THE ROLE OF INTERFERON GAMMA IN THE STROMA OF GROWING AND REGRESSING TUMOURS

vorgelegt von
BSc (Honours)
Felicia Pradera Elsley
Aus Perth

von der Fakultät III – Prozesswissenschaften
der Technischen Universität Berlin
zur Erlangung des akademischen Grades

Doktor der Naturwissenschaften
-Dr. rer. nat.-

genehmigte Dissertation

Promotionsausschuss
Vorsitzender..Prof. Dr. Roland. Tressl
Gutachter: Prof. Dr. Ulf Stahl
Gutachter: Prof. Dr. Roland Lauster

Tag der Aussprache: 21/09/06

Berlin 2006
D83

TABLE OF CONTENTS

1 INTRODUCTION

1.1 TUMOUR STROMA

The microenvironment, which encompasses the tumour body, is termed the tumour stroma and its role in malignancy is poorly understood (Seljelid et al., 1999). All solid tumours are made up of cancer cells and stroma. Tumour cells can modify the resident stroma by altering the surrounding connective tissue and modulating the metabolism of the resident cells, thus resulting in production of a stroma convenient for the tumour cells instead of maintaining the physiological composition of the tissue. In addition to a variety of extracellular matrix components, the stroma contains a rich cellular population, which includes fibroblasts that provide the connective tissue framework for adipose, vasculature, resident immune cells, and a milieu of cytokines and growth factors (Figure 1) (Pupa et al., 2002). Therefore, tumour stroma is composed of a variety of normal cell types which appear to be actively recruited by the tumour, for example, to provide blood supply (O'Reilly et al., 1994).

1.1.1 EXTRACELLULAR COMPONENTS OF THE TUMOUR STROMA

A network of interacting extracellular macromolecules that constitute the extracellular matrix (ECM) surrounds most cells in multicellular organisms. These proteins and polysaccharides serve as 'biological glue', and are secreted locally into an organised meshwork within the extracellular space of most tissues. They have the capability to form highly specialised structures such as basal laminae, tendons and cartilage; and are an essential component of the tumour stroma.

In recent years, it has become clear that the extracellular matrix plays an active and complex role in regulating the behaviour of cells. The two main domains of extracellular matrix are the basement membrane and the interstitial matrix, while the two primary classes of extracellular macromolecules are collagens and glycosaminoglycans. Communication between the matrix and cells are conducted through matrix receptors of which integrins and cadherins are the most important classes. Additionally, almost all classes of matrix molecules are involved in the control of proliferation, differentiation, and motion. Each tumour type has a different composition of these molecules providing a stable microenvironment for tumour growth.

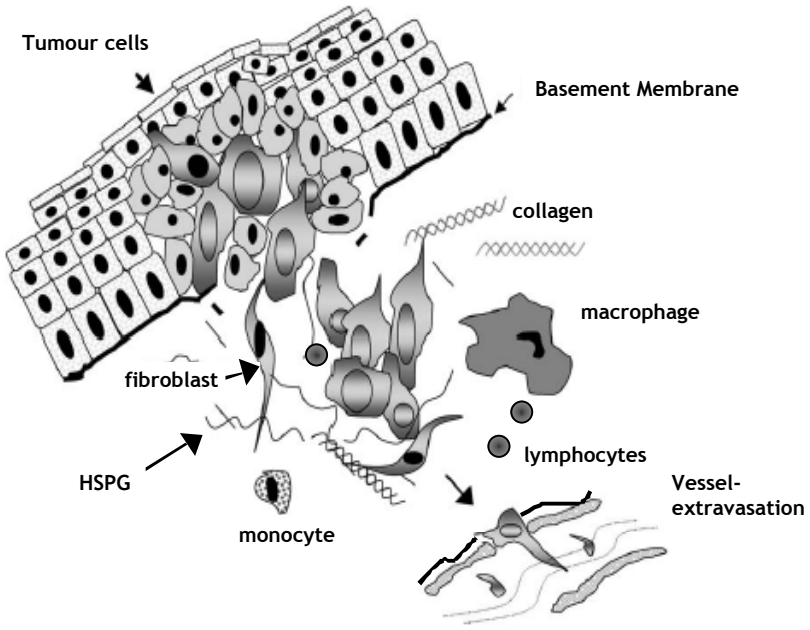

Figure 1: Tumour Stroma
The tumour stroma consists of a variety of cellular and extracellular molecules which mediate cell-cell and cell-matrix interactions. The invasion of tumour cells requires that the natural barriers between the various compartments, such as basement membranes consisting of heparan sulphate proteoglycan (HSPG) and collagen, are overcome to facilitate the passage of tumour cells and enable them to intravasate and generate distant metastasis. Adapted from (Zigrino et al., 2005).

1.1.2 MOLECULES MAKING UP THE BASEMENT MEMBRANE ASSOCIATED TUMOUR STROMA

Basement membranes constitute a specific compartment of the extracellular matrix, which occur as thin sheet-like structures located in the adherent cell microenvironment, at the basal side of a cell or as a pericellular envelope. These matrices are mainly composed of collagen type IV, the glycoproteins laminin and entactin/nidogen and proteoglycans. Basement membranes provide anchoring cell support, divide tissue compartments by forming selective barriers, may control the access of regulatory molecules such as growth factors to the cell surface, and can act as solid-phase regulators of growth and differentiation (Lortat-Jacob and Grimaud, 1992).

The basement membrane represents a barrier to invasive tumour cell growth, separating the epithelium from connective tissue and the vascular endothelium. Remodelling or loss of the basement membranes is required for tumour cells to reach vessels and thus allow for access distant organs. This involves upregulation of the various matrix metalloproteinases (MMPs) that act on the ECM (Kalluri, 2003).

A PROTEOGLYCANS (PG)

Proteoglycans are the most highly charged components of the basement membrane. They contain 90-95% carbohydrate by weight, compared to the 1-60% for other glycoproteins. Virtually all mammalian cells produce proteoglycans and secrete them into the ECM, insert them into the membrane or store them in secretory granules.

In the panoply of signals from the extracellular matrix, proteoglycans appear to play a predominant role. Proteoglycans can be grouped into several families based on their protein core design (Iozzo, 1998). There are three main family members:

1. Lecticans:
   Stimulate the proliferation of fibroblasts and chondrocytes.
2. Small Leucine Rich Repeats (SLRP's):
   Primary organisers of collagen networks, involved in signal transduction and modulation/differentiation of epithelial and endothelial cells.
3. Heparan Sulphate Proteoglycans (HSPG):
   Effects cell adhesion and migration, proliferation and differentiation. Binds cytokines and growth factors. Involved in pathological processes.

Proteoglycans are continuously modified due to cleavage caused by heparanases, exoglycosidases and sulphatases. They can also regulate enzyme activity by binding ligands (such as various cytokines and chemokines) to their specific receptors, and protecting proteins from degradation. Some of these proposed functions are likely to depend on a large polyanionic domain supported by the glycosaminoglycan (GAG) component.

B GLYCOSAMINOGLYCANS (GAGS)

Glycosaminoglycans are a group of negatively charged molecules present in many tissue components of the extracellular matrix, basement and cellular membranes. Most GAGs exist naturally as non-associated forms or as covalent complexes with the core proteins, proteoglycans. Glycosaminoglycans assume extended structures in aqueous solution because of their strong hydrophilic nature based on extensive sulphation, which is further exaggerated when they are covalently linked to core proteins. They hold a large number of water molecules in their domain and occupy hydrodynamic space in solution.

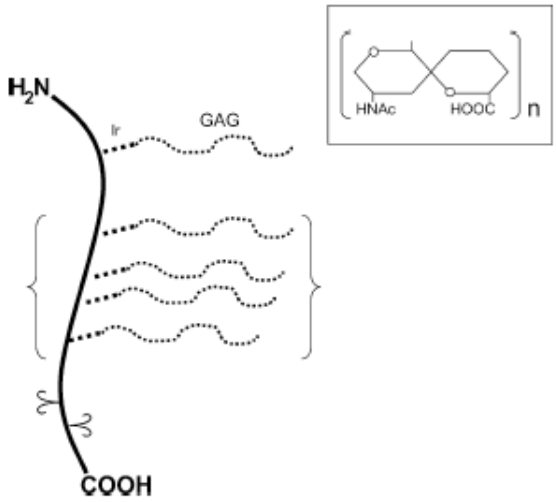

Figure 2: General schematic representation of proteoglycan structure.
The core protein (thick line) undergoes post-translational modification by covalently attached one or more (braces) glycosaminoglycan chains (dotted lines, GAG) via the linkage region (thick dots). Insert shows the general structure of the disaccharide units in GAGs. The protein core may also be modified by sulphation, phosphorylation, myristilation or glycosylation of the amino acid chain (γ). (Wegrowski and Maquart, 2004)

GAGs are linear polysaccharides whose building blocks consist of an amino sugar and an uronic acid (Figure 2). Binding of proteins to the GAG chains of proteoglycans can result in immobilisation of the respective proteins at their sites of production for matrix storage and future mobilisation in response to immunological and environmental stimuli. As a result, the interaction between GAGs and proteins can have physiological effects on cell growth, migration and development, haemostasis, lipid transport and absorption.

Within the tumour stroma and the tumour fibrotic tissue there are often higher proportions of proteoglycans than in normal tissues. While the stromal proteoglycans of the SLRP family possess antiproliferative properties, the GAGs liberated after PG degradation promote cancer cell migration (Wegrowski and Maquart, 2004).

C HEPARAN SULPHATE GAG CHAINS

Heparan sulphate proteoglycan is a component of all basement membranes. Heparan sulphate (HS), is a GAG composed of alternating sequences of glucosamine and either glucuronic or iduronic acid (Gallagher and Walker, 1985). It is structurally related to heparin which is produced mainly by mast cells. HS arises from the same biosynthetic pathway, but heparin is more heavily sulphated and contains a greater amount of iduronic acid.

HS chains are characterised by complex sulphation patterns resulting in distinct protein binding domains (Qiao et al., 2003). The HS side chains have been found to be involved in the sequestration of heparin-binding growth factors (Noonan et al., 1991). In part this is due to the molecular impermeability of these structures, imparting anionic charges across the basement membrane.

HS molecules are ubiquitous in animal tissues where they function as ligands that are involved in the regulation of the proteins that they bind (Lortat-Jacob et al., 2002). Cells have the ability to rapidly adjust their HS in response to a changing microenvironment (Nurcombe et al., 1993). *In vivo* the vast majority of HS exists in covalent linkage to core proteins, the HSPGs. HSPGs can be divided into the cell surface forms (syndecans and glypicans) and secreted extracellular matrix forms (e.g. perlecan). There are divergent reports suggesting that the role of HSPGs (either stimulatory or inhibitory) depends on the core protein and its association with a cell type (Qiao et al., 2003).

HSPGs at the tumour cell surface can actively modulate the tumourigenic process by regulating autocrine signalling loops that lead to unregulated cell growth. They can also influence how an organism responds to a growing tumour, including the recruitment of cells of the immune system to the tumour site, the formation of a fibrin shell around the tumour that acts as a protective barrier and the development of new blood vessels to the site of the growing tumour (Sasisekharan et al., 2002).

There are numerous biological effects of factors bound to HSPGs.

- Fibroblast growth factor (FGF) can result in receptor specific oligomerisation and in cancer HSPGs bind FGF, thereby acting as a storage depot and activating an autocrine signalling loop (Iozzo and San Antonio, 2001).
- Vascular endothelial growth factor (VEGF) bound to HSPGs results in low affinity receptor interaction, which can block angiogenesis in cancer (Jiang and Couchman, 2003).
- Interleukin 8 (IL-8) can stimulate growth factor sequestration, which in turn can modulate the host immune response to tumour cells (Capila and Lindhardt, 2002).

1.1.3 CELLS WITHIN THE TUMOUR STROMA

A FIBROBLASTS

The term fibroblast is ascribed to an heterogeneous multifunctional population of cells that play a role in wound healing and developmental processes. They can be described as connective tissue stem cells, matrix and protein synthesising cells (i.e. fibrocytes), contractile cells (i.e. myofibroblasts) and, in some instances, tissue phagocytic cells (i.e. histiocytes) (Silzle et al., 2004).

Fibroblasts are a relevant source of ECM and ECM-modulating molecules in tumours, suggesting that tumour-associated fibroblast (TAF) alterations in ECM composition profoundly impact the recruitment and function of immune cells (Silzle et al., 2004). They are also capable of producing a number of paracrine immune modulators such as peptide growth factors, cytokines, chemokines and inflammatory mediators. These modulators can contribute to the development of transformed cells and the formation of tumour mass (Elenbaas and Weinberg, 2001).

The production of MMPs by fibroblasts, enables tumour cells to cross structural barriers and metastasise into distant organs, as well as regulate angiogenesis. These proteinases are also responsible for the release of growth factors from the ECM such as FGF (Klein et al., 2004), transforming growth factor-beta (TGF-β1) (Stamenkovic, 2003), and platelet derived growth factor (PDGF) (Kalluri, 2003), which influence tumour development and rejection.

B ENDOTHELIAL CELLS

The endothelium is a single layer of flattened, polygonal cells lining the vertebrate heart, blood, and lymph vessels. Endothelial cells are the building blocks of angiogenesis, new vessel formation. This is an important phenomenon during normal development and tissue repair, as well as during various pathological processes such as tumour growth (Iivanainen et al., 2003).

Angiogenesis depends on specific molecular interactions between vascular endothelial cells and their surrounding microenvironment, composed of neighbouring cells and the extracellular matrix (Iivanainen et al., 2003). This process involves a cascade of events characterised by induction of vascular hyperpermeability, local degradation of the basement membrane, migration and sprouting into the local stroma, cell proliferation and formation of granulation tissue, reconstruction of the basement membrane and formation of new blood vessels (Li and Thompson, 2003). Within tumours, vessels are organised in a chaotic fashion and do not follow the hierarchical branching network of normal vascular networks (Jain and Duda, 2003).

C HAEMATOPOIETIC CELLS

Tumours contain numerous different haematopoietic cell types, of the myeloid line as granulocytes, macrophages and dendritic cells, and the lymphoid line, as B, T and natural killer (NK) cells. Depending on the type of inflammation, haematopoietic cells can aid in tumour growth (chronic inflammation) or tumour rejection (acute inflammation) (Philip et al., 2004).

1.1.4 CYTOKINES AND CHEMOKINES WITHIN THE TUMOUR STROMA

There is a functional relationship between inflammatory infiltrates and malignant growth, in which the infiltrates can contribute to regression or development of cancer. In addition to tumour cells, infiltrating cells such as macrophages and T cells are often responsible for

cytokine and chemokine production. Normal cells produce cytokines only transiently, however malignant cells can produce considerable and sustained amounts of cytokines and pleiotropic chemokines such as IL-8, TGF-ß and macrophage chemotactic proteins (MCPs) (De Wever and Mareel, 2003). These factors can enable the production of an array of cytokines such as IL-2, IL-4, tumour necrosis factor (TNF) and interferon gamma (IFN-γ), which influence tumour growth progression or inhibition.

Depending upon the cytokine milieu, cytokines and chemokines can be anti-tumour effector molecules or alternatively they can contribute to tumour progression. Nevertheless, the origin of these molecules (matrix bound or cellularly produced) and their influence in tumour stromal interactions are not fully understood.

1.2 THE PROTEIN INTERFERON GAMMA (IFN-γ)

IFN-γ is a potent, pro-inflammatory cytokine produced primarily by activated T cells and NK cells. It is a lymphoid factor that possesses powerful anti-viral and anti-parasitic functions, which is also capable of inhibiting proliferation in a number of normal and transformed cells. IFN-γ has several properties related to immuno-regulation:

i. Activator of macrophages to stimulate the release of reactive oxygen species
ii. Increases major histocompatability class I (MHC-I) molecule expression, and induces MHC-II molecules on a wide variety of cell types
iii. Acts directly on T and B lymphocytes to promote differentiation and maturation
iv. Strong activator of NK cells

1.2.1 STRUCTURE

IFN-γ is a dimeric protein. The active form of this cytokine is a homodimer consisting of two intertwining 143-amino acid polypeptides (Sadir et al., 1998). The protein is glycosylated at

two sites and the isoelectric point is 8.3-8.5. The (amino) N-terminus of IFN-γ is directly involved in receptor binding and the integrity of the (carboxyl) C-terminus is critical for biological activity. A basic amino acid cluster located in this C-terminal domain is involved in the organisation of the three dimensional structure of the protein. This cluster is also important as it increases the on rate of the IFN-γ - IFN-γ receptor (IFN-γ–R) binding reaction (Lortat-Jacob and Grimaud, 1991).

Fernandez-Botran and co-workers, 1999, found that by removing stretches of more than 11 amino acids (aa) from the C-terminal portion of human IFN-γ, receptor binding and specific activity were greatly reduced. This is due to the fact that the C-terminus of IFN-γ, encompassing residues 95-133 in mouse and residues 95-134 in human IFN-γ, interact with high affinity at a membrane proximal site on the cytoplasmic domain of the alpha chain of the receptor (Subramaniam et al., 2000). It has been postulated that this domain could be a regulatory element of the cytokine (Wetzel et al., 1990).

1.2.2 IFN-γ SIGNAL TRANSDUCTION

IFN-γ is a pleiotropic cytokine involved in aspects of immune regulation including transcription. Upon engagement of IFN-γ with the receptor, janus tyrosine kinases (JAK) are activated and subsequently phosphorylate the signal transducer and activator of transcription-1α (STAT-1α) protein, which dimerises and translocates to the nucleus to induce target gene transcription by binding to gamma activated sequences (GAS) in the promoter of IFN-γ-responsive genes (Ma et al., 2005).

1.2.3 INTERACTION WITH THE MATRIX

IFN-γ molecules of different species display only modest homology at either cDNA or amino acid levels (Fernandez-Botran et al., 1999). However, there is a conserved sequence within the molecule present in many species and defined by the amino acids, KRKRS (Figure 3). This homologous motif of the IFN-γ molecule is a high affinity binding site ($K_d = 10^{-9}$ M) for heparan sulphate from basement membranes within the extracellular matrix (Lortat-Jacob and Grimaud, 1992).

ECM components have been hypothesised to be involved in storing IFN-γ and thereby providing a local pool of cytokine (Lortat-Jacob et al., 1996b). Cell surface heparan sulphate bound to IFN-γ was shown to delay the nuclear accumulation of IFN-γ, providing extra evidence that HS molecules act as a storage depot around the cell for local delivery of the cytokine (Sadir et al., 2000).

Once IFN-γ is bound to heparan sulphate, the extent of its C-terminal cleavage is reduced to less than 10 amino acids and this increases the cytokine activity. This may be due to the protein folding in a new relaxed conformation with increased stability (Lortat-Jacob and Grimaud, 1991). IFN-γ is generally thought of as a soluble factor and, *in vivo*, is eliminated from the bloodstream with a half-life ($t_{1/2}$) of 1.1 minutes. However, after heparin stabilisation plasma clearance is reduced to a half-life ($t_{1/2}$) of 99 minutes (Lortat-Jacob et al., 1996a).

It has been demonstrated (Fernandez-Botran et al., 1999) that IFN-γ molecules bound to immobilised GAGs, such as heparan sulphate, are still capable of retaining their activity and can induce MHC class II expression on target cells. Lortat-Jacob and colleagues, suggested a novel model for the interaction of HS with a protein in which two sulphated terminal sequences of the binding domain interact directly with the two IFN-γ C-termini and bridge the two cytokine monomers through an internal N-acetyl-rich sequence (Figure 4).

This interaction could be biologically relevant as basement membranes could provide a local concentration of this soluble cytokine, direct the range of its action and act as a physiological storage depot around cells. IFN-γ is sequestered at the surface of endothelial cells by electrostatic interactions between specific basic amino acid residues KRKRS of the conserved motif, and the sulphated domains of HS, the most abundant endothelial GAG (50-90%) (Douglas et al., 1997). At present little is known about the *in vivo* influence of IFN-γ on the matrix of both normal and malignant tissues.

SPECIES	TOTAL IFN-γ HOMOLOGY (%)	MC-2 SEQUENCE	% HOMOLOGY OF MC-2 SEQUENCE
Mouse		**LRKRKRSR**	
Rat	87	********	100
Hamster	56	********	100
Duck	33	**SKRKRSQS**	60
Gallus	35	**FKRKRSQS**	60
Turkey	35	**SKRKRSHP**	60
Pheasant	36	**SKRKRSQS**	60
Quail	36	**SKRKRSQC**	70
Guinea fowl	36	**LKRKRNQP**	50
Fugu	18	**LEKR*R*R**	50
Zebra fish	23	***KNKE*K***	50
Rainbow trout	18	**DNR***RQ**	20
Guineapig	46	**Q***R*TQ**	60
Baboon	48	**IG*****Q**	70
Macaque	48	**IG*****Q**	70
Human	42	**TG*****Q**	60
Marmoset	49	**IG**R**Q**	60
Squirrel monkey	48	**IG*****Q**	70
Rabbit	47	***K*****Q**	80
Woodchuck	51	*******Q**	90
Donkey	53	*******Q**	90
Cat	51	*******Q**	90
Dog	52	*******Q**	90
Camel	53	*******Q**	90
Llama	52	******RQ**	80
Cow	51	*******Q**	90
Water buffalo	51	*******Q**	90
Goat	51	*******Q**	90
Dolphin	50	****R**Q**	80
Pig	51	*******Q**	90

Figure 3: Species consensus of the IFN-γ molecule and the C-terminal (mIFN-$\gamma_{128-135}$) fragment responsible for binding to heparan sulphate as determined by Vector-Alignment™. Sequence homology was also described previously (Zou et al., 2005). (*) Indicates consensus with the mouse sequence.

Amino acids; Green – non polar / hydrophobic, **Black** – No charge/ non-acidic amino acid/ polar/ hydrophilic, Blue – Positive charge/ basic amino acid/ polar /hydrophilic, Red – Negative charge/ acidic amino acid/ polar / hydrophilic. For phylogenetic tree and complete sequences see Appendix (Figure 27).

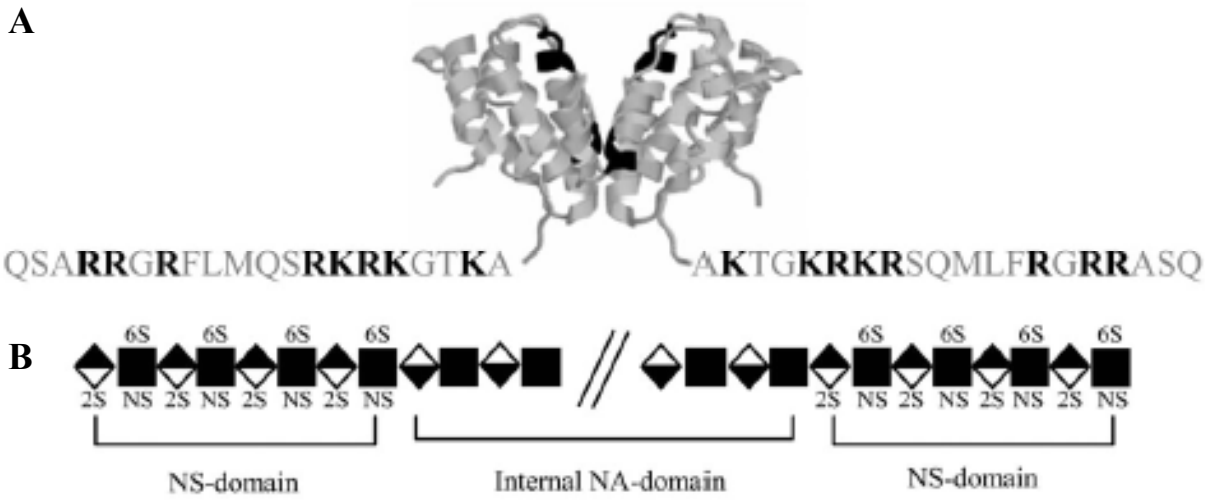

Figure 4: Molecular organisation of the HS binding site of Human IFN-γ
(A) IFN-γ is a C_2-symmetric homodimer in solution and binds (bold type-site of interaction) to (B) HS by virtue of basic residues located at the C terminus of the two subunits. A model of the interaction between IFN-γ and HS was thus proposed in which the KRKRS domains, located at the C terminus of each subunit of the IFN-γ dimer, would interact with the highly charged NS domains of the fragment (Lubineau et al., 2004).
N-acetylated regions (NA-domains) are mainly composed of D-glucuronic acid and N-acetylated glucosamine, and thus with low global charge, separate domains rich in L-irduronic acid and N-sulphated glucosamine (NS-domains), which are hypervariable and highly charged.

1.2.4 ROLE OF IFN-γ IN TUMOURS

Several mechanisms have been proposed to explain the role of IFN-γ in tumours using defined experimental models. These include:

- **Effects on tumour growth and survival**. Studies have shown that IFN-γ and IFN–γ receptor are essential for tumour rejection (Blankenstein and Qin, 2003). Tumours that have been transfected to secrete IFN-γ are rejected in immunocompetent mice (Hock et al., 1993) and blocking endogenous IFN-γ with neutralising antibodies inhibits

tumour rejection (Dighe et al., 1994). The ability of $CD8^+$ T cells to mediate tumour rejection upon adoptive transfer correlates with interferon gamma production (Becker et al., 2001). However, the mechanism by which IFN-γ exerts tumouricidal activity is still not completely resolved.

- **Angiogenesis.** It is well known that a growing tumour requires new blood vessels. Inhibition of angiogenesis by $CD4^+$ (Qin and Blankenstein, 2000) and $CD8^+$ (Qin et al., 2003) T cell-derived IFN-γ, is an effective way to prevent rapid tumour burden thereby allowing other, perhaps direct killing mechanisms to eliminate residual tumour cells (Blankenstein and Qin, 2003). Evidence suggests that there is a critical dependence on expression of IFN-γ–R on the vasculature in order to mediate destruction of blood vessels, and ultimately of the tumour (Ibe et al., 2001).

- **Effects on both innate and adaptive immune reponses against tumours.** IFN-γ is known to be a macrophage activating factor capable of inducing non-specific kill of a variety of tumour targets as well as up-regulating expression of cytotoxic ligands such as TNFα and FAS-ligand (Farrar and Schreiber, 1993). Additionally, IFN-γ also stimulates B cell proliferation and differentiation and enhances MHC-I expression on the tumour surface (Mocellin et al., 2001).

1.3 TUMOUR THERAPY

The reasons why the immune system does not effectively destroy tumour cells is not fully understood and therefore is controversially discussed. The concept of immune surveillance was first formulated by Thomas (Thomas, 1959). They assumed that the immune system would recognise pre-cancerous and cancerous cells as non-self and reject them. This concept is valid only for virally transformed cells. Tumours arising from non-virus related mechanisms are regarded by the immune system as "self", and therefore attempts to manipulate the immune system to recognise the tumour as "non self" are difficult (Klein and Klein, 2005).

Initially it was believed that tumours could escape immune recognition as there was no detectable adhesion or costimulatory molecules, and no peptides that could be presented by

MHC molecules, thereby creating low immunogenicity. Later it was thought tumours could express antigens to begin with, to which the immune system could respond but that later these were lost by antibody-induced internalisation or antigenic variation. Essentially, when tumours were attacked by cells responding to a particular antigen, any tumour cell that did not express that tumour antigen, would have a selective advantage.

Recently, it has been demonstrated that immune responses could be suppressed directly as tumours can often produce substances such as TGF-ß and IL-10. Willimsky and Blankenstein, (2005) demonstrated that spontaneously developed sporadic tumours of high antigenicity are initially ignored by the immune system. The expansion of antigenic-spceific T cells occurs later, but the T cells are dysfunctional at this later stage (Willimsky and Blankenstein, 2005).

The fact that cancer cells are genetically and phenotypically less stable than normal cells enables them to rapidly change and escape immune destruction. Aided by the tumour stroma, tumour cells can become resistant to destruction. In an effort to combat tumours various therapies have been developed. These include radiation, surgery, chemotherapy, vaccination and adoptive immunotherapy. Often combinations of these therapies have elicited the best response in patients.

1.3.1 CYCLOPHOSPHAMIDE

Cyclophosphamide (Cy) is an alkylating agent widely used in chemotherapy. It has a bimodal effect on the immune system, depending on the dose and the schedule of administration (Matar et al., 2002). Large doses of Cy bring about impairment of host defence mechanisms, therefore leading to severe immunodepression. However, the administration of low doses leads to an enhancement of immune responses in both experimental animals (Awwad and North, 1988) and humans (Berd et al., 1982).

Cy is an inert lipophilic prodrug that requires enzymatic conversion regulated by the hepatic cytochrome P450 2B1 gene for its anticancer effect (Figure 5) (Pass et al., 2005). As Cy toxicity is not dependent on a particular phase in the cell cycle, it is well suited for the treatment of solid tumours.

The anti-tumour response induced by Cy has been investigated previously, and the interactions of stroma cell components were analysed during rejection of established tumours (Ibe et al., 2001). It was shown that 6 h after Cy-treatment T cells in the tumour were inactivated and tumour infiltrating macrophages (TIMs) switched to IFN-γ production. Both, IL-10 production before and IFN-γ production after Cy-treatment by TIMs required T cells. Under certain experimental conditions Cy can induce tumour rejection by host cell modulation rather than direct tumouricidal activity (Awwad and North, 1988). For example, a single injection of a defined amount of Cy induced tumour rejection in immunocompetent mice but had no effect on tumour growth in immunodeficient mice (Hengst et al., 1980). It was discovered that during low dose therapy using Cy, IFN-γ played a crucial role in mediating tumour rejection, however whether the cytokine originates from T cells (Tsung et al., 1998), or macrophages (Ibe et al., 2001) remains in question.

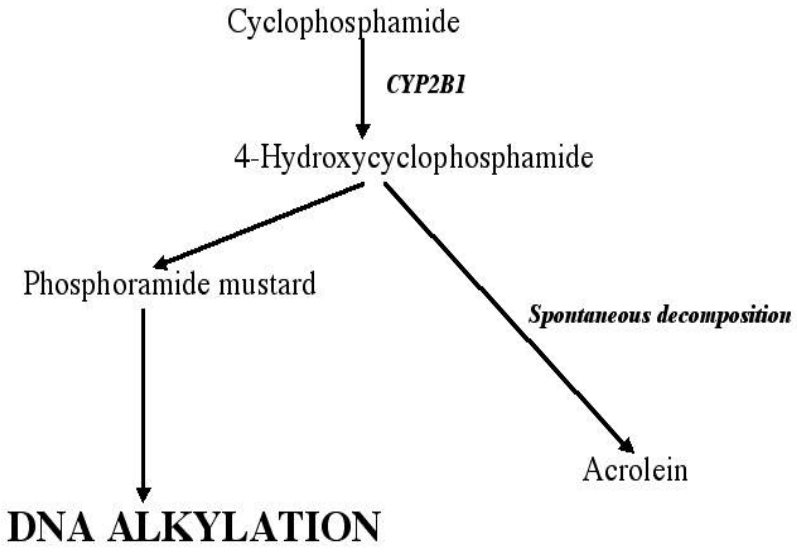

Figure 5: Pathway of the Bioactivation of Cyclophosphamide (Chiocca, 1995)

1.4 AIMS

The goal of this study was to investigate the origin of IFN-γ during chemotherapy induced, immune response mediated tumour rejection.

The role of IFN-γ in mediating tumour rejection is known, yet all previous studies have focused on the cellular origin of the cytokine. Matrix bound IFN-γ may play an important role in immune responses. This hypothesis was based on experiments carried out by Fernandez-Botran and coworkers, (2002) in which the survival of an allotransplanted skin graft was prolonged by inhibiting this interaction. Additionally, it was shown that the tertiary structure of IFN-γ changed when bound to the matrix and this provided the molecule with higher affinity for its receptor. Therefore, major attention in this work was given to the presence and role of matrix bound IFN-γ within the tumour microenvironment.

By analysing the tumour stroma interactions in an established model during cyclophosphamide (Cy)-induced tumour rejection the aim was to determine:

- Whether IFN-γ played a role in tumour rejection in this model
- Which cells produced IFN-γ in response to tumour therapy?
- Could IFN-γ bind to the matrix *in vivo*?
- Could the interaction of IFN-γ with the matrix be disturbed and were there functional consequences?

The role of IFN-γ in tumour immunity was investigated by inoculation of the plasmacytoma J558L in IFN-$\gamma^{-/-}$ and IFN-$\gamma^{+/-}$ BALB/c mice and bone marrow chimeras followed by treatment with a previously established amount of Cy (15mg/kg) (Ibe et al., 2001). Tumour growth kinetics, histological analysis and radioactive cytokine accumulation were used to determine whether there was a matrix/IFN-γ interaction within the model, and if interference of this interaction could inhibit tumour rejection.

2 MATERIALS AND METHODS

2.1 MATERIALS

2.1.1 CELL LINES

The plasmacytoma cell line J558L grows aggressively in BALB/c mice. It is a heavy chain loss variant of the BALB/c derived line J558 that synthesises and secretes the λ light chain. The cell line was induced using mineral oil and expresses H-2^d and the antigen PC.1. Additionally, J558L express cellular adhesion molecule ICAM-1 (Cavallo et al., 1995), but no detectable MHC class II molecules. Cells are sensitive to dexamethasone and cortisol.

The J558L-interferon gamma transfectants were generated by Hock and colleagues, 1993. Essentially the tumour cell line was transfected with the pLTR-IFN plasmid along with pWLneo. Under G418 selection the cell line is capable of producing 120 ng/ml IFN-γ as detected by ELISA.

TS/A is a spontaneous mammary adenocarcinoma, which developed from a 20 month old retired BALB/c breeder. The cell line expressed MHC class I but not MHC class II molecules and grows in H-2 matched, minor histocompatability antigen incompatible hosts such as DBA/2 mice (Nanni et al., 1983).

Mc51.9 was induced by MCA in 129/Sv/Ev IFNγR-/- mice ($H2^b$). These tumour cells express MHC class I molecules (both H-$2D^b$ and H-$2K^b$) and are negative for MHC class II. The interferon gamma transfectant was created using the pLTR-IFN and pWLneo plasmid and under G418 selection pressure is capable of producing 70 ng/ml of IFN-γ.

The XMG-6 mAb neutralising IFNγ was obtained from ATCC (American Type Cell Culture). It was originally derived from a Lewis rat after immunizing on eight sequential days with soluble recombinant mouse IFN-γ (170 μg/injection). This rat was later boosted with IFN-γ (100 μg) in CFA. After 21 days, the rat was boosted again with 100 μg IFN-γ without adjuvant. 3 days later, the spleen cells were fused with P3X63Ag myeloma cells using 50% polyethylene glycol. The cytokine production was identified by ELISA and neutralisation capability determined. The isotype for XMG-6 was concluded to be IgG1.

2.1.2 MICE

Wild type BALB/c mice and Severe Combined Immune Deficient (SCID) mice were obtained from Jackson laboratories. IFN-γ deficient mice backcrossed to the BALB/c background, 11 generations, were bred and maintained from birth at the Max-Delbrueck-Centrum in Berlin. All mice were used in experiments when they were 8-12 weeks old. Genotypes of IFN-γ deficient mice (Dalton et al., 1993) were confirmed by polymerase chain reaction (PCR) using a thermocycler. (PCR conditions: 12 cycles, annealing 64°C for 30 sec; 25 cycles, annealing 58°C for 30 sec, elongation 72°C for 2 min).

2.1.3 PEPTIDE

The sequence specific for the basic amino acid cluster responsible for IFN-γ binding to heparan sulphate was identified (Fernandez-Botran et al., 1999). The fragment of the murine IFN-$\gamma_{128-135}$ named MC-2 (LRKRKRSR) was produced and purified by HPLC (Biosynthan, Berlin). The peptide was diluted in phosphate buffered saline (PBS) to a 1 mM concentration and sterile filtered. Aliquots were stored at –20°C.

2.1.4 OLIGONUCLEOTIDES

Oligonucleotides were obtained from TIB^R Molbiol (Berlin, D).

A PCR PRIMERS

Intact IFN-γ:

fwd: 5’-AGA-AGT-AAG-TGG-AAG-GGC-CCA-GAA-G-3’

rev: 5’-AGG-GAA-ACT-GGG-AGA-GGA-GAA-ATA-T-3’

fragment: 260 bp

IFN-γ disrupted by neomycin:

fwd: 5’-TCA-GCG-CAG-GGG-CGC-CCG-GTT-CTT-T-3’

rev: 5’-ATC-GAC-AAG-ACC-GGC-TTC-CAT-CCG-3’

fragment: 320 bp

pSecTag/EF1α:

fwd: 5’- ATC AGG GTT ATT GTC TCA T -3’

rev: 5’- GGA ACC CAG AGC AGC AGT -3’

fragment: 1466 bp

pMC2sec:

MC21: 5’- TAC CGA GCT CGG ATC CTC TCA GGA AG -3’

MC22: 5’- CAG CAT GCC TGC TAT TGT CTT CCC AA -3’

Fragment: 406 bp

β-Actin:

U12: 5’- TGG AAT CCT GTG GCA TCC ATG AAA CTA CAT-3’

U13: 5’- AAA CGC AGC TCA GTA ACA GTC GCG CTA GAA-3’

Fragment: 347 bp

B INSERTS

Murine IFN-γ $_{128–135,}$ C-2) insert:

5’- GAT CCT CTC AGG AAG CGG AAA AGG AGT CGC TGC G -3’

5’- AA TTC GCA GCG ACT CCT TTT CCG CTT CCT GAG AG -3’

Fragment: 34 bp

Murine neutral insert:

5’- GAT CCT GCC GCA GCG GCT GCA GCC GCC GCT GCC G –3’

5’- AAT TCG GCA GCG GCG GCT GCA GCC GCT GCG GCA G –3’

Fragment: 34 bp

2.1.5 REAGENTS

A CHEMICALS

CHEMICAL	ABBREVIATION	COMPANY
1-kb-DNA Ladder	M	Invitrogen, Karlsruhe, G
2-Mercaptoethanol	ME	Merck, Darmstadt, G
4-2-hydroxyethyl-1-piperazineethanesulfonic acid	HEPES	Serva, Heidelberg, G
5x First strand buffer		Invitrogen, Karlsruhe, G
Acrylamide		Bio-rad, München, G
Agarose		Serva, Heidelberg, G
Ammonium chloride	NH_4Cl	Merck, Darmstadt, G
Ampicillin (50ug/ul)		Sigma, Taufkirchen, G
Ammonium persulphate (10%w/v)	APS	Bio-rad, Munich, G
Borgal solution (24%)		Intervet, Unterschleißheim, G
Bovine serum albumin	BSA	Serva, Heidelberg, G
Chloroform		Roth, Karlsruhe, G
Concavalin A	Con A	Sigma, Taufkirchen, G
Cytofix/Cytoperm		Becton Dickinson, Heidelberg, G
Deoxy-nucleotide triphosphate	dNTP's	Roche, Mannheim, G
Diethylether		Otto Fischer, Berlin, G
Diethylpyrocarbonate	DEPC	Fluka, Taufkirchen, G
Dimethylsulfoxide	DMSO	Sigma, Taufkirchen, G
Dithiothritol	DTT	Merck, Darmstadt, G
Dnase I (Rnase-free)		Roche, Mannheim, G
Dulbecco's modified Eagles medium	DMEM	Gibco, Karlsruhe, G
Dulbecco's PBS (1x)	D-PBS	Invitrogen, Karlsruhe, G
Ethanol	Et-OH	Merck, Darmstadt, G
Ethidium bromide		Serva, Heidelberg, G
Ethylene diamine tetra-acetic acid	EDTA	Merck, Darmstadt, G
Extracellular matrix gel from Engelbreth-Holm-Swarm murine sarcoma	Matrigel/ ECM gel	Sigma,Taufkirchen,G
Fetal calf serum	FCS	Greiner, Solingen, G

Gel/mount		Vector Laboratories, Peterborough, UK
Geneticin	G418	Gibco, Karlsruhe, G
Glutamine	Glu	Gibco, Karlsruhe, G
Golgi plug		Becton Dickinson, Heidelberg, G
Haemotoxylin		Merck, Darmstadt, G
Histoacryl		B/Braun, Melsungen,G
Hydrochloric acid	HCl	Roth, Karlsruhe, G
Interferon gamma (murine)	mIFN-γ	R&D Systems,
Interferon gamma (human)	hIFN-γ	Bohringer Ingelheim,G
Isoamyl alcohol		Merck, Darmstadt, G
Isopropanol		Roth, Karlsruhe, G
Kaisers gelatine		Merck, Darmstadt, G
Magnesium chloride	$MgCl_2$	Merck, Darmstadt, G
Magnesium sulfate	$MgSO_4$	Merck, Darmstadt, G
Nusieve GTG agarose		Cambrex, Hess Oldendorf,G
Tissue-Tek®	OCT	Sakura Finetek, USA
Penecillin/Streptomycin	P/S	Gibco, Karlsruhe, G
Perm/Wash Buffer		Becton Dickinson, Heidelberg, G
Phenol		Gibco, Karlsruhe, G
Phenol/Chloroform (1:1)		Roth, Karlsruhe, G
Polyoxyethylene sorbitan monolaureate	Tween-20	Sigma, Taufkirchen, G
Phosphate buffered saline	PBS	Gibco, Karlsruhe, G
Potassium chloride	KCl	Merck, Darmstadt, G
Potassium bicarbonate	$KHCO_3$	Roth, Karlsruhe, G
Proteinase K		Roche, Mannheim, G
Sodium acetate		Fluka, Taufkirchen, G
Sodium chloride	NaCl	Fluka, Taufkirchen, G
Sodium citrate		Sigma, Taufkirchen, G
Sodium-dodecyl-sulphate	SDS	Serva, Heidelberg, G
Sodium hydroxide	NaOH	Merck, Darmstadt, G

Sodium pyruvate		Gibco, Karlsruhe, G
RNAse-inhibitor		Promega, Manheim, G
RPMI 1640-Medium	RPMI	Gibco, Karlsruhe, G
Reverse transcriptase (Superscript II)	RT	Invitrogen, Karlsruhe, G
T4 DNA ligase		Promega, Manheim, G
T4 ligation buffer		Promega, Manheim, G
Taq polymerase		Roche, Mannheim, G
Taq polymerase buffer (10x)		Roche, Mannheim, G
Tetramethylethylenediamine	TEMED	Bio-rad, Munich, G
TOTO-3 iodide	TOTO-3	Invitrogen, Karlsruhe, G
Tricine		Bio-rad, Munich, G
Tris (hydroxymethyl) aminomethane	Tris	Sigma, Taufkirchen, G
Tris-HCl	Tris-HCl	Sigma, Taufkirchen, G
Triton X-100		Serva, Heidelberg, G
Trizol		Invitrogen, Karlsruhe, G
Trypan blue		Sigma, Taufkirchen, G
Trypsin		Gibco, Karlsruhe, G
Zeocin	Zeo	Invitrogen, Karlsruhe, G

B KITS

KIT	**COMPANY**
DAB Substrate Kit	Sigma, Taufkirchen, G
DAKO Fast-Red	DAKO, Hamburg, G
DC Protein Assay Kit	Bio-Rad, Munich, G
DNA Blunting/Ligation Kit	TAKARA BIO. INC, Japan
Gel Extraction Kit	Qiagen, Hilden, G
Human IFNγ ELISA Set	Becton Dickinson, Heidelberg, G
In Vivo Capture Assay for Mouse IFN-γ	Becton Dickinson, Heidelberg, G
Micro Protein Determination	Sigma, Taufkirchen, G
Mouse IFNγ ELISA Set	Becton Dickinson, Heidelberg, G
Plasmid Mini/Maxi Preparation Kit	Qiagen, Hilden, G

TitaniumTM One-Step RT-PCR Kit	Clontech, Heidelberg, G

C BUFFERS

BUFFER	INGREDIENTS
Annealing buffer	10 mM Tris, pH 7.5-8.0, 50 mM NaCl, 1 mM EDTA
Blocking buffer (IHC)	10% FCS, 1 x PBS, 0.1% NaN_3
Chloroform/Isoamyl alcohol	Chloroform (29 ml), Isoamylalcohol (1 ml)
Diethylpyrocarbonate (DEPC) water	500 µl DEPC, 500 ml Aqua dest.
Ethidium bromide	10 mg ethidium bromide/ml A.dest
Gel buffer concentrate/500ml	181.5 g Tris, 1.5 g SDS, pH to 8.45 w/ HCl
LB medium	10 g NaCl, 5 g Yeast extract, 10 g trypton, 1L aqua dest
Lysis buffer for spleen	0.15 M NH_4Cl, 1 mM $KHCO_3$, 0.1 mM Na_2EDTA, pH 7.2
Lysis buffer for mouse tail biopsies	100 mM Tris-HCl, pH 8.5; 5 mM EDTA, pH 8; 0.2% SDS, 200 mM NaCl
PBS-T	PBS containing 0.05% Tween-20
1x SDS PAGE buffer	24 g Tris base, 115.2 g glycine, 20 ml 20% SDS, H_2O to 4 litres
SOC-medium	2% Bactotrypton, 0.5% Bacto-yeast extract, 10 mM NaCl, 2.5 mM KCl, 10 mM $MgCl_2$, 10 mM $MgSO_4$, 20 mM Glucose
TAE (50x)	242 g Tris, 57.1 ml concentrated acetic acid, 100 ml EDTA pH8; 1 L H20
TE buffer (DNA dilution buffer)	100 mM Tris-HCL, 5 mM $MgCl_2$, pH 7.6 at 16°C

D ANTIBODIES

ANTIBODIES	ISOTYPE	COMPANY
Rat anti-mouse CD31, (390)	Rat IgG2a, κ	Becton Dickinson, Heidelberg, G
Rat anti-mouse Interferon gamma (XMG1.2, F1, XMG6, R4-6A2-Biotinylated).	Rat IgG1	Abcam, Cambridge UK, Becton Dickinson, Heidelberg, G
Rat anti-mouse Heparan sulphate (A7L6)	Rat IgG2a, κ	Abcam, Cambridge UK
Rat anti-mouse ERTR7	Rat IgG2a	DPC Biermann, Bad Neuheim, G
Rat IgG1 (isotype standard)	Rat IgG2a, κ	Becton Dickinson, Heidelberg, G
Rat IgG2a (isotype standard)	Rat IgG2a, κ	Becton Dickinson, Heidelberg, G
Rat IgG2b (isotype standard)	Rat IgG2a, κ	Becton Dickinson, Heidelberg, G
Goat anti-rat FITC	Goat IgG	Abcam, Cambridge UK
Goat anti-rat Texas Red	Goat IgG	Abcam, Cambridge UK
Goat anti-rat Alkaline Phosphatase	Goat IgG	Dianova GmbH, Hamburg, G
Goat anti-rat Horse Radish Peroxidase	Goat IgG	Dianova GmbH, Hamburg, G
Goat anti-rabbit Alkaline Phosphatase	Goat IgG	Dianova GmbH, Hamburg, G
Rabbit anti-mouse Collagen I	Rabbit IgG	Abcam, Cambridge, UK
Rabbit anti-mouse Collagen II	Rabbit IgG	Abcam, Cambridge, UK
Rabbit anti-mouse Collagen III	Rabbit IgG	Abcam, Cambridge, UK
Rabbit anti-mouse Collagen IV	Rabbit IgG	Abcam, Cambridge, UK

E EQUIPMENT

PRODUCT	COMPANY
96 well cell culture plates (flat or round bottom)	Corning Costar, Bodenheim, G
96 well breakaway plates (flat bottom)	Corning Costar, Bodenheim, G
Cell culture flasks (T-25, T-75, T-150)	TPP, Trasafingen, Switzerland

CELLine™ system	Integra-Bioscience, Fernwald, G
Centrifuge tubes (15 ml, 50 ml)	BD Falcon, Heidelberg G
Disposable cuvettes	Roth, Karlsruhe, G
Disposable syringes (25 ml, 10 ml, 5 ml, 1ml)	Braun, Mesungen, G
Eppendorf tubes (2 ml, 1.5 ml, 0.5 ml)	Eppendorf, Hamburg, G
FACS tubes	Becton Dickenson, Heidelberg G
Filter (0.2 μm, 0.45 μm)	Schleicher and Schüll, Dassel, G
Needles (0.8 x40 bwz. 0.4 x20 mm)	Sanimed, Berlin, G
PAP™ pen	DAKO,Hamburg, G
Petri-dishes (10 cm Diameter)	Greiner, Solingen, G
Pippette tips	Roth, Karlsruhe, G
Quartz cuvettes	Hellma, Müllheim,Baden, G
Scapel	NeoLab, Heidelberg, G
Scissors	Roth, Karlsruhe, G
Sieve (40 μm)	Becton Dickinson, Heidelberg, G
Superfrost slides	Roth, Karlsruhe, G
Sterile glass pippettes	Brand, Wertheim, G
Sterile pipettes (5, 10, 25 ml)	Costar, Bodenheim, G
Tweezers	Roth, Karlsruhe, G

F MACHINERY

MACHINE	**COMPANY**
Bio-Freezer (-80°C)	Forma Scientific, Cotech, Berlin, G
Centrifuge 3K12	Sigma, Taufkirchen, G
Centrifuge 5415C	Eppendorf, Hamburg, G
Centrifuge RT 6000D	Sorvall, Langenselbold, G
Confocal LSM 510	Zeiss, G
Counter	Mitutoyo, Neuss, G
Electrophoresis chamber for gels	Bio-rad, München, G
Electroporation machine	Amaxa, Köln, G
ELISA reader MR 5000	Dynatech, Berlington, USA

FACSCalibur flow cytometer	Becton Dickinson, Heidelberg, G
Fluorescent image analyser FLA-5000	FujiFilm, Dusseldorf, G
Frost free fridge	Labotect, Göttingen, G
Gene ray UV-photometer	Biometra, Göttingen, G
Haemocytometer	Roth, Karlsruhe, G
Liquid nitrogen tank	Messer Griesheim, Griesheim, G
Lysis machine	Coulter, Krefeld, D; Bector Dickinson, Heidelberg, G
Microscope Leitz DM IL	Leica, Wetzlar, G
Olympus BX51	Olympus, Hamburg, G
PCR machine	Biometra, Göttingen, G
pH meter	Hanna Instruments, Kehl/Rhein, G
Pippetes (single or multichannel)	Eppendorf, Hamburg, G
Print-Scale-Timer BF2306P	Ortec, Meerbusch, G
Scales	Sartorius, Göttingen, G
Spectrophotometer UV-160A	Shimadzu, Berlin, G
Sterile bench	BDK, Sonnbuhl, G
Thermomixer	Eppendorf, Hamburg, G
Ultracentrifuge	Beckmann, Krefeld, G
Vortex	Janke & Kunkel IKA-labortechnik, Staufen,G
Wallac-Wizard-Gamma counter 1470	Perkin Elmer, Jügesheim, G
Waterbath	GFL, Burgwedel, G

2.2 METHODS

2.2.1 CELL CULTURE

A INCUBATION

All cells were incubated in a 5% CO_2 oven at 37°C. All cells and cell lines were processed in appropriate cell culture flasks and dishes.

B ADHERENT CELL CULTURE

When the cell monolayer (TS/A) had reached 80% confluency the cells were passaged. Essentially, the culture medium was removed and cells washed with PBS. Cells were treated with 0.3% Trypsin/2.7 mM EDTA diluted in PBS to cover the monolayer. After a 5 minute incubation period at 37°C the cells had detached and were transferred to a tube for centrifugation (5 min at 1200 rpm). The supernatant was discarded and cells were resuspended in medium or frozen for storage.

C SUSPENSION CELL CULTURE

Semi-confluent cell cultures (J558L, J558L-IFN-γ or XMG6) were split and transferred to new medium. This process involved centrifuging the cells for 5 minutes at 1200 rpm before splitting or freezing for storage.

D COUNTING AND VIABILITY

10 µl of cell suspension was added to 90 µl of trypan blue and thoroughly mixed. After incubation at room temperature for 2 minutes, trypan blue excluded cells were considered viable and counted using a cell counting chamber (haemacytometer). The cell concentration is then determined by the following equation:

$$\text{Cell number} \times \text{dilution factor} \times \text{total volume} \times 10^4$$

E FREEZING AND THAWING

Cells that had reached 80% confluency in a T-75 cell culture flask were centrifuged and pelleted. They were washed in PBS and counted. After further centrifugation, the new pellet was then resuspended in a solution of 10% DMSO and 90% FCS so that $1x10^7$ cells per 1 ml could be frozen slowly to –80°C. For long term storage cells were transferred to a liquid nitrogen tank. When aliquots were required, cells were defrosted in a 37°C water bath and then resuspended in 5 ml of medium.

F ANTIBODY PRODUCTION

The hybridoma XMG-6 produces a neutralising anti-IFN-γ monoclonal antibody. INTEGRA CELLine CL1000 enables high cell culture densities and consequently augmented concentrations of antibody via membrane technology. The lower chamber was inoculated with 25 x 10^6 cells in 15 ml of complete DMEM supplemented with 10% FCS. The upper nutrient compartment contained complete medium without serum. When harvesting the lower chamber for antibody, 7.5 ml of mixed cell suspension was removed and replaced with 7.5 ml of fresh complete medium. The harvest supernatant, which contained the antibody was centrifuged for 15 min at 12000 rpm. The pellet was discarded and the supernatant stored until purified by HPLC. Cultures were harvested every three days for 6-8 weeks.

2.2.2 *IN VIVO* EXPERIMENTS

A TUMOUR CELL INJECTION AND *IN VIVO* TREATMENT

J558L, J558L-IFN-γ, TS/A and plasmid transfected tumour cells were injected subcutaneously in the left abdominal region of BALB/c IFN-γ competent or deficient mice at a concentration of 1 x 10^6 – 5 x 10^6 cells per 0.2 ml of PBS. At day 11 mice were treated with 15 mg/kg Cyclophosphamide (Cy) in Dulbeccos PBS. Injections of Cy were administered intraperitoneally (i.p). Tumour size was measured by a caliper and determined as the mean of the largest diameter and the diameter at right angle. Tumours had an average size of 1 cm in diameter or approximately 0.63 grams, 11 days after injection as previously determined by Ibe and coworkers, 2001. Tumour rejection was defined as complete regression after treatment and the absence of recurrent tumour for the entire follow up period (60 days).

B NEUTRALISATION

To neutralize the IFN-γ activity *in vivo*, BALB/c mice were i.p. injected with 1 mg of purified XMG6 (rat anti-mouse IFN-γ mAb) in 0.5 ml D-PBS 1 day before tumour cell injection. As control, another group of mice were injected with affinity purified total Rat-IgG (1mg/mouse).

C BONE MARROW CHIMERAS (BMC)

IFN-γ competent and deficient mice were separated one day before irradiation. On the day of transfer five mice of each subset were euthanised and the bone marrow extracted from the femurs. The bone marrow of one donor mouse was used to reconstitute four to five recipient mice. To isolate the bone marrow, the ends of the femurs were cut off and the bone marrow was flushed out with serum-free DMEM using a 25-gauge needle attached to a 1ml syringe. The bone marrow was dispersed into a single cell suspension, and debris and cell clumps were removed by filtration through a 40 μm filter. Typical yield from two femurs was between 1 and 1.5 x 10^7 cells. Recipient mice were irradiated on the day of transfer with 10 Gy and subsequently injected intravenously with 0.2ml bone marrow cells from a 10^7 cells/ml bone marrow cell suspension. Mice were monitored for 3 months and treated with Borgal intermittently throughout that time period. After which the success of the chimerism was determined by PCR of both blood and tail DNA. Mice were then injected with J558L tumour cells and treated as above.

D *IN VIVO* CINCINNATI CYTOKINE CAPTURE ASSAY

Principle: Normal or experimentally treated mice are injected with a biotin-labelled cytokine-binding monoclonal antibody. This allows the target cytokine, which normally has a very short half-life, to accumulate *in vivo* for a defined period of time (2-72 hours) as a soluble cytokine-anti-cytokine antibody complex. This complex increases the cytokines subsequent cytokine measurement because it inhibits the cytokines utilisation, degradation or excretion. The level of *in vivo* captured cytokine present in serum is measured using ELISA with a monoclonal antibody directed against a different epitope.

Tumour bearing IFN-γ wild type mice treated with or without Cy treatment were injected i.p. with 10 μg of a no azide/low endotoxin biotin-conjugated anti-mouse IFN-γ antibody in 200 μl of sterile PBS. Blood was collected 24 hours later and allowed to clot for 30-60 minutes. Samples were centrifuged for 10 minutes at 4°C at 4000 rpm. Serum was removed and aliquoted for immediate ELISA and storage at –80°C.

2.2.3 IMMUNOHISTOCHEMISTRY

A LIGHT MICROSCOPY

Principle: Detection of protein in tissues can be determined by a specific antibody, which is chemically coupled to an enzyme that converts a colourless substrate into a coloured product *in situ*. The localised deposition of the coloured product where antibody has bound can be directly observed under a light microscope. The antibody binds stably to its antigen, allowing unbound antibody to be removed by thorough washing.

Mice were inoculated with tumours and 10 days later they were removed, embedded in OCT and frozen in liquid nitrogen. Blocks were mounted and 4 μm sections were cut using a Micron cryostat. Sections were allowed to dry on Superfrost slides for two hours and either used directly or stored at –80°C long term. Sections were fixed in acetone and sections were circled with a PAP^{TM} pen. They were placed in a humid chamber and 50-75 μl of blocking buffer was added to each section for 30 minutes to 1 hour at room temperature. After removal of the blocking buffer, sections were incubated with 5 μg/ml dilution of primary antibody (50-75μl per section) for 1 hour at room temperature or overnight at 4°C. Slides were washed with blocking buffer and then the (7 μg/ml) secondary antibody (50-75 μl per section) applied and incubated for 1 hour at room temperature. The enzyme substrate alkaline phosphatase (AP) or diaminobenzidine (DAB) was used according to the manufacturers instructions and left on the sections for 5-10 minutes. After thorough rinsing with water, sections were washed in haematoxylin counterstain for 10 minutes. After a further wash, slides were dried carefully and sealed using Kaisers Gelatine for analysis using an Olympus BX51 microscope.

B FLUORESCENT MICROSCOPY

Fluorescent antibodies can also be responsible for the visualisation of certain structures within tissue sections. However, when two or more structures are visualised, fluorescence is the most appropriate and safe method. Sections were not fixed. The slides were blocked with (50-75μl per section) the appropriate buffer for 1 hour. They were washed and incubated for 1 hour with 50-75μl per section primary heparan sulphate unconguated antibody (5 μg/ml). A secondary anti-Rat Texas red (615 nm emission) was applied at 5 μg/ml was applied for 1 hour. After washing with blocking buffer, 100 μl of an anti-IFN-γ-FITC conjugated antibody (100 μg/ml) was incubated for 48-72 hours in the dark at 4°C. After washing slides were sealed with Gel/mount (Vector Laboratories).

2.2.4 LASER SCANNING CONFOCAL MICROSCOPY

Principle: The confocal microscope uses computer-aided techniques to produce ultra-thin optical sections of tissue. Confocal images have high resolution without the need for elaborate sample preparation. The resolution of the confocal can be further increased using low-intensity illumination so that two photons are required to excite the fluorochrome. A pulsed laser beam is used, and only when it is focused into the focal plane of the microscope is the intensity sufficient to excite fluorescence. By this the fluorescence emission itself can be restricted to the optical section.

2.2.5 *IN VIVO* MATRIGEL BINDING ASSAY

Matrigel was thawed to 4°C and 0.2 ml was injected subcutaneously into the belly of IFN-$\gamma^{-/-}$ or IFN-$\gamma^{+/-}$ mice. After a 5 day rest period, mice were treated with human IFN-γ. After 1-24 hours the gel was extracted from the mouse and homogenised with 500 μl cold PBS. A diluted sample (100 μl sample: 1 ml PBS) was then analysed for IFN-γ by ELISA.

2.2.6 ENZYME LINKED IMMUNOSORBENT ASSAY (ELISA)

Principle: A typical sandwich ELISA involves a specific capture antibody, samples, a biotinylated detection antibody, a streptavidin-HRP conjugate (SAV), chromogen and stop solution. Antigen will bind to the immobilised capture antibody and to the biotinylated detection antibody. The SAV binds to the detection antibody to complete the sandwich. A substrate solution is added, acted upon by the enzyme conjugated SAV, and effects a colour change. The intensity of the colour change is proportional to the amount of antigen in the original sample.

A IFN–γ ELISA

Murine interferon gamma produced by J558L-IFNγ cells or murine spleens after stimulation with ConA were determined using the mouse IFN-γ kit. Essentially, supernatant samples from murine cell culture were purified by filtration so that no debris was present.

Human interferon gamma was determined using a human IFN-γ kit. Human samples were prepared by washing and mashing matrigel, isolated from mice, in cold D-PBS and filtering the supernatant with 40μm filters.

Serum samples isolated from Cy treated and untreated mice for the *in vivo* capture assay were analysed using the BD *In Vivo* Capture ELISA.

Standards and samples were added to 96 well plates that had been treated with the respective capture antibody and were processed according to manufacturer's instructions. The plates were read at 450 nm with a λ correction at 570 nm.

2.2.7 CONSTRUCTION OF TUMOUR CELLS EXPRESSING MC-2 PEPTIDE

A PLASMID CONSTRUCTION

PsecTag2 is a 5.2 kb expression vector, which was selected from Invitrogen Life Technologies to produce high-level stable expression in mammalian cells. Proteins expressed

from pSecTag2 are fused at the N-terminus to the murine Ig κ-chain leader sequence for protein secretion and at the C-terminus to the c-myc epitope and six tandem histidine residues for detection and purification.

Due to the presence of the human cytomegalovirus intermediate-early promoter/enhancer (P_{CMV}) the plasmid becomes methylated *in vivo* and subsequently shuts down. Hence, the substitution of another promoter was required. Therefore, P_{CMV} was substituted with the human elongation factor 1α (EF-1α) promoter, which was removed from the PEF/Bsd vector (Invitrogen Life Technologies) (4.3 kb). This promoter remains functional within the mouse and thus is optimal to drive the constructed plasmid and the production of the MC-2 peptide.

B FRAGMENT DETERMINATION

The P_{CMV} fragment was excised from pSecTag2 using the BglII restriction site and NheI. Two fragments resulted, 883bp and 4276bp, the latter being required. P_{EF-1} was excised using the restriction enzymes NheI and Acc65I to create 2 fragments of 1291bp and 3013bp. The former was essential for ligation to create a functional plasmid (Figure 28-Appendix).

In order to identify the required fragments, digestions were subjected to gel electrophoresis and run on 1.2% Nusieve GTG Agarose. DNA was eluted from the gel using QIAquick gel extraction kit according to the manufacturers instructions using a vacuum manifold. Essentially, the kit allows recovery of DNA and the removal of contaminants by incubating the gel in a buffer containing guanidine thiocyanate and adsorbing the DNA to a silica-membrane on the spin column. Guanidine thiocyanate solubilizes the DNA, denatures proteins and acts as a pH indicator to ensure optimal adsorption.

C BLUNTING

DNA blunting took place using the DNA blunting kit from TAKARA according to the manufacturer's instructions. This converts the 3' and 5' protruding ends of DNA fragments to blunt or flush ends. To deactivate the T4 polymerase the mixture was vigorously vortexed and then diluted to a concentration of 1μg/ 50 μl in TE buffer.

D DEPHOSPHORYLATION

In order to minimise self-circularisation/ligation the plasmid fragment was dephosphorylated. Shrimp alkaline phosphatase was used as, unlike the calf enzyme, it is completely and irreversibly inactivated by Tris-buffers at pH 8.0-8.5 by simply heating for 15 minutes at 65°C. Using 3 μl of DNA termini, 0.2 μl of phosphatase at 37°C for 1 hour was the minimum effective amount.

E LIGATION

The DNA fragment for insertion should be present in 5 fold molar excess relative to the vector DNA. Ligation was carried out according to manufacturer's instructions, TAKARA BIO INC. Essentially, buffer containing T4 DNA Ligase enabled sufficient ligation efficiency to be achieved at 25°C for 3 minutes. The resultant solution was aliquoted for bacterial transformation.

The remaining ligation DNA was extracted by phenol/chloroform 1:1. Then 1/10 volume of sodium acetate (3 M) and 2.5 volumes of ethanol were added. The solution was left at –20°C overnight and the following day it was centrifuged at 14000 rpm for 30 minutes at 4°C. The supernatant was removed and the precipitated DNA kept at -80ºC for long term storage.

F TRANSFORMATION

UltraMAX™ DH5α-FT™ (Invitrogen) competent cells were used for generation of the plasmid DNA. One of the easiest ways to get large amounts of DNA is to place the desired DNA into bacteria, grow and harvest the bacteria, and subsequently isolate the DNA. Transformation efficiency of the ligated circular DNA into competent cells could be improved by the addition of one tenth the volume of Transformation Enhancer provided by TAKARA Bio Inc. before transformation. 100 μl of cells and 10 ng of ligation DNA were then incubated on ice for 30 minutes. The cells were heat shocked in a water bath at 42°C and placed on ice for 2 minutes. SOC medium (Super optimal broth plus glucose) was added and the resultant

1ml mixture was placed at 37°C for one hour. The solution was then divided and spread on LB agar plates.

2.2.8 PLASMID PREPARATIONS

A MINI AND MAXI PREPARATIONS

Colonies from the LB transformation plates were used to inoculate 5 ml of LB medium (mini) or 200 ml of LB medium (maxi). These cultures were incubated at 37°C overnight. 750 µl of bacteria was mixed with 150 µl glycerol to form stocks which were stored at –80°C. The cultures were then centrifuged and the resultant pellet was treated according to the manufacturer instructions for QIAprep Spin Miniprep Protocol (using a vacuum manifold) or Qiagen plasmid maxi protocol, respectively.

B ENZYME DIGESTION

In order to ascertain whether the transfer of the EF1-α promoter had correctly inserted into the pSecTag2 vector, 3 µl of plasmid from the mini-preps were digested with 10 Units of each enzyme for 2h at 37°C. Digestion was with either AgeI/BamHI for fragment sizes of 1236bp/4331bp or BglII/BamHI for fragment sizes of 748bp/4819bp. To check the resulting fragments 5 µl of sample was run on a 1% agarose electrophoresis gel for 1 hour and visualised under a 354 nm UV-light.

C OLIGONUCLEOTIDE ANNEALING AND INSERTION INTO PSECTAG2-EF1α

The murine IFN-γ oligonucleotides (34bp) (LRKRKRSR – MC-2 insert) or the neutral oligonucleotide (34bp) were resuspended in annealing buffer. Equimolar volumes of oligonucleotides were mixed and placed in tubes within a thermal cycler. A program was constructed to heat to 95ºC and remain at 95ºC for 2 minutes and then ramp cool to 25ºC over a period of 45 minutes. Tubes were spun in a microfuge to draw all moisture from the lid. Later unused samples were stored at 4ºC.

PSecTag2-EF1α was cut using the EcoR1 and BamH1 restriction sites between the T7 and TAA region (Stop codon). This created two fragments of 16bp and 5551bp. As the oligonucleotide had been engineered to have the corresponding ends for insertion into the vector, ligation and transformation was carried out as in 2.2.7E/F. Plasmids were prepared according to protocol 2.2.8A/B. These plasmids were intentionally misaligned so that the excreted peptide fragment did not contain the Myc/HIS-Tag. A realigned plasmid was created by cutting PSecTag2-EF1α containing the MC-2 oligonucleotide with EcoR1, and filling with Klenow before re-ligation (Figure 6).

INSERT	HIS/MYC TAG	COMMON NAME
Murine IFN-γ (128-135)	Yes	J558L-pMC2-Tag
Murine IFN-γ (128-135)	No	J558L-pMC2-NoTag
Alanine^{8}	No	J558L-pAlanine^{8}-NoTag
None	Yes	J558L-pTag

Table 1: Components within the plasmid transfected cell lines.
All plasmids contained the EF1-α promoter and the Igκ-leader sequence responsible for extracellular excretion of the peptide fragment.

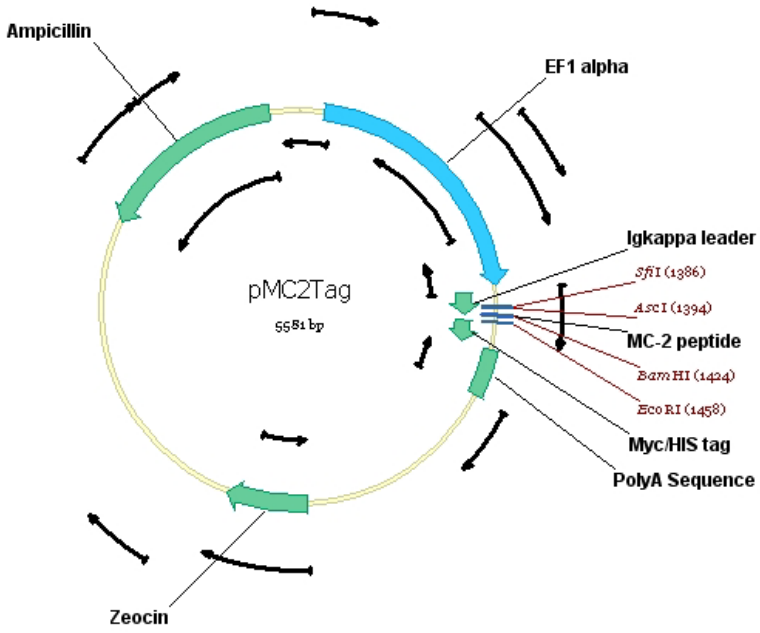

Figure 6: Arrangement of the completed plasmid. In this case the plasmid can secrete the murine IFN-γ fragment responsible for ECM binding The Myc/HIS-Tag was optional. For more detailed plasmid map and sequences review Figures 28 and 29 (Appendix).

D PCR OF MC-2 INSERT

Principle: A powerful technique for amplifying small fragments of the genome is provided by PCR. A preparation of DNA is denatured by heat and the single strands are annealed with two short primer sequences that are complementary to sites on the opposite strands on either the side of the target region. DNA polymerase is used to synthesise a single strand from the 3'-OH end of each primer. The entire cycle can then be repeated by denaturing the preparation and starting again. The number of copies of the target sequence grows exponentially. In practice, it doubles with each cycle until reaching a plateau at which more primer-template accumulates than the enzyme can extend during the cycle; then the increase in target DNA becomes linear. For all PCR's the heat stable DNA-polymerase from *Thermus aquaticus* (*Taq*-Polymerase) was used. It remains stable up to 95°C.

To ensure the correct insertion of the LRKRKRSR (MC-2) fragment into the plasmids PCR was carried out. The temperature for annealing of the MC-2 primers had been determined by the producers TIB® MolBiol to be around 66°C. However, when the PCR was run the required band was not clear. Therefore, a temperature gradient PCR was run. It follows the same principle as a normal PCR except that across the plate the annealing temperature in each well increases in 0.8°C increments. It was determined that the strongest band for the MC-2 primers occurred at a temperature of 58°C.

Conditions using the MC-2 primers for the amplification of the MC-2 fragment from plasmid and cellular DNA were: 94°C for 3 minutes; amplification by 40 cycles of 94°C for 40sec, 58°C for 40sec, 72°C for 40sec; elongation for 10 minutes at 72°C.

E SEQUENCING

To confirm the results of the PCR reactions, the sequences of pSecTag2-EF1α and the plasmids containing the inserts, were determined by Invitek, Berlin.

2.2.9 TUMOUR CELL TRANSFECTION

J558L were transfected using the Gene Pulser® Electroporator and Electroprotocol from Bio-Rad. The tumour cells were suspended in RPMI medium with 10% FCS at a concentration of

$1x10^7$ cells/ml. 10 µl plasmid DNA (1 mg/ml) was suspended in TE buffer was added to 800 µl of cells. A cuvette gap of 0.4 cm was used and the voltage maintained between 0.2 to 0.4 kV. A field strength of 0.5 to 1 kV/cm and the capacitor at 960 µF was set. Cells were then transferred to 5 ml RPMI-Medium in a T-25 flask and incubated overnight. The following day 1.5 mg/ml Zeocin was added to select for transfected cells.

2.2.10 ISOLATION OF GENOMIC DNA

Genomic DNA was isolated from 0.5 cm tail biopsies, blood and plasmid transfected tumour cells for genotyping and analysis. Essentially samples were incubated in 700 µl lysis buffer with 17.5 µl 20 mg/ml Proteinase K at 55°C overnight. A 0.5 ml solution of phenol-chloroform-isoamyl alcohol (25:24:1) was added and the tube mixed well by repeated inversion. After centrifugation at 14000 rpm for 5 minutes the aqueous phase was transferred to a fresh tube and 0.5 ml chloroform-isoamyl alcohol (24:1) was added and the tube mixed. The aqueous phase was again transferred to a fresh tube and 100% volume isopropanol added. The tube was centrifuged and the supernatant removed. The pellet was then washed with 1ml 70% ethanol and later resuspended in 50 µl TE buffer.

2.2.11 ISOLATION OF RNA

Cells transfected with the 4 different plasmids were subject to total RNA isolation by TRIzol™ reagent. RNA was prepared when $1x10^7$ tumour cells were pelleted and resuspended in 1ml of TRIzol™. 0.2 ml chloroform per 1 ml TRIzol™ was added and the tube vortexed for 15 seconds. Samples were then centrifuged for 10 minutes at 14000 rpm at room temperature. The aqueous phase was transferred to a fresh tube and 0.5 ml of isopropanol added and mixed by inversion. The sample was then centrifuged again at 12000 x g but this time at 4°C for 15 minutes. The RNA was pelleted, the supernatant decanted, and 1 ml of ethanol added to wash the pellet. Once the ethanol was removed the pellet was air-dried and resuspended in RNAse-free DEPC water.

The concentration of RNA was determined by diluting the recovered RNA 1:250 in a quartz curvette for spectrophotometric analysis at 260 nm. An absorbance of 1 indicates around 40

µl/ml RNA. To check the purity of the RNA a measurement at 280 nm was also carried out. The quotient of the measurement between 260 nm and 280 nm was evaluated. An OD_{260}/OD_{280} greater than 1.6 indicated a clean preparation. The RNA was stored at –80°C.

2.2.12 RT-PCR

RT-PCR is a technique used for measuring gene expression in tissues and cultured cells. Traditionally, RT-PCR is performed in two steps: a first strand cDNA synthesis step using reverse transcriptase, followed by a PCR step using a thermostable DNA polymerase. However, we used a one step procedure according to the manufacturer's instructions. The TITANIUM™ One-Step RT-PCR Kit allows cDNA synthesis and PCR to be performed in a single optimised buffer with a single enzyme mix.

2.2.13 PROTEIN DETERMINATION

The concentration of protein in the samples from antibody production and tumour cells were determined by the Bio-Rad DC Protein Assay, which is a colorimetric assay which functions similarly to the Lowry assay.

Principle: The protein in the sample reacts with copper tartrate solution and Folin reagent. Colour development is primarily due to the amino acids tyrosine and tryptophan and to a lesser extent cystine, cysteine and histidine. Proteins effect a reduction of the Folin reagent by the loss of 1, 2 or 3 oxygen atoms, thereby producing one or more of several reduced species which have a characteristic blue colour with a maximum absorbance at 750 nm and a minimum absorbance at 405 nm. Protein was determined by the microplate assay protocol, essentially 5 µl of sample and standard was incubated with 25 µl of reagent A (alkaline copper tartrate) and 200 µl of reagent B (dilute Folin reagent) and left for 15 minutes to develop. The plate was then measured at 750 nm.

2.2.14 IODINE^{125} LABELLED IFN-γ EXPERIMENTS

Iodine 125 is used to iodinate proteins on the cell surface and/or intracellular proteins. It is a moderately volatile radioisotope, which emits relatively weak gamma radiation as it decays. It is commonly used as a radiotracer in life sciences research as well as in clinical applications.

Principle: IODO-BEADS® Iodination Reagent is a N-chloro-benzenesulfonamide (sodium salt) immobilsed on nonporous, polystyrene beads. Radioactive I^{125} can be incorporated into protein by either enzymatic or chemical oxidation. IODO-BEADS is milder than the traditional chloramine-T, generates sufficient radioactive iodine, and does not require a reduction step, which makes it advantageous for maintaining biological activity of proteins. IODO-BEADS allows easy separation of the reagent from the reaction mixture and allows for a two-phase system, a more easily controlled reaction, which limits direct contact of the oxidant with the protein.

A PROCEDURE FOR PROTEIN IODINATION AND PURIFICATION

Just before use, one or more beads were washed with 500 µl of reaction buffer per bead. This wash step removes any loose particles and reagent. The beads were added to a solution of carrier-free NaI^{125} (approximately 1 mCi per 100 µg of protein) diluted in PBS and allowed to react for 5 minutes. The protein was dissolved or diluted in reaction buffer and added to the Eppendorf tube, which was allowed to react for 2-15 minutes. The bead was removed from the solution and the reaction subsequently stopped. The solution was then passed over D-Salt™ Desalting Columns to remove excess NaI^{125} or unincorporated I^{125} from the iodinated protein. The columns were equilibrated with 5 column volumes of PBS. The tip of the column was placed in a test tube and the sample applied. The sample entered the gel and the column stopped flowing. The tip of the column was placed in a new tube and a volume of buffer equal to the fraction volume was added. After the buffer entered the gel, the column was transferred to a new tube. This continued until the protein had emerged from the column.

B MEASURING THE COUNTS AND QUANTITY OF RADIOACTIVE PROTEIN

The counts of the extracted fractions were determined by the Print-Scale-Timer BF2306P.

Protein was visualised using a 12.5% SDS-PAGE gel to determine which fraction of the flow through from the columns contained iodinated protein. Gels were run at 100V for 60 minutes and then placed on a BIOMAX-MS film (Kodak) for 10 minutes. The film was then developed according to the manufacturers instructions.

The quantity of protein could be monitored by measuring the absorbance of each fraction at 280nm. The absorbance depends on the presence of tyrosine and tryptophan in the protein and this method is entirely advantageous as the sample can be recovered. The first peak in absorbance will generally emerge when 1 void volume of buffer has been added after the sample is applied. This peak is the protein. Molecules smaller than the exclusion limit of the gel (i.e., buffer salts) will emerge from the column in subsequent fractions. These fractions can be discarded after confirming that all fractions containing protein have been collected.

C IMMOBILISATION OF COLLAGENS AND MATRIGEL

The coating of microtitre plates and the calculation of coating efficiencies were performed as described previously (Somasundaram et al., 2000). Native collagens were immobilised on polystyrene microtitre plates at concentrations of 2μg/100μl/well for binding studies. Immobilisation was done with 50 mM ammonium bicarbonate, pH 9.6, overnight at 4°C followed by three washes with PBS, pH 7.4, with the exception of glycoproteins, which were coated in PBS. Matrigel from an Engelbrecht Holm Swarm sarcoma was pre-coated 20 minutes at room temperature and then overnight at 4°C with 114 μg/well solution in D-PBS. As 1-3% of Matrigel is made of heparan sulfate approximately 17 μg/ml coated the wells. Non-specific binding sites were blocked with PBS-T for 2 hours at room temperature.

For binding studies 0.1-10 ng of I^{125}-IFN-γ□□ in PBS-T was added to the collagen or matrigel coated wells and incubated for 2 hours at 4°C. Finally, after three washes in binding buffer, radioactivity bound to the coated wells was measured using a gamma counter.

For inhibition studies matrigel wells were incubated with either MC-2 peptide (1ng-1mg), supernatants from transfected tumour cell lines or buffer overnight at 4°C. They were washed with blocking buffer and then radioactive IFN-γ (7.5 ng/ml or $4x10^{-7}$ mol/L) was added to wells to incubate from 2h to overnight at 4°C. The supernatants were discarded and the wells washed three times with buffer (PBS-T). Bound IFN-γ was then was measured with a gamma counter.

D ANIMALS TREATED WITH I^{125}-IFN-γ

Adult female BALB/C interferon gamma competent and deficient mice were housed in the Nuclear Medicine facility of the Benjamin Franklin Clinic on a 12 hour light/dark cycle, with *ad libitum* access to food and water. After mice had grown J558L or transfected tumours over a 8-10 day period they were injected intravenously (iv) through the tail vein with 5 μg of IFN-γ containing counts between 100000 and 500000 cpm, depending on the success of protein iodination, as a tracer. Mice were sacrificed at selected times (1h, 24h, 72h after injection), and organs extracted (heart, lung, liver, spleen, kidney and tumour).

E MEASUREMENT OF THE ORGAN DISTRIBUTION OF I^{125}-IFN-γ

Samples of tissues, excised at the various time points after I^{125}-IFN-γ, were weighed and counted. For each organ the radioactivity per gram was calculated as a percentage accumulation of I^{125}-IFN-γ.

3 RESULTS

3.1 GENOTYPING INTERFERON GAMMA KNOCKOUT MICE

Mice with a non-functional IFN-γ gene were generated by Dalton and colleagues, 1993, and obtained from Jackson Laboratories (USA). Mice were created by replacing one normal IFN-γ allele with a defective allele in mouse embryonic stem cells. The targeting vector had a 2kb neomycin resistance gene inserted into exon 2, which introduced a termination codon after the first 30 amino acids of the mature IFN-γ protein. Mice appear to have no gross or histological abnormalities, and no alterations of splenic and thymic populations. Knock-out mice remain normal, healthy and fertile (Dalton et al., 1993). Thus, IFN-γ is not required for the development of the immune system but is essential for the immune response.

Mice were crossed heterozygote to homozygote. In order to correctly type the IFN-$\gamma^{+/-}$, BALB/c and IFN-$\gamma^{-/-}$ BALB/c mice by PCR, genomic DNA from the tail was prepared and the IFN-γ gene amplified. Mice that contained the neomycin resistance gene in exon 2 generated a PCR band of 320 bp, whilst mice with DNA for an intact IFN-γ gene produced a PCR band of 260 bp.

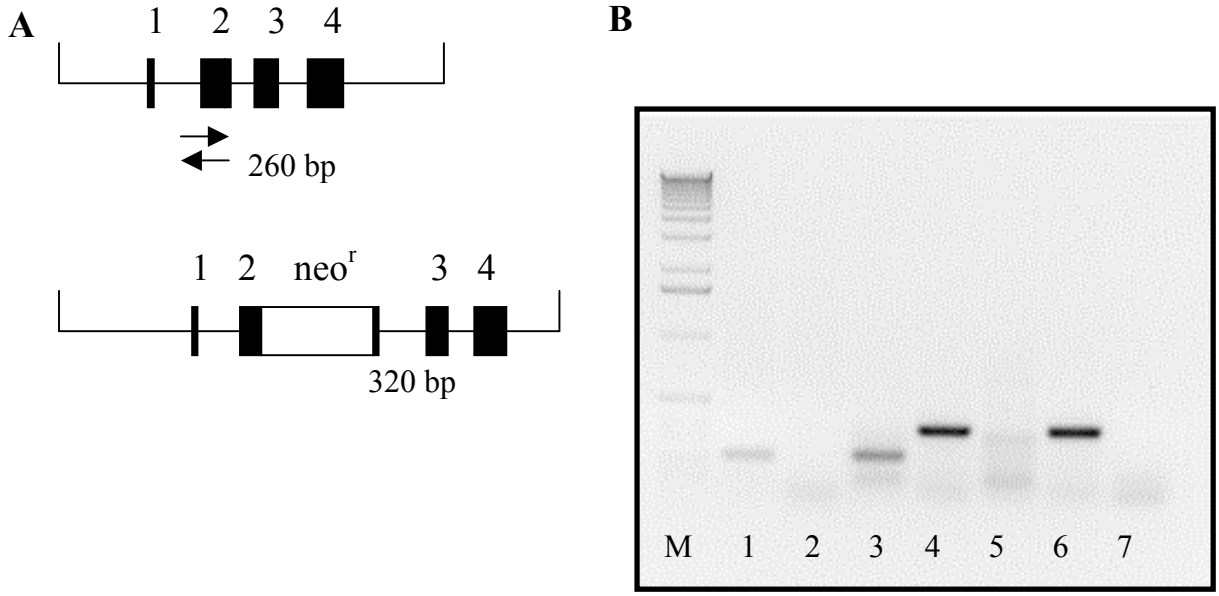

Figure 7: PCR analysis of genomic DNA for typing IFN-γ mice.
(A) IFN-γ gene structure on a genomic fragment. Primers were derived from exon 2. Insertion of the 2-kb neo^r gene into exon 2, meant new primers were derived from the neomycin gene. **(B)** IFN-γ gene 260 bp, neomycin disrupted gene 320 bp. Lane M Marker, Lanes 1-2 BALB/c mouse, Lanes 3-4 IFN-$\gamma^{+/-}$ mouse (both bands), Lanes 5-6 IFN-$\gamma^{-/-}$ mouse (neo band only), Lane 7 H_2O.

3.2 THE EFFECT OF INTERFERON GAMMA ON TUMOUR GROWTH

In several studies, IFN-γ has been associated with tumour rejection. To investigate this, the influence of IFN-γ produced by tumour cells rather than host cells was investigated. The J558L parental line had previously been transfected with a plasmid encoding IFN-γ. Subcutaneous injection of J558L-IFN-γ producing cells demonstrated that IFN-γ inhibited the outgrowth of the tumour in BALB/c mice whereas the parental cell line grew rapidly in immuno-competent hosts.

Effective neutralisation of IFN-γ is important to determine the role it plays when derived from the host. Therefore the ability of the neutralising antibody XMG6 was tested in a model where J558L cells were known to produce a specific concentration of IFN-γ (120ng/ml). In this experiment, 1mg/mouse of XMG6 (Isotype – Rat IgG1) was administered 1 day before tumour cell injection. From the kinetics of the growth curve in Figure 8, the antibody was capable of completely neutralising IFN-γ *in vivo* and allowed the transfected cells to grow with similar kinetics compared to the parental line.

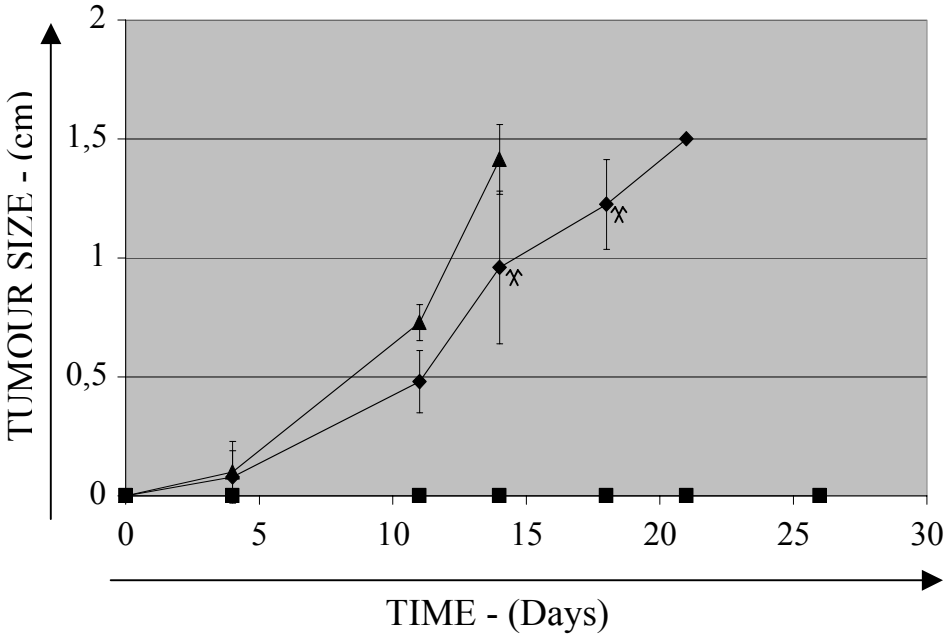

Figure 8: IFN-γ inhibits tumour growth.
BALB/c mice were inoculated with 1 x 10^6 J558L ( ) or 5 x 10^6 J558L-IFN-γ ( ) on day 0. Another group of BALB/c were neutralised for IFN-γ using 1mg/mouse XMG6 antibody on day -1 and then inoculated with 5 x 10^6 J558L-IFN-γ ( ) on day 0. Tumour growth was monitored over 30 days (n=5/group). Single experiment. NB: Indicates mouse removed from experiment.

3.3 CYCLOPHOSPHAMIDE INDUCES IFN-γ DEPENDENT REJECTION OF J558L TUMOURS

3.3.1 WILD TYPE MICE BUT NOT IFN-γ KNOCKOUTS CAN REJECT J558L TUMOURS.

The previous experiment demonstrated that IFN-γ inhibits tumour growth. Therefore, the role of IFN-γ in Cy-mediated tumour rejection was analysed. Under certain conditions cyclophosphamide can induce rejection through host cell modulation rather than direct tumouricidal activity. It was shown that T cell deficient mice were incapable of rejecting a solid tumour of J558L plasmacytoma cells, by this mode of treatment. However BALB/c mice, which were treated similarly with a single injection of 15mg/kg of Cy 9-11 days after tumour injection, rejected the tumour mass. Three days after Cy treatment, these tumours became severely necrotic in immunocompetent mice and were rejected within 10-20 days (Figure 9A).

Recently, it was demonstrated by Ibe and co-workers, 2001, that expression of IFN-γ–R on host cells but not tumour cells was required for Cy-mediated tumour rejection. Therefore, Cy was tested in a murine IFN-γ knockout model. The tumours grew similarly in this model, and mice were treated when tumours ranged between 0.6 - 1cm. 11 days after inoculation with J558L cells, the tumour was treated with Cy. IFN-$\gamma^{-/-}$ mice were unable to reject whereas IFN-$\gamma^{+/-}$ mice rejected tumours. The tumours of the IFN-$\gamma^{-/-}$ mice did appear to reduce slightly in size however, they eventually grew out aggressively (Figure 9B). All mice had succumbed to tumour burden by day 21 and had to be euthanized.

From histological stainings of J558L tumours in Cy treated IFN-$\gamma^{+/-}$ and IFN-$\gamma^{-/-}$ mice there appears to be rapid destruction of the endothelial vasculature (Figure 10). Approximately 24 hours after Cy treatment CD31 positive blood vessels in J558L tumours of IFN-$\gamma^{+/-}$ mice have become shorter and appear to be less densely arranged when compared to IFN-$\gamma^{-/-}$ tumour tissue. By 72 hours after Cy treatment tumour vasculature appears to be single dots with a few small vessels intact.

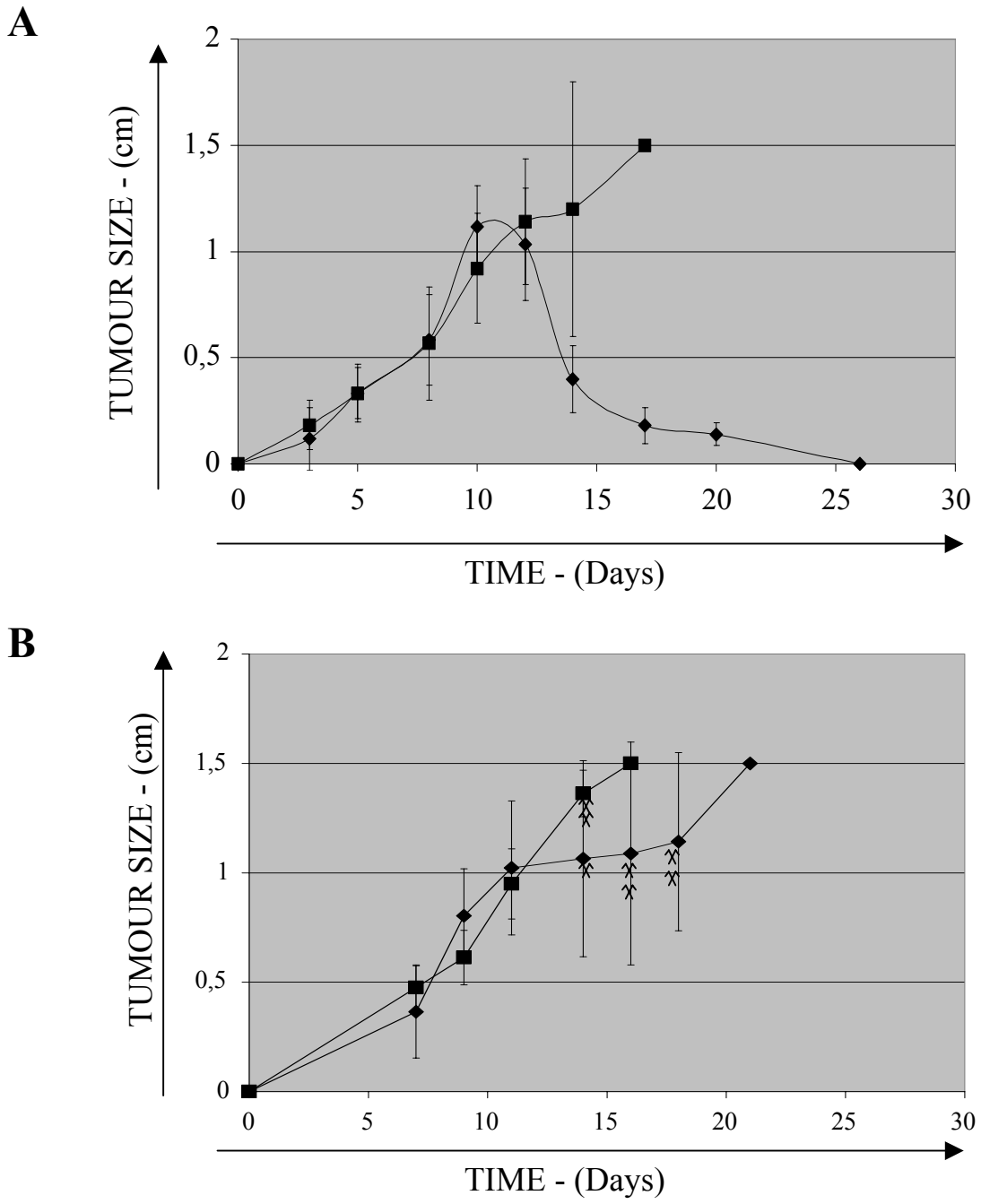

Figure 9: IFN-γ is required for Cy mediated tumour rejection.
Tumours were established by subcutaneous injection of 1x 10^6 J558L cells into mice. 11 days later, when tumours reached a size of around 1 cm in diameter, mice were treated intraperitoneally with 15 mg/kg Cy. **(A)** IFN-$\gamma^{+/-}$ mice (, n=10) with treatment, IFN-$\gamma^{+/-}$ mice (, n=10) which had not received Cy treatment served as controls. All Cy-treated BALB/c mice rejected the tumour. **(B)** IFN-$\gamma^{-/-}$ mice treated with Cy (, n=10). IFN-$\gamma^{-/-}$ mice treated with No Cy (, n=10). Representative of 3 experiments. NB. ^ Indicates mouse removed from experiment.

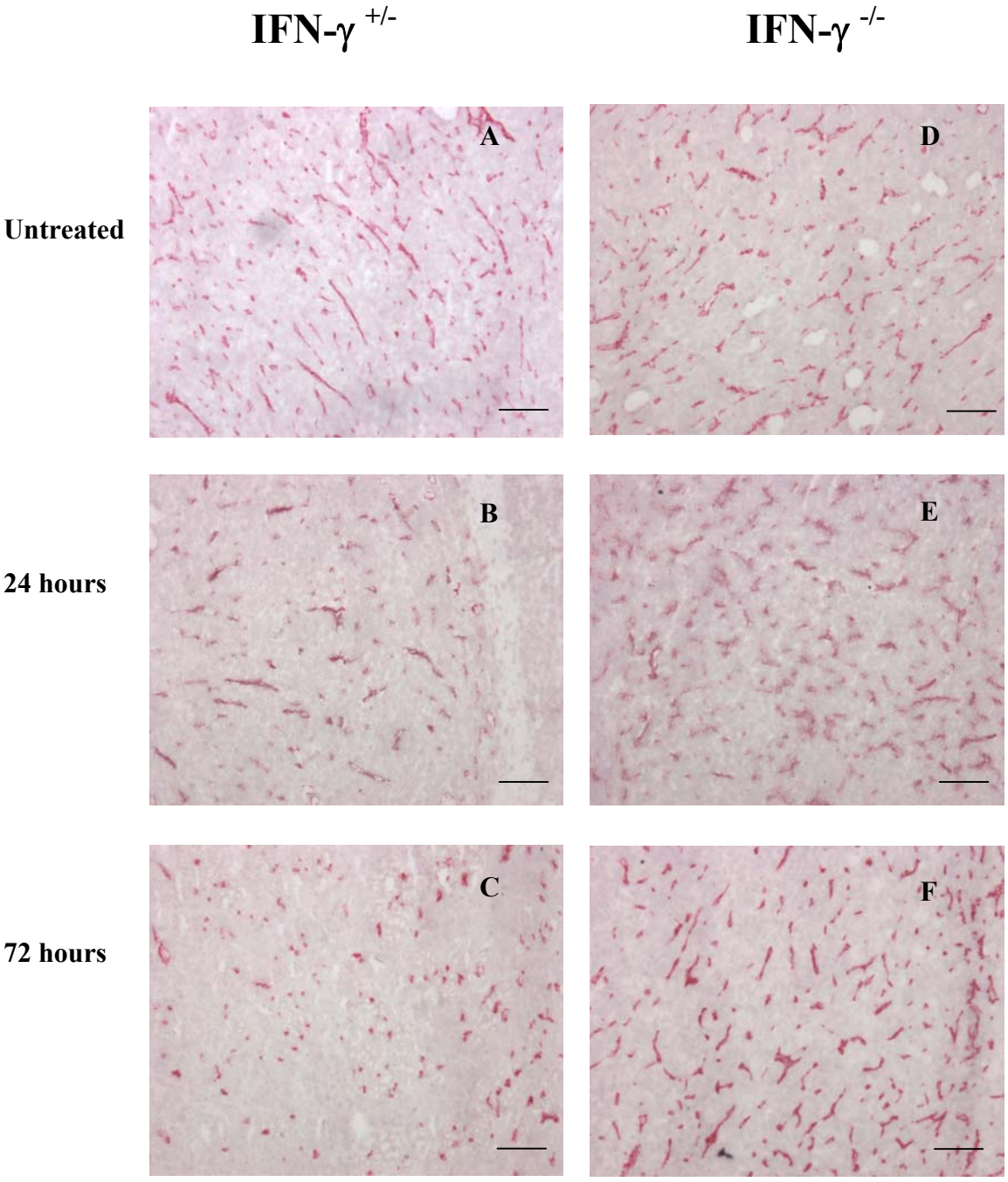

Figure 10: Cy induces IFN-γ dependent destruction of the vasculature. Tumours were established in IFN-$\gamma^{+/-}$ and IFN-$\gamma^{-/-}$ BALB/c mice by subcutaneous injection of 1 x 10^6 J558L cells. 11 d later, mice were injected intraperitoneally with 15 mg/kg Cy and tumours were excised before, 24 h, and 72 h after Cy treatment. Immunohistochemical analysis of tissue sections from IFN-$\gamma^{+/-}$ mice **(A–C)** and IFN-$\gamma^{-/-}$ mice (**D–F)** was performed with mAb CD31 **(A-F)**. Scale bar equals 100μm. A representative staining of tumours from 3 mice per group.

3.3.2 NEUTRALISATION OF IFN-γ PRODUCTION IN WILD TYPE MICE EFFECTS TUMOUR REJECTION.

Mice with targeted gene deletions, have a specific gene removed or inactivated. They are unable to produce the gene product throughout the life of the animal. There are significant advantages such as avoidance of inadequate dosing, specificity, affinity or penetration of drugs and the lack of response to exogenous antibodies and soluble receptors. However, the lack of clinical relevance arises from the absolute absence of the gene throughout the animals life and the possible indirect effects such as the over compensatory expression of other genes that can not be controlled.

The most effective way to validate the role of a particular cytokine in disease is by specific blockage of its activity in a complex model. This works as a temporary blockade of a specific signalling pathway. The results of the knockout model were confirmed by neutralisation of IFN-γ using the anti-IFN-γ antibody XMG6. The mAb antibody was prepared from hybridoma supernatant by the CELLine^{TM} system and purified by HPLC to generated 76 mg of XMG6 antibody.

The minimal neutralisation dose in which all J558L-IFN-γ producing cells grew in wild type mice had been previously established to be 1 mg/mouse of anti-IFN-γ mAb (Figure 8). Wild type mice were separated into groups of animals treated with (day -1 alone or day -1, day 5, day 10) and without XMG6 mAb. On day 0 all animals received 1x10^6 J558L tumour cells. Tumours in IFN-γ mAb treated animals grew with similar kinetics to the wild type untreated controls. At day 11 all groups were treated with cyclophosphamide (15 mg/kg) and the response monitored. Figure 11 demonstrates that neutralisation of IFN-γ prevents rejection of tumours. All mice that were not treated with cyclophosphamide from each group (n=3), including mice neutralised for IFNγ and injected with 1x10^6 J558L-IFNγ cells (n=9), grew out by day 22.

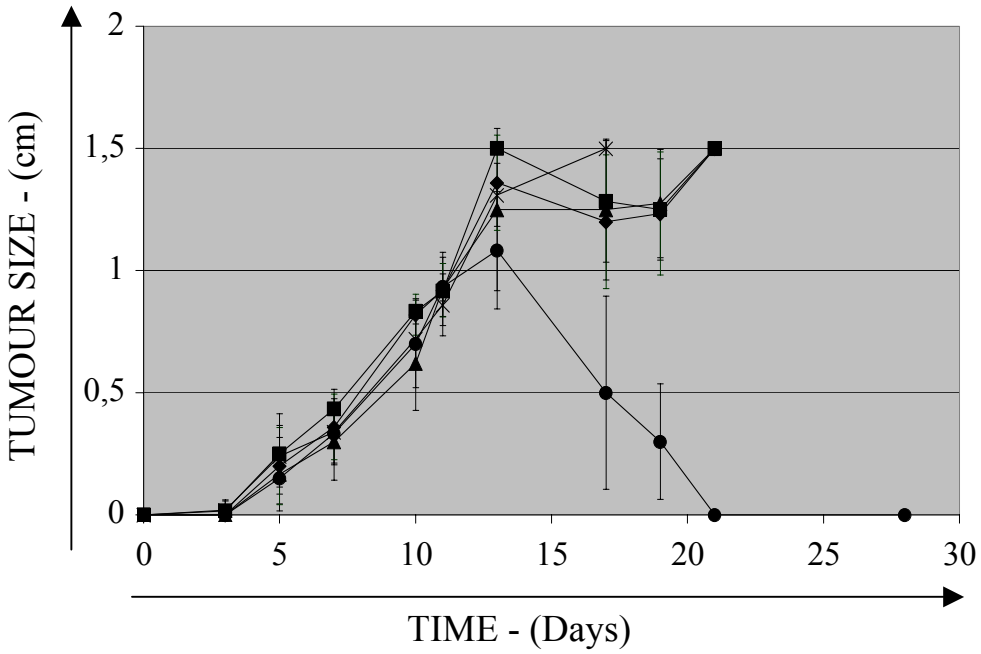

Figure 11: The neutralisation of IFN-γ inhibits J558L tumour rejection induced by cyclophosphamide.
IFN-γ competent mice were treated with the neutralising antibody XMG-6 (1 mg/mouse). Mice were given a single injection of antibody on day -1 (, n=6) or multiple injections on day -1,5 and 10 (, n=6). As control XMG-6 untreated IFN-$\gamma^{+/-}$ mice (, n=6) and IFN-$\gamma^{-/-}$ mice (, n=6) were also included. Mice in these four groups were injected with $1x10^6$ J558L tumour cells on day 0 and treated with cyclophosphamide (15 mg/kg) on day 11. Additionally, IFN-$\gamma^{+/-}$ mice were treated with 1 mg of XMG on day –1 and injected with $1x10^6$ J558L-IFNγ cells on day 0, there was no Cy treatment in this group ( ). Representative of 2 experiments.

3.3.3 IFN-γ IS RELEASED INTO THE SERUM AFTER CYCLOPHOSPHAMIDE TREATMENT

The short *in vivo* lifespan of IFN-γ makes it difficult to measure its concentration. An assay was developed to measure cytokine production *in vivo* (Finkelman and Morris, 1999). The amount of cytokine measured is directly proportional to the amount produced and relatively independent of the site of cytokine production. Mice were injected with 10 μg of a biotin-labelled neutralising rat IgG anti-IFN-γ mAb (R4-6A2). The antibody is able to capture the cytokine to produce a complex that has a relatively long *in vivo* half-life, and consequently accumulates in the serum.

Six hours after treatment of the tumours with Cy there is a little difference in systemic IFN-γ followed by increasing amounts of cytokine from 24-72 hours (Figure 12). The result shows that three days after Cy treatment there is double the amount of IFN-γ in the serum compared to naïve mice.

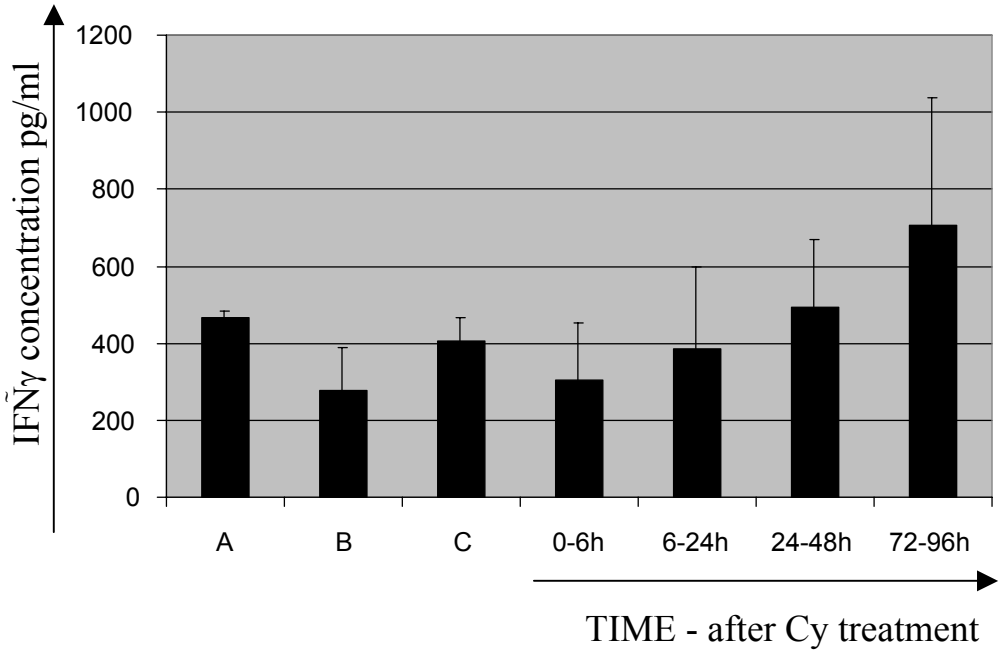

Figure 12: IFN-γ is released into the serum after Cy treatment.
Serum containing murine IFN-γ bound to a biotinylated detection antibody was isolated from mice. C57BL/6 tumour free **(A)**, BALB/C tumour free **(B)**, and day 10 tumour bearing **(C)** mice without Cy treatment served as baseline controls. Mice in groups (0-6h) were given the antibody day 11 just before treatment with Cy on day 11. In the other groups antibody was given on the initial time point and extracted on the final time point. Serum was analysed at various time points after treatment by an IFN-γ ELISA developed by Finkelman and Morris (n = 4/group). Representative of 1 experiment.

3.3.4 HAEMATOPOIETIC CELLS PRODUCE IFN-γ REQUIRED FOR TUMOUR REJECTION

In experiments aimed at determining the origin of IFN-γ required for rejection of J558L tumours, bone marrow chimeras were made using the IFN-γ BALB/c heterozygous and homozygous negative mice. All four possible combinations were made (IFN-$\gamma^{-/-}$ BM to IFN-$\gamma^{-/-}$ host, IFN-$\gamma^{-/-}$ BM to IFN-$\gamma^{+/-}$ host, IFN-$\gamma^{+/-}$ BM to IFN-$\gamma^{-/-}$ host, IFN-$\gamma^{+/-}$ BM to IFN-$\gamma^{+/-}$ host). In bone marrow chimeras all blood borne cell lineages were derived from donor cells. This was confirmed first by PCR from blood (Appendix - Figure 30), and then by ConA stimulation of PBMC's followed by a murine IFN-γ ELISA. The reconstituted, host derived lymphoid compartments contained IFN-γ producing cell populations as determined after ConA stimulation in Figure 13.

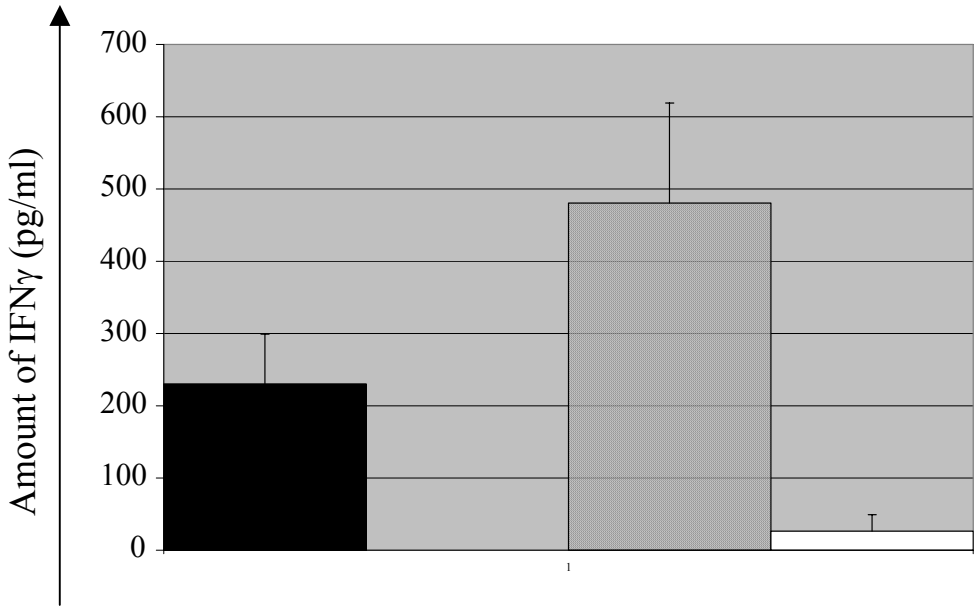

Figure 13: Haematopoietic cells produce IFN-γ upon Con-A stimulation.
Whole blood was removed from individual mice of each group and red blood cells were lysed. The remaining cells were washed and incubated with Con-A for 72 hours. Supernatants were then subjected to an ELISA and the quantity (pg/ml) of IFN-γ determined. Groups include WT to WT ■ , KO to KO ▩ , WT to KO▪ , KO to WT□ - Each group n = 3.

In general, J558L tumours grew with similar kinetics when compared with their unirradiated counterparts. At day 11 all tumours were 0.8 cm in diameter with a standard deviation of 0.25 cm. The BMC tumour response to Cy is shown in Table 2. Four days after cyclophosphamide injection those mice that received bone marrow from IFN-γ competent mice began to reduce

tumour burden. This was seen through a reduction of tumour size and central necrosis of the tumour. Tumours in these mice were characterised by a bloody core and 3-7 days after cyclophosphamide, holes became visible within the tumour mass (Figure 14).

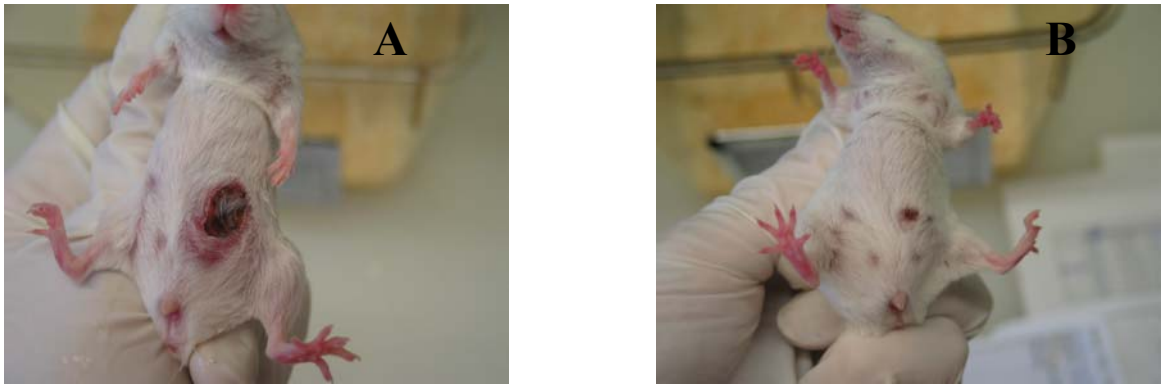

Figure 14: Mice with haematopoietic cells capable of producing IFN-γ reject a J558L tumour.
IFN-γ competent mice, which bare 11 day old J558L tumours, were treated with Cy (15 mg/kg). Rejection was characterised by central necrosis and scab formation 3-7 days after Cy **(A)** and complete destruction 10-15 days after Cy **(B).**

	IFN-$\gamma^{+/-}$ to IFN-$\gamma^{+/-}$	IFN-$\gamma^{+/-}$ to IFN-$\gamma^{-/-}$	IFN-$\gamma^{-/-}$ to IFN-$\gamma^{-/-}$	IFN-$\gamma^{-/-}$ to IFN-$\gamma^{+/-}$
CYCLOPHOSPHAMIDE				
Experiment 1	6/6	6/7	0/5	0/6
Experiment 2	5/6	6/7	0/7	0/6
NO CYCLOPHOSPHAMIDE				
Experiment 1	0/2	0/2	0/3	0/2
Experiment 2	0/2	0/2	0/2	0/2

Table 2: Haematopoietic cells produce IFN-γ that is required for Cy mediated tumour rejection.
The table shows a summary of the number of mice, which rejected the tumour after Cy treatment. IFN-γ bone marrow chimeras were made by irradiating competent and knock out mice with 10 Gy and then transferring $2x10^6$ bone marrow cells. After 12 weeks the chimeras were tested for IFN-γ gene locus by PCR of tail and blood (Appendix - Figure 30). Mice were injected with $1x10^6$ J558L tumour cells on day 0 and treated with cyclophosphamide (15 mg/kg) on day 11.

Tumours of mice that received bone marrow unable to produce IFN-γ continued to grow after Cy treatment. A few mice in the IFN-$\gamma^{-/-}$ haematopoietic to IFN-$\gamma^{+/-}$ non haematopoietic group had a reduction in tumour burden of approximately 0.1 cm - 0.3 cm four days after Cy treatment but shortly after continued to grow (Figure 15). The IFN-$\gamma^{-/-}$ haematopoietic to IFN-

$\gamma^{+/-}$ non haematopoietic group indicated that there was a small amount of IFN-γ that was influencing the response of the mice. It was speculated that this could have been non-haematopoeitic cell derived or from the matrix. Therefore, the relationship of matrix bound cytokine was further investigated. All mice that were not treated with cyclophosphamide had maximal tumour burden between days 20-25 and had to be euthanised.

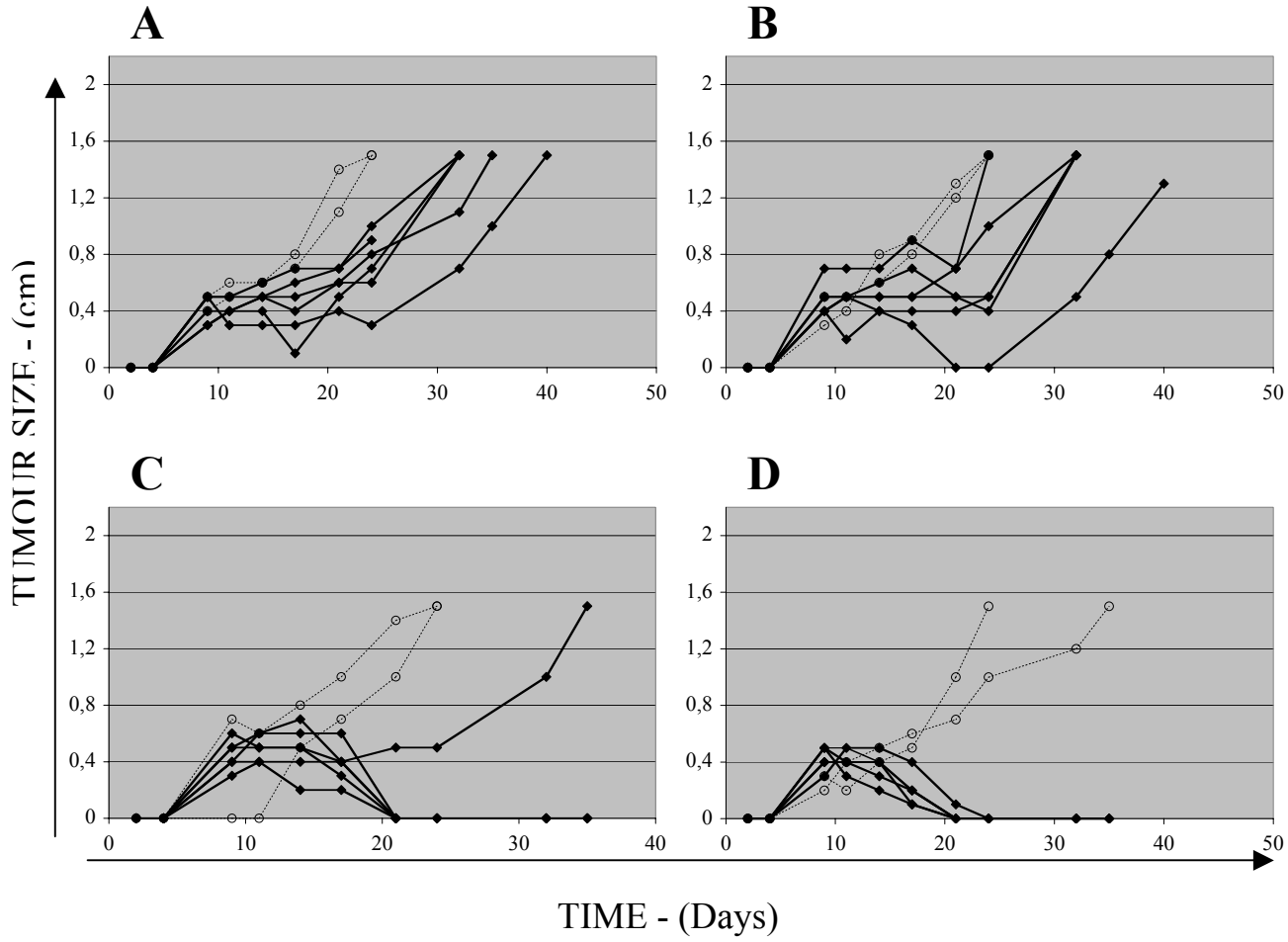

Figure 15: Haematopoietic cells produce IFN-γ that is required for Cy mediated tumour rejection.
Kinetics of tumour growth in IFN-$\gamma^{+/-}$ and IFN-$\gamma^{-/-}$ mice, which were irradiated with 10 Gy and injected i.v. with $2x10^6$ cells of bone marrow isolated from the femurs of IFN-γ deficient or competent mice. Four groups of bone marrow chimeras were generated. **(A)** IFN-$\gamma^{-/-}$ BM to IFN-$\gamma^{-/-}$ host, **(B)** IFN-$\gamma^{-/-}$ BM to IFN-$\gamma^{+/-}$ host, **(C)** IFN-$\gamma^{+/-}$ BM to IFN-$\gamma^{-/-}$ host, **(D)** IFN-$\gamma^{+/-}$ BM to IFN-$\gamma^{+/-}$ host. After 12 weeks mice were given $1x10^6$ J558L tumour cells and treated 11 days later with Cy (15mg/kg). Individual mice treated with Cy bold circles. Untreated mice in dotted circles.

3.4 IFN-γ CO-LOCALISES TO HEPARAN SULPHATE PROTEOGLYCAN *IN VIVO* AND BINDS HEPARAN SULPHATE GLYCOSAMINOGLYCAN *IN VITRO*

It has been shown that *in vitro* IFN-γ can bind to HS found in the extracellular matrix (Fernandez-Botran et al., 2004; Subramaniam et al., 1999). This association of IFN-γ has not been validated *in vivo*. Therefore, the presence of this matrix bound cytokine within the tumour microenvironment was examined due to the rapid destruction of the vasculature after Cy treatment (Figure 10) and retarded outgrowth of tumours in the bone marrow chimeric group where haematopoietic cells could not produce IFN-γ (Figure 15).

3.4.1 IFN-γ CAN CO-LOCALISE WITH HEPARAN SULPHATE IN GROWING TUMOURS

To determine whether IFN-γ might associate with elements of the extracellular matrix *in vivo*, we microscopically examined various tumours (J558L, J558L-IFN-γ) excised from mice for evidence. BALB/c, IFN-γ deficient BALB/c and SCID mice were inoculated with $1x10^6$ tumour cells. Tumours were then extracted at day 5 and 10 and prepared for histology.

Optimal conditions were determined for sectioning and staining the tumours. Similar to the experiments carried out by Van der Loos and colleagues, 2001, four murine monoclonal (XMG1.2, XMG6, R46A-2, F1) and two polyclonal IFN-γ antibodies were screened, as were the fixatives used on the tissues. It was eventually determined that little difference could be seen between acetone, paraformaldehyde and non fixed tissues. Two monoclonal antibodies (XMG1.2 and R46A-2) showed poor but detectable staining in light microscopy and therefore were considered for immunofluorescence co-localisation by confocal microscopy.

IFN-γ was detected using confocal microscopy (Figure 16) and specific staining was confirmed by finding a lack of specific fluorescence in tissues from mutant mice deficient in IFN-γ. Similarly, all sections with isotype control antibodies (IgG1-FITC) showed no fluorescence under the confocal microscope.

The distribution of IFN-γ was limited in tumours from IFN-γ WT mice. Those tumours that arose from haematopoietic cells (J558L) had detectable levels of IFN-γ in sections. The pattern of staining was weak and widely dispersed in different areas of the tumour. However, the most significant signal was generated from SCID mice that had J558L-IFN-γ producing tumours and 129/Sv/Ev mice with MC51.9-IFN-γ producing tumours. As there was a strong signal within these tumours, the parameters of the confocal were adjusted to identify only those areas which had especially high deposits of IFN-γ. The staining was characterised by single strong deposits with dull positive areas encircling.

Heparan sulphate was detected in all tumours in all mice (n=20). It was fairly evenly distributed around the tumour. Nevertheless, within the IFN-γ knockout mice the deposits were shorter and thicker than those seen in the wild type mice.

There was clearly binding of IFN-γ to heparan sulphate but it was restricted to some spots around the tumour. Additionally, there were areas where IFN-γ was shown in close proximity with what could be the nucleus (TOTO-3 - blue) as seen in Figure 16A. This possibly indicates cellular accumulation of IFN-γ. The diffusion of interferon gamma into the matrix can be seen through interaction with heparan sulphate. The strength of co-localisation is seen by the yellow/orange colour in the overlaid images.

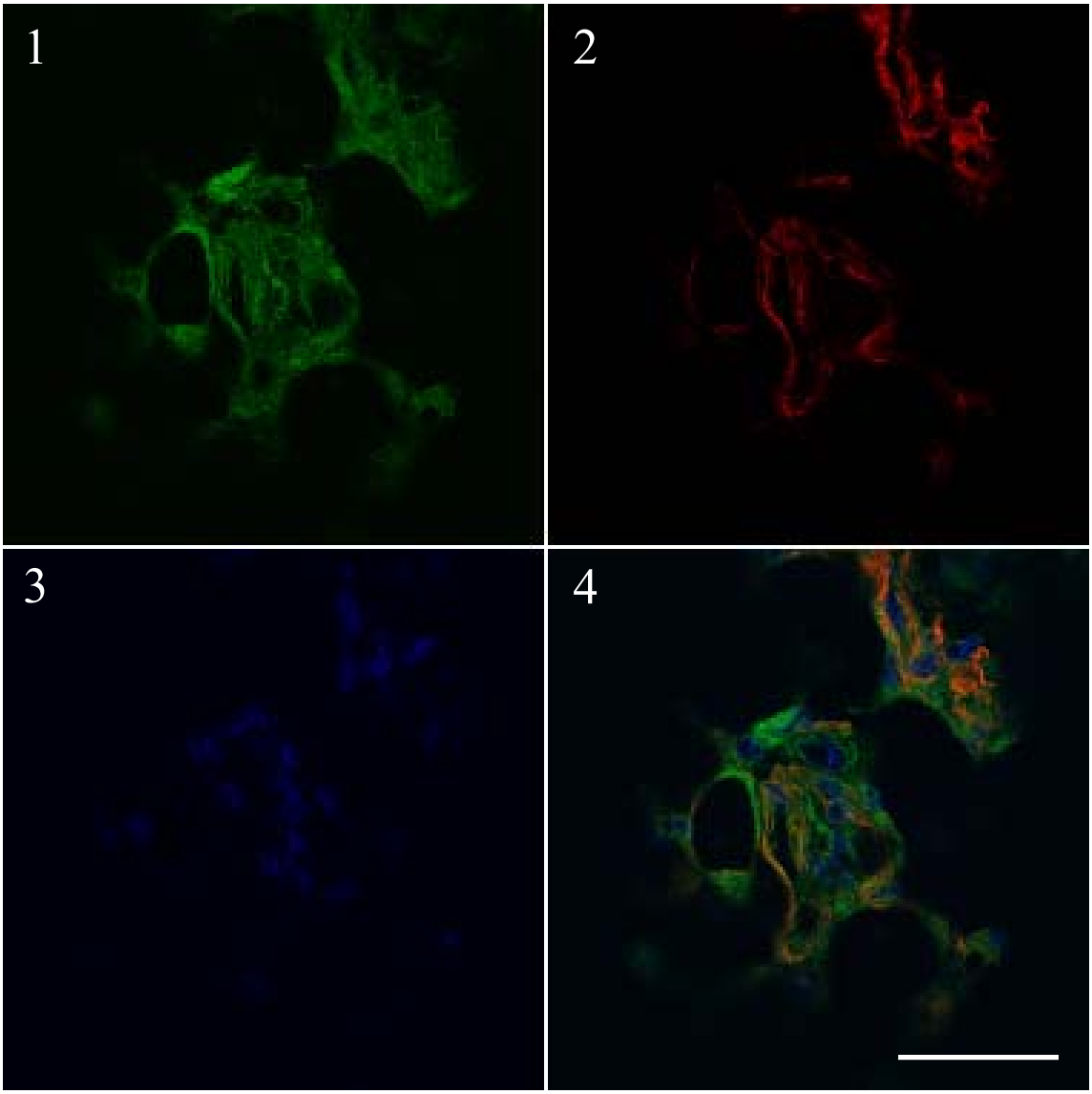

Figure 16 A: Matrix bound IFN-γ.
Interferon gamma (FITC) in association with heparan sulphate (TEXAS RED) in day 10 J558L-IFN-γ tumours in SCID mice. Nuclei are stained with TOTO-3 (blue). **1**: Interferon gamma, **2**: Heparan Sulphate; **3**: Nuclei; **4**: Overlay. Representative of 3-4 mice per group. Scale bar 50 μm.

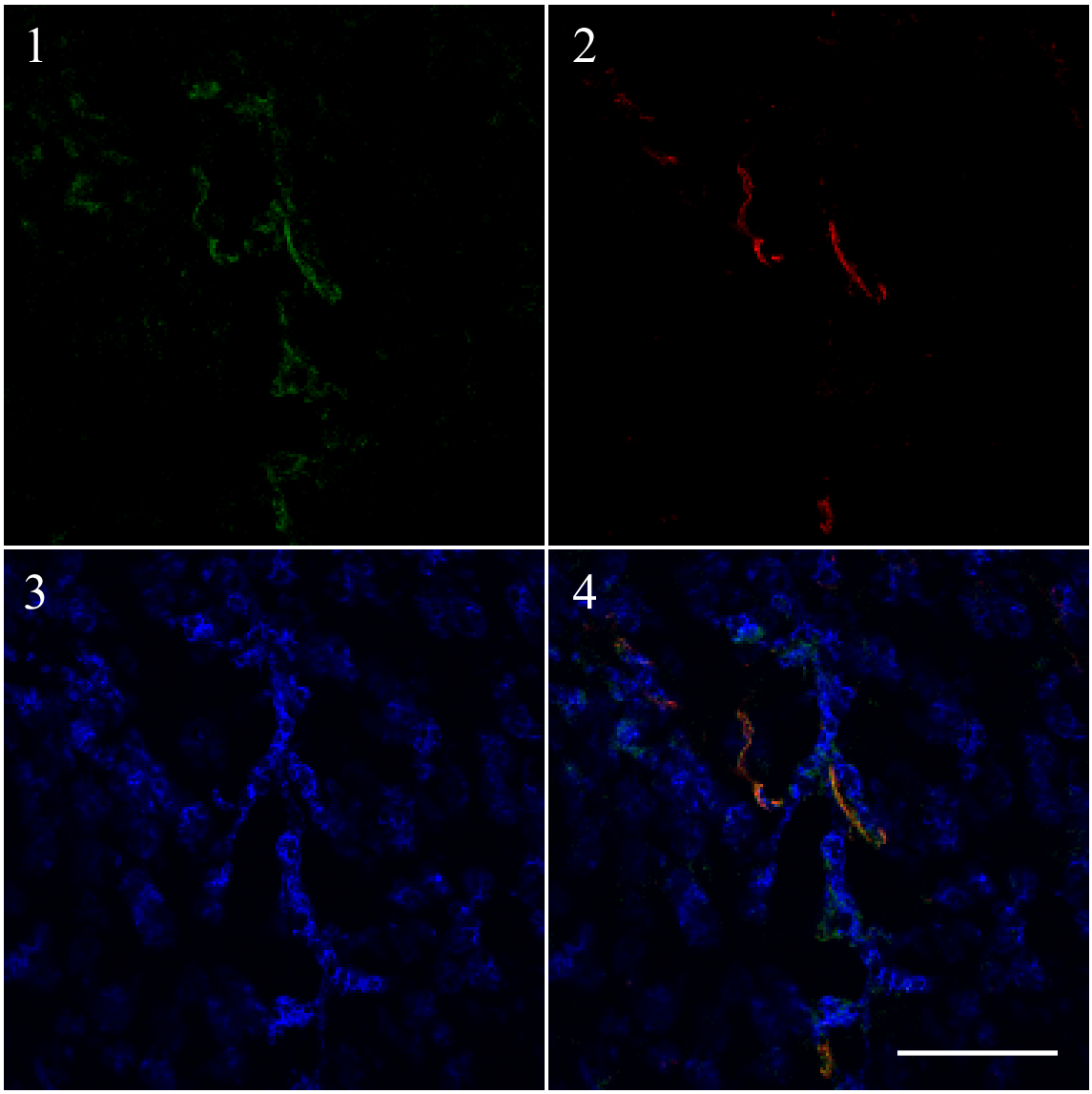

Figure 16 B: Matrix bound IFN-γ.
Interferon gamma (FITC) in association with heparan sulphate (TEXAS RED) in day 10 MC51.9-IFN-γ tumours in wild type mice. Nuclei are stained with TOTO-3 (blue). **1**: Interferon gamma, **2**: Heparan Sulphate; **3**: Nuclei; **4**: Overlay. Representative of 3-4 mice per group. Scale bar 50 μm.

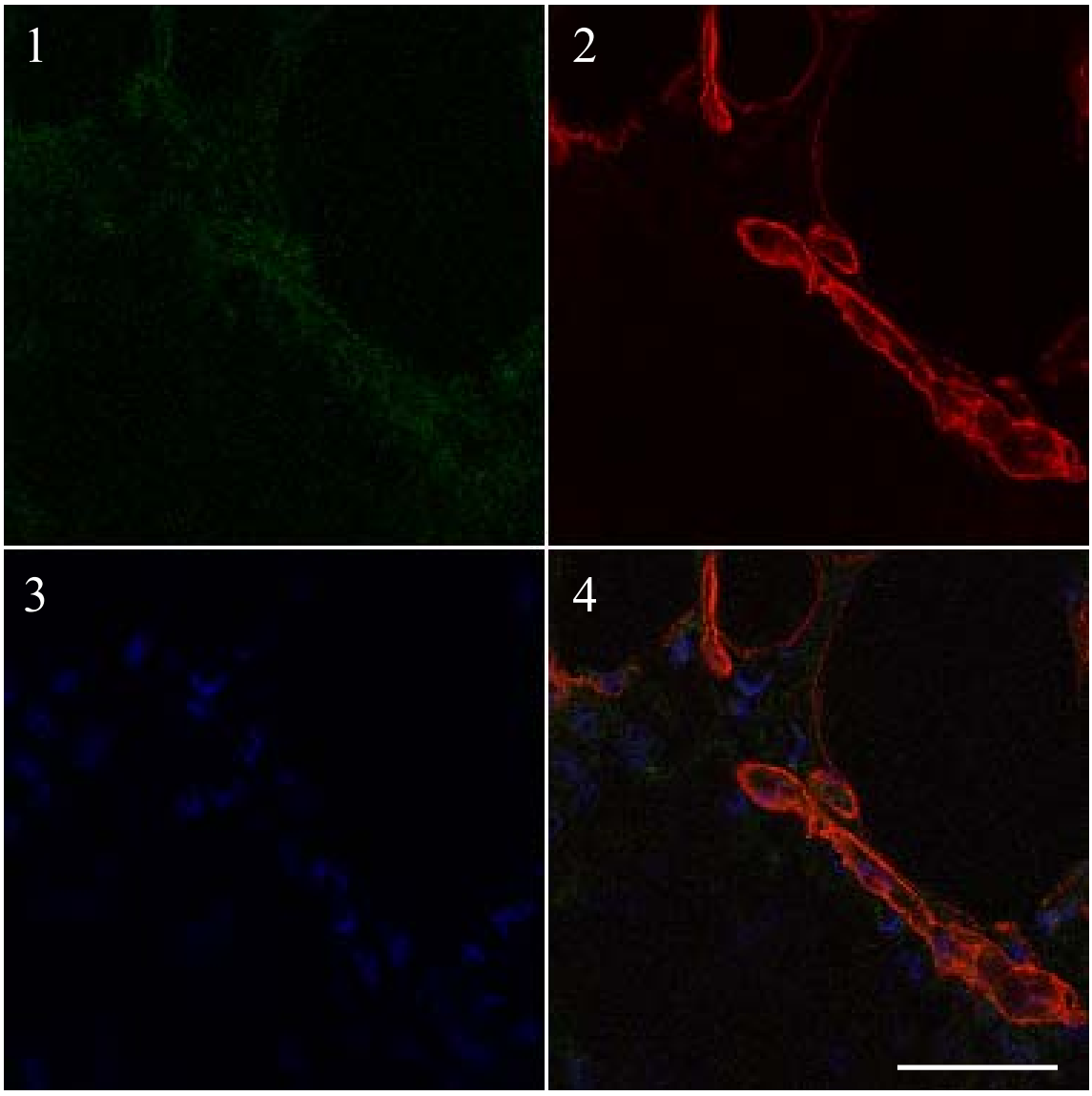

Figure 16 C: Matrix bound IFN-γ.
Interferon gamma (FITC) in association with heparan sulphate (TEXAS RED) in day 10 J558L tumours in wild type mice. Nuclei are stained with TOTO-3 (blue). **1**: Interferon gamma, **2**: Heparan Sulphate; **3**: Nuclei; **4**: Overlay. Representative of 3-4 mice per group. Scale bar 50 μm.

3.4.2 IFN-γ INFLUENCES THE MATRIX PRODUCTION OF TUMOURS

Not only does IFN-γ bind to the matrix, but its presence can influence matrix structure. Tumours have been described as wounds that do not heal (Dvorak, 1986), as there are many parallels between tumour stroma generation and wound healing. In wound healing the presence or absence of certain cytokines has been shown to influence the formation of scar tissue (Azouz et al., 2004). While the majority of the components of the extracellular matrix appear to remain the same in both the knock out and the wild type mice, the structural formation of each matrix element varies.

To support the significance of the differences seen in the J558L model, the TS/A mammary carcinoma was additionally analysed as it grows with similar kinetics in BALB/c mice. Mice were injected with $1x10^6$ cells of either tumour type and the tumours were extracted and frozen for sectioning on day 10. Being of non-haematopoietic origin the TS/A tumours tended to have larger quantities of matrix than the plasmacytoma J558L (grown as a solid tumour), therefore the signal from histology was stronger due to the density of the matrix molecules.

The pan fibroblast marker, ERTR-7, was used to determine the distribution of fibroblasts within growing tumours. In both the J558L and TS/A models there was dense staining in wild type mice and tendrils were long and thin. These tended to be slightly thicker in the IFN-$\gamma^{-/-}$ mice (Figure 17A-A & 17B-A).

The signal for heparan sulphate proteoglycan was markedly reduced in the wild type mice in comparison with the IFN-$\gamma^{-/-}$ mice. Within the WT group the structures were very fine, long and thin. The knockout mice had denser structure formations and these were a little more restricted in distribution within the TS/A model. In general, there appeared to be more heparan sulphate in the TS/A model.

Within the TS/A tumour collagen II had similar coverage in both WT and IFN-$\gamma^{-/-}$ groups. The significant difference was that tendrils of collagen were long and wispy in the WT but short and stubby in the IFN-$\gamma^{-/-}$ mice. There were larger amounts of deposited collagen II in WT mice with J558L tumours compared with the tumours of IFN-$\gamma^{-/-}$ mice. However, the finding of long tendrils in WT and shorter tendrils in knockout remained the same.

The most significant difference between the WT and IFN-$\gamma^{-/-}$ tumours was seen with collagen IV. The staining was consistent in both the J558L and the TS/A model. Collagen IV is a staple of basement membranes that make up the support for the blood vessels within the tumours. The WT tumours were covered completely in thick, long, intertwined sheets of collagen IV. Knockout tissues, while still having significant staining, consisted primarily of shorter tendrils and dots of collagen IV.

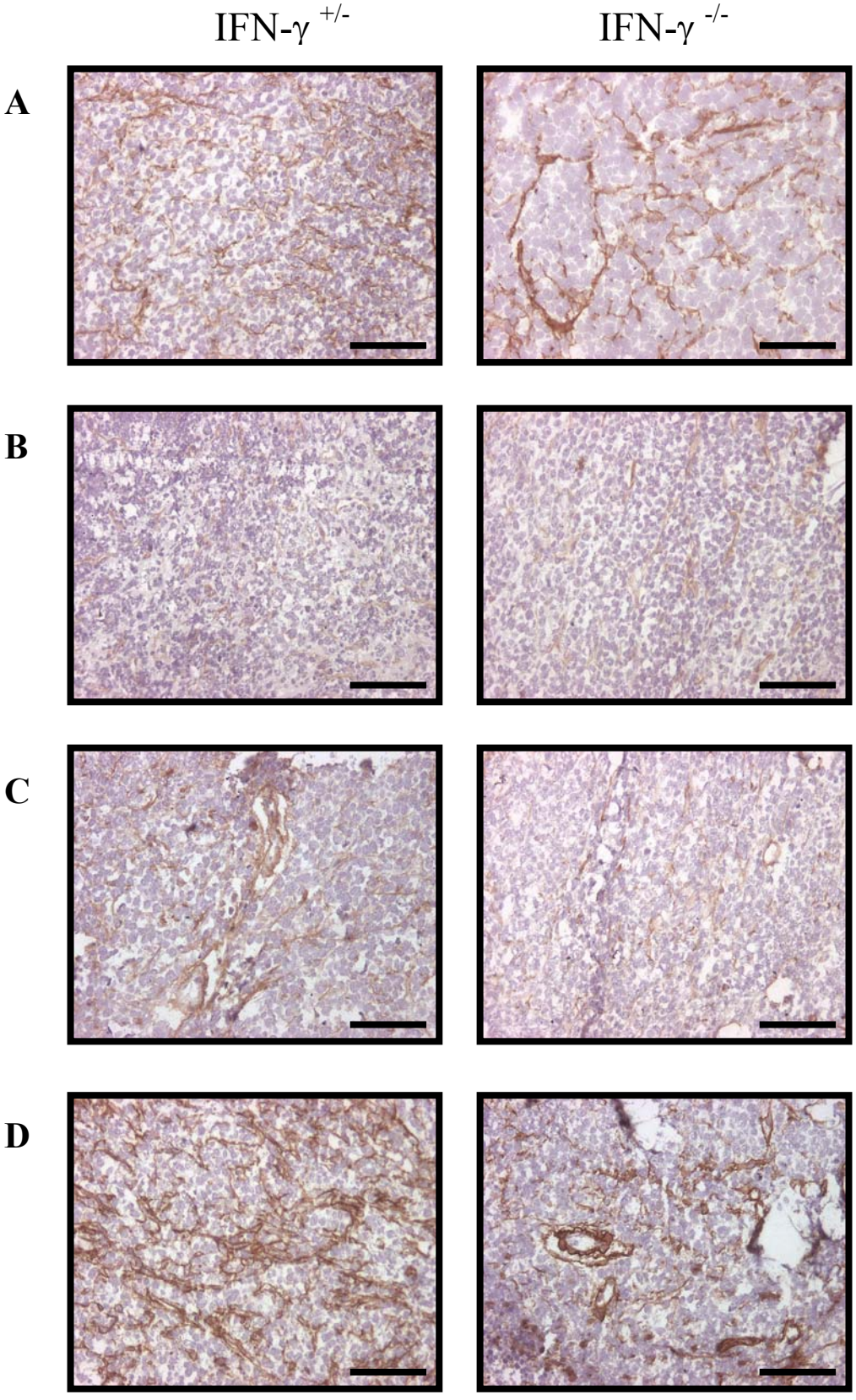

Figure 17 A: J558L matrix differences between wild type and IFN-γ knockout mice.
Mice were injected with $1x10^6$ J558L tumour cells. Sections were made 10 days later tumours were excised and cut. Tumours were stained for (A) ERTR-7; (B) Heparan sulphate proteoglycan; (C) Collagen II; (D) Collagen IV, and then counterstained with Haematoxylin. Scale Bar 100μm. Representative of 3-4 mice per group

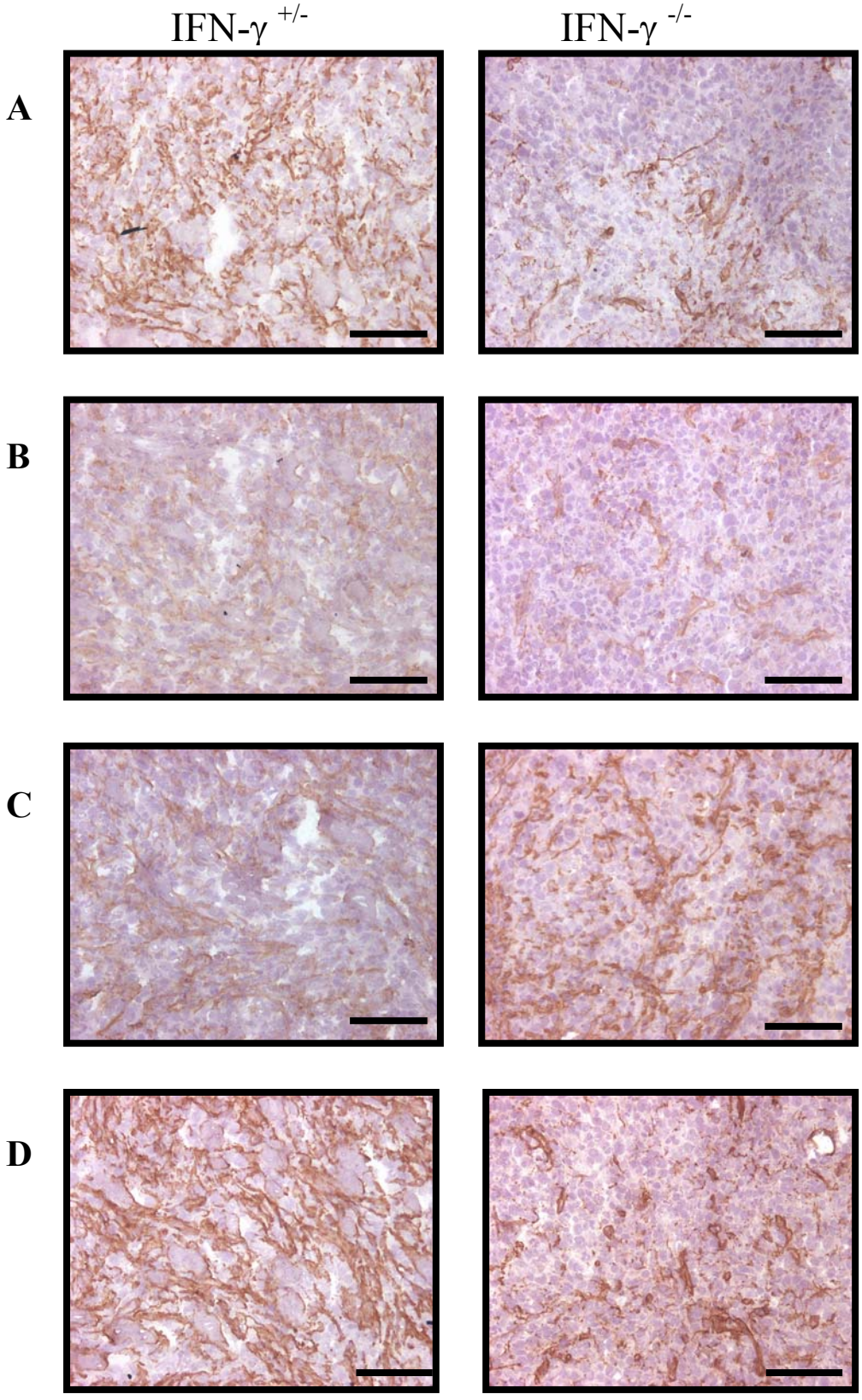

Figure 17 B: TS/A matrix differences between wild type and IFN-γ knockout mice.
Mice were injected with $1x10^6$ TS/A tumour cells. Sections were made 10 days later tumours were excised and cut. Tumours were stained for (A) ERTR-7; (B) Heparan sulphate proteoglycan; (C) Collagen II; (D) Collagen IV, and then counterstained with Haematoxylin. Scale Bar 100μm. Representative of 3-4 mice per group.

3.4.3 EXOGENOUS HUMAN IFN-γ CAN BIND TO MATRIGEL PLUGS *IN VIVO*

Matrigel is a purified form of basement membrane from the Engelbreth-Holm-Swarm (EHS) sarcoma (Lortat-Jacob et al., 1991). It contains collagen type IV, laminin and heparan sulphate proteoglycans. It can provide a suitable biologically relevant environment where the matrix is devoid cells. Previously, it had never been demonstrated that IFN-γ and heparan sulphate could interact *in vivo*. In order to confirm the confocal histological analysis, matrigel (0.2 ml) was injected subcutaneously into IFN-$\gamma^{-/-}$ mice. After 5 days, mice were treated with 200 μg of recombinant human IFN-γ. Upon removal of the plug, vasculature was macroscopically visible throughout. The amount of IFN-γ detectable by ELISA had decreased 24 hours after the first matrigel extraction time point of 1 hour. The detection level was limited to 1.6ng/ml (Figure 18).

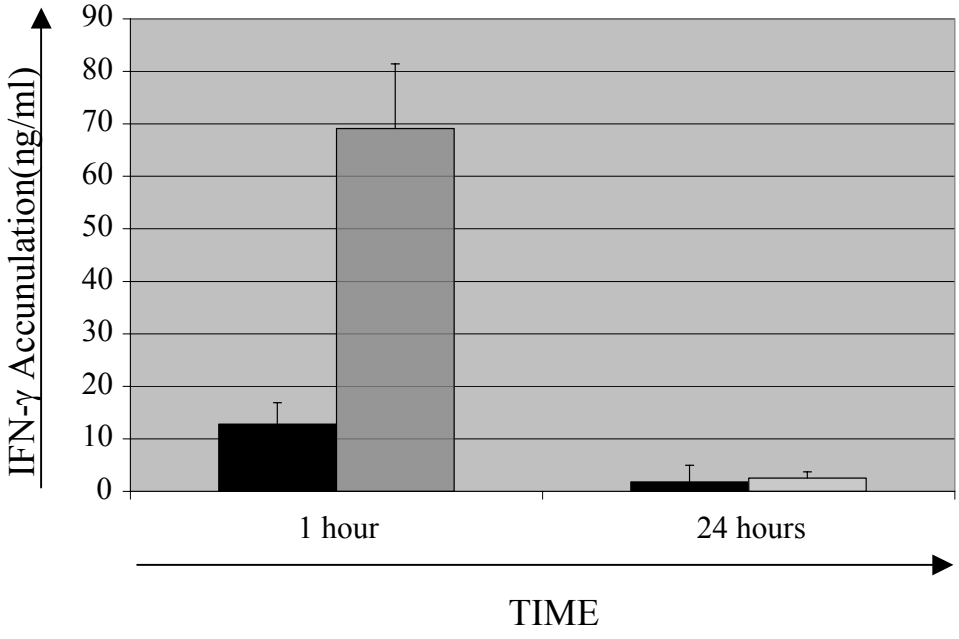

Figure 18: IFN-γ can bind to Matrigel plugs *in vivo*.
Five days after matrigel injection, mice received 200μg recombinant human IFN-γ, 1 hour or 24 hours later gel fragments (■) were extracted and mulched with PBS. Serum IFN-γ levels (▩) were also analysed at the corresponding time points (n=3). Matrigel from mice that were not treated with recombinant human IFN-γ had undetectable levels of cytokine.

3.5 THE KRKRS SEQUENCE OF THE CYTOKINE IFN-γ INFLUENCES *IN VITRO* AND *IN VIVO* RESPONSES.

3.5.1 IODINATION OF IFN-γ

It is known that IFN-γ has a dissociation constant for heparan sulphate similar to its affinity for its receptor (Lortat-Jacob and Grimaud, 1992). As the competition for matrix free sites within the tumour had never been analysed it seemed appropriate to investigate this relationship. Human IFN-γ contains the conserved KRKRS sequence responsible for matrix binding and, whilst it is capable of electrostatic interaction with the murine heparan sulphate, it is incapable of binding to the murine IFN-γ receptor (Lortat-Jacob et al., 1996a).

Human IFN-γ was iodinated using the chloramine-T method primarily because the sites of iodination (tyrosines) were not closely associated with the specific binding sequence. Purified bound protein was obtained and identified in samples of the desalting column washes which were run on a protein gel (Figure 19)

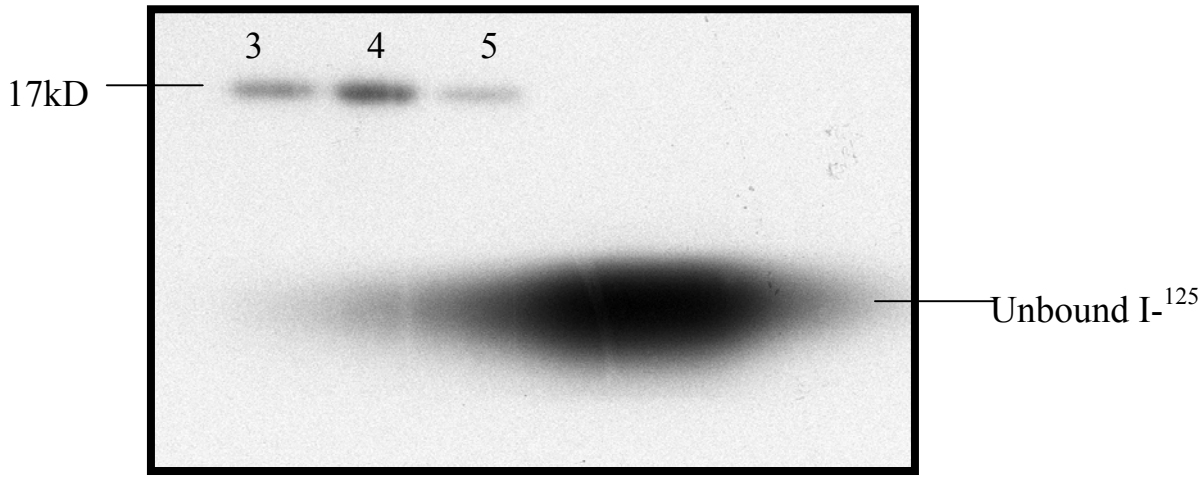

Figure 19: Radioactive labelling of IFN-γ.
Bands on an SDS gel of I^{125} IFN-γ from the different eluent fractions off a desalting column. Lanes 3-5 show single bands of bound IFN-γ protein, Lanes 6-10 show unbound radioactivity. Representative of 2 experiments.

3.5.2 *IN VITRO* INHIBITION

A RADIOLABELLED IFN-γ CAN BIND TO MATRIX

In vitro the best way to determine the binding of human I^{125} IFN-γ to heparan sulphate within a tumour was to analyse its association with matrigel isolated from an EHS sarcoma. Whilst matrigel contains basement membrane components such as laminin and collagen IV, it is also composed of 1-3% heparan sulphate. Radioactively labelled cytokine was incubated in wells with matrigel and individual matrix components such as Collagen I, III, IV, VI, XIVα and fibronectin. Significant binding was seen only in wells containing matrigel and the optimal concentration of IFN-γ binding per well was determined to be 5 ng – 7.5 ng using I^{125} IFN-γ (Figure 20).

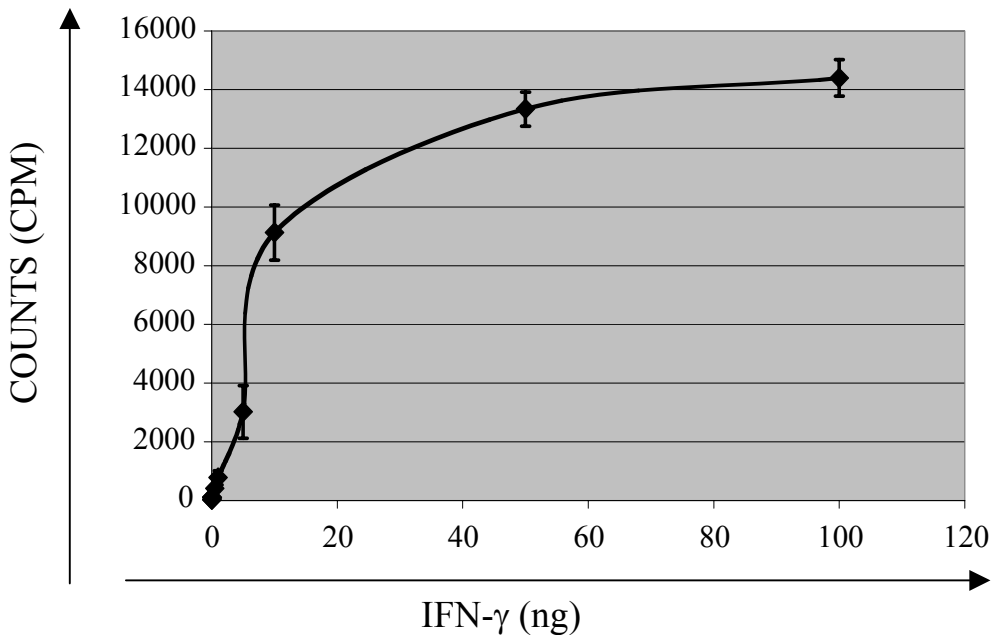

Figure 20: Radioactively (I^{125}) labelled human recombinant IFN-γ can bind to EHS matrigel.
Wells were incubated with 114 ug per well of matrigel overnight. After washing wells were incubated for 24 hours with varying concentrations of I^{125} IFN-γ, washed again and counted. Representative of 3 experiments.

B THE MURINE PEPTIDE CAN PREVENT BINDING OF IFN-γ TO MATRIGEL

The basic sequence of amino acids at the C-terminus of the IFN-γ molecule are essential for matrix binding (Fernandez-Botran et al., 2004) and for mediating receptor interaction (Sadir et al., 1998). Utilising the murine peptide MC-2 (LRKRKRSR) *in vitro* inhibition of human I^{125}-IFN-γ binding to the matrigel complex was observed. Inhibition of 50% was seen using 400μg of the peptide and 1000μg of peptide caused 80% inhibition of radio-labelled cytokine interaction with the matrigel (Figure 21). The molar ratio of IFN-γ, 4 $x10^{-7}$ mol/L, to heparan sulphate within the ECM gel 17 μg/ml was comparative to previously published reports.

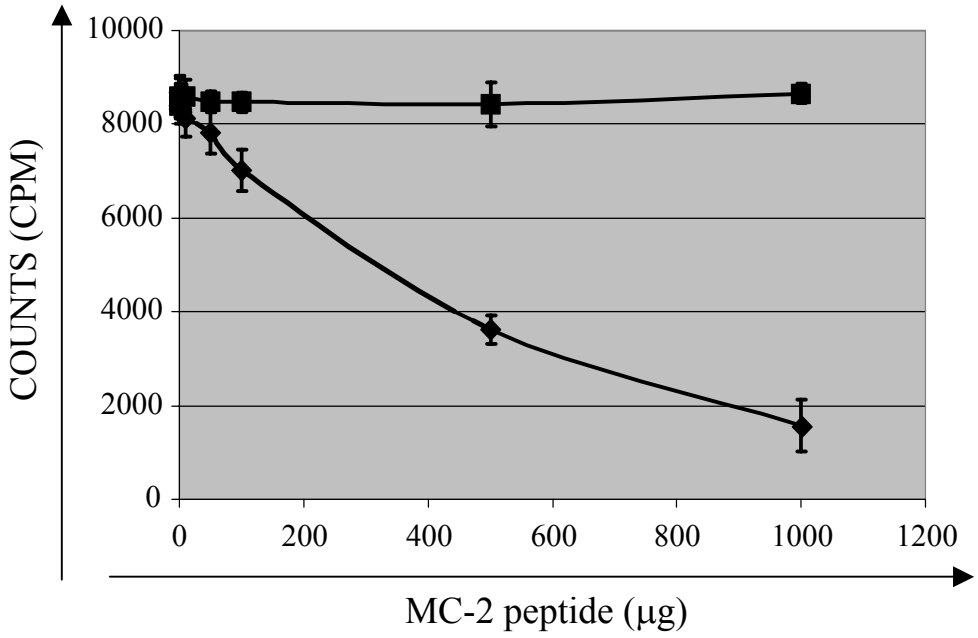

Figure 21: The murine peptide MC-2 (LRKRKRSR) can inhibit 7.5 ng/ml human I^{125}-IFN-γ binding to matrigel.
Matrigel coated wells were incubated with MC-2 peptide dissolved in PBS (◆) and the MC-2 dissolved in 100% DMSO (■). The negative charge of the DMSO interferes with the effect of the peptide. Representative of 3 experiments.

C MC-2 PEPTIDE IN THE SUPERNATANTS FROM TRANSFECTED TUMOUR CELLS CAN INHIBIT IFN-γ BINDING

The J558L tumour cell line was transfected with four different plasmids to create, 2 cell lines that were capable of secreting the murine peptide and 2 cell lines that acted as negative controls. At all times the transfected cell lines (bulk culture) were kept under selection with Zeocin™. The supernatants were conditioned by $4x10^6$ cells/ml of RPMI medium overnight. They were then collected and analysed for their ability to inhibit binding of human I^{125}-IFN-γ to matrigel coated wells. The results indicated that both tumour lines containing plasmids for the secretion of MC-2 into the supernatant were indeed producing significant quantities of MC-2 peptide, independent of the presence of a HIS-Tag. In both of these tumour lines IFN-γ binding was inhibited by approximately 50%. The control supernatant with HIS-Tag alone showed minimal difference to the parental untransfected J558L supernatant, while low level inhibition was seen in the tumour line secreting the neutral alanine peptide fragment into the supernatant. The results were titratable as seen in Figure 22.

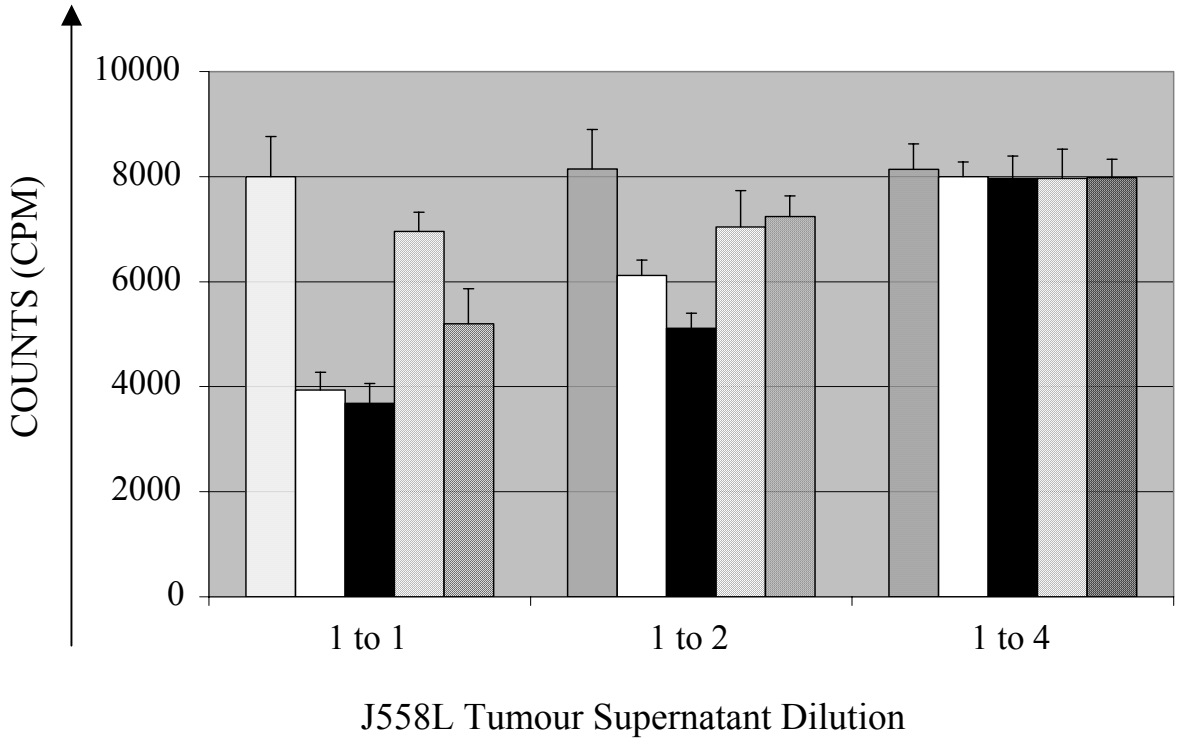

Figure 22: MC-2 from tumour cell supernatants inhibit human I^{125}-IFN-γ binding to plate bound matrigel.
Supernants were incubated for 24 hours on ECM gel coated plates at 4°C at various dilutions in RPMI. Groups include; Parental – untransfected (⊟), J558L – pMC-2NoTag (□), J558L – MC-2Tag (■), J558L –pTag (◫), J558L – pAlanine[8] NoTag (◪) tumour cells.

3.5.3 *IN VIVO* INHIBITION

A RADIOLABELLED IFN-γ CAN BIND TO MATRIX *IN VIVO*

It has been previously been shown that 20μg of radioactive IFN-γ injected into rats was enough to determine the specific counts and location of the protein. As the IFN-$\gamma^{-/-}$ and wild type mice are much smaller than the rat, the amount of protein thought to give similar results was reduced to 5μg per mouse in order to get a similar result. Organs were extracted 1 hour, 24 hours and 72 hours after injection, however the most significant results were seen after the 1 hour time point. This corresponds to previously published reports where it was shown the half life of IFN-γ was increased from 1.1 minutes to 99 minutes when bound to heparin (Lortat-Jacob et al., 1996a).

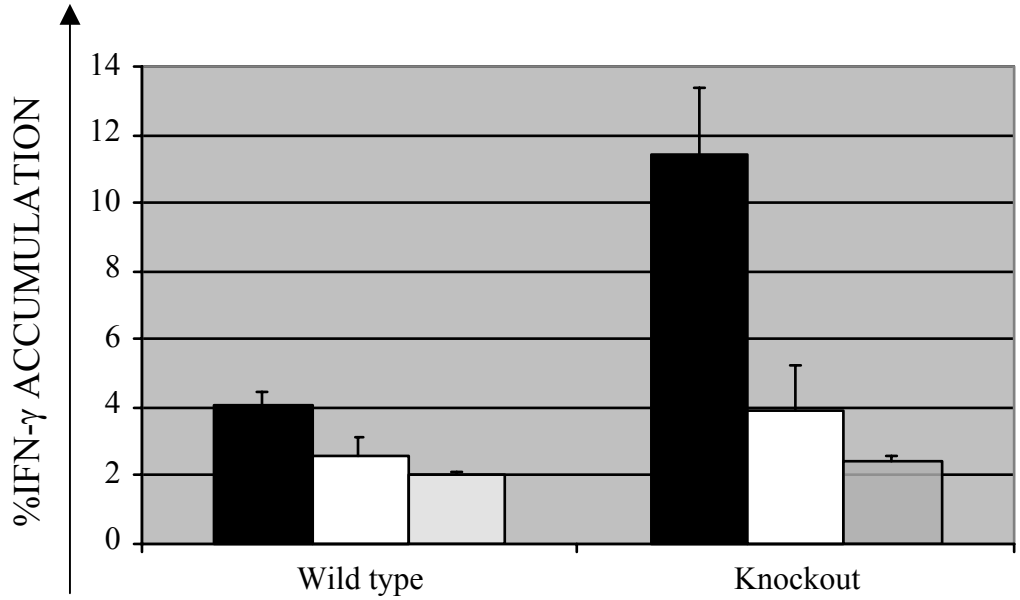

Figure 23: Distribution of I^{125} labelled human IFN-γ 1 hour after injection (% Dose/gram).
Mice from both WT and IFN-$\gamma^{-/-}$ groups (n=3) were injected with 5 μg of I^{125} labelled IFN-γ on day 5 or day 8 of tumour growth. One hour later blood and organs were extracted for cpm analysis. Day 5 tumour burden (■); Day 8 tumour burden (□), representative organ - spleen (▣) day 8.

The differences in the amount of radioactive IFN-γ that had accumulated per gram of tumour can be seen in Figure 23. It was clear that between organs on both day 5 and day 8 there was little difference in both the WT and IFN-$\gamma^{-/-}$ groups (spleen as representative organ other data not shown). However, the tumours of the IFN-$\gamma^{-/-}$ groups, on both days, had larger amounts of

accumulated IFN-γ. This indicated that there was no competition by endogenous IFN-γ for heparan sulphate binding sites in the knock out mice.

B HUMAN I^{125} IFN-γ BINDS LESS IN MC-2 TRANSFECTED TUMOURS

To test the ability of the tumour transfectants in preventing exogenous human I^{125}-IFN-γ binding *in vivo*, the tumours without the HIS-Tag expressing MC-2 or alanine[8] were injected in IFN-γ deficient mice. At day 8 the mice were given a single shot of 5 μg human I^{125}-IFN-γ and one hour later the tumours were excised. The MC-2 secreting tumour line was capable of preventing accumulation of IFN-γ by approximately 30% when compared to the alanine secreting control tumour.

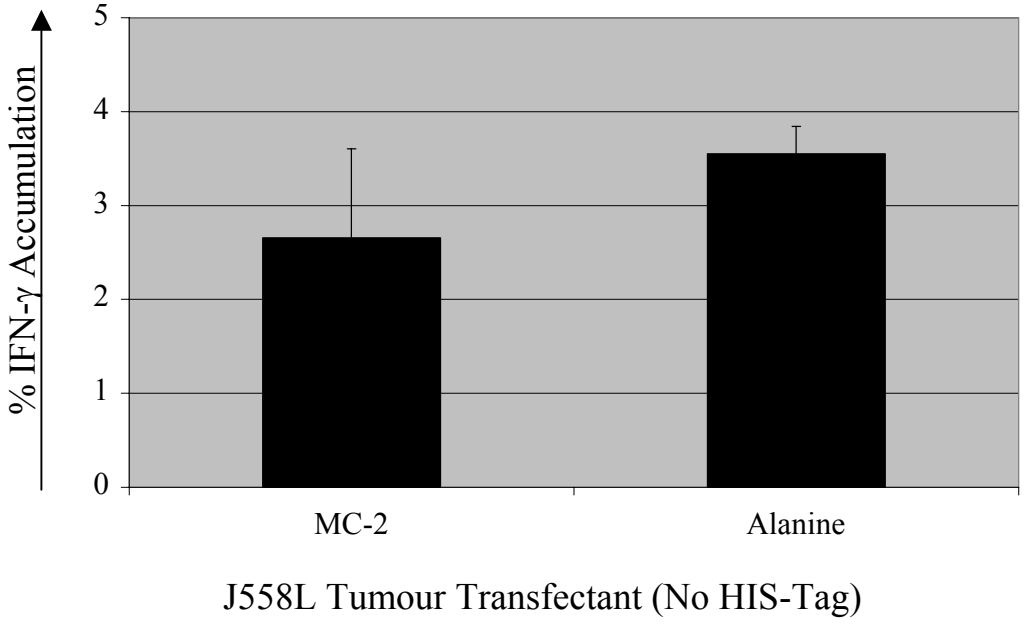

Figure 24: Tumours secreting the MC-2 peptide accumulate less human I^{125}-IFN-γ *in vivo*.
Percentage dose per gram of tissue. Transfected tumours grown for 8 days without the HIS-Tag were treated with human I^{125}-IFN-γ and 1 hour later the tumours (and organs) were excised and counts determined. Little difference was seen in the other organs or blood between the two groups, (n=3).

Similarly, single mice were given 3 tumour lines and matrigel in order to compare the accumulation of human I^{125}-IFN-γ within the organs and at the different sites. Tumours were allowed to grow to 0.4-0.8cm in size. Both the pTag alone and parental tumours appeared to grow with the same kinetics, however the pMC-2-Tag were always noticably larger. From Figure 25 it is clear that there is less accumulation of I^{125}-IFN-γ in the pMC-2-Tag tumours compared with the parental tumour and the matrigel. The gel was the highest accumulator of the human I^{125}-IFN-γ even though less than 3% of the gel by weight is actually heparan sulphate.

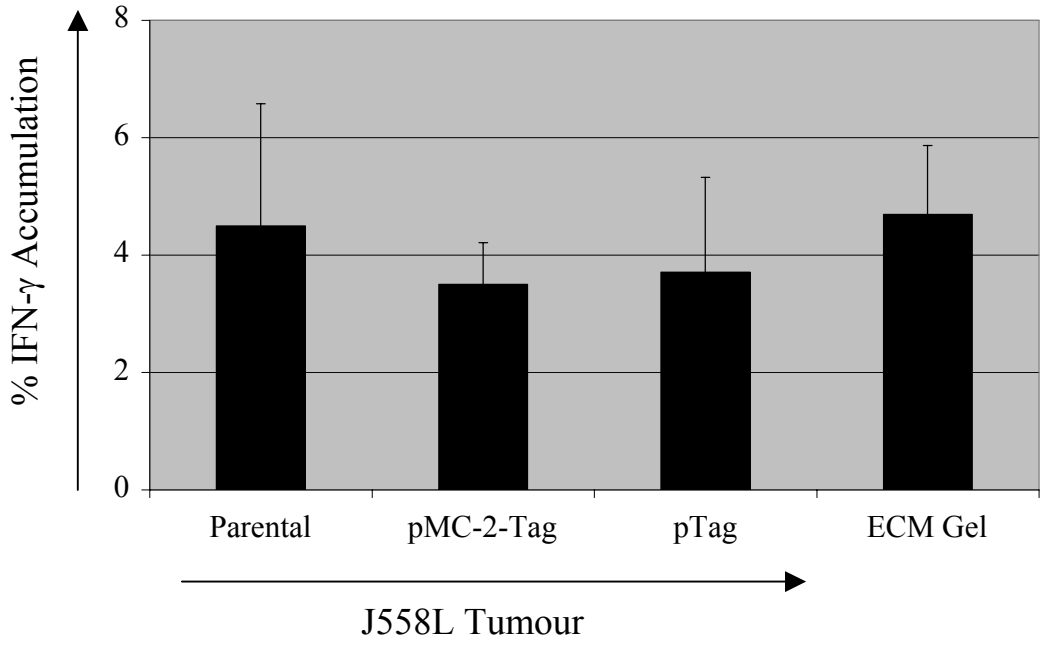

Figure 25: MC-2 secreting tumours can prevent human I^{125}-IFN-γ accumulation.
Percentage dose per gram of tissue. Eight days after s.c. injection of tumour cells and EHS-ECM gel on single mice, 5μg human I^{125}IFN-γ was injected i.v. and one hour later tumour and gel excised and counts determined, (n=3).

C TRANSFECTED TUMOUR RESPONSE TO CYCLOPHOSPAMIDE TREATMENT

The model in which the rejection of J558L tumours by cyclophosphamide is IFN-γ dependent has been previously described in earlier experiments (Figure 9, 10 and 11). In order to show a function of the LRKRKRS fragment *in vivo*, IFN-γ competent mice were given $1x10^6$ tumour cells and treated with Cy eleven days after tumour injection. Five groups were included:

J558L Parental, J558L-pMC2-NoTag, J558L-pMC2-Tag, J558L-pAlanine^{8}-NoTag and J558L-pTag. From the growth kinetics it was clear that mice that received tumours with the MC2 fragment grew similarly to the control lines. Tumours that contained the neutral fragment appeared to have a larger tumour volume, however after Cy treatment, tumours grew out completely. Mice bearing the J558L-pMC2-NoTag and J558L-pMC2-Tag groups were also unable of rejecting tumours upon treatment with Cy, whilst mice with the J558L-pTag group rejected tumours 30% of the time. Parental J558L tumours and those mice bearing parental tumours, treated daily with MC-2 peptide (i.p.) were rejected after Cy treatment.

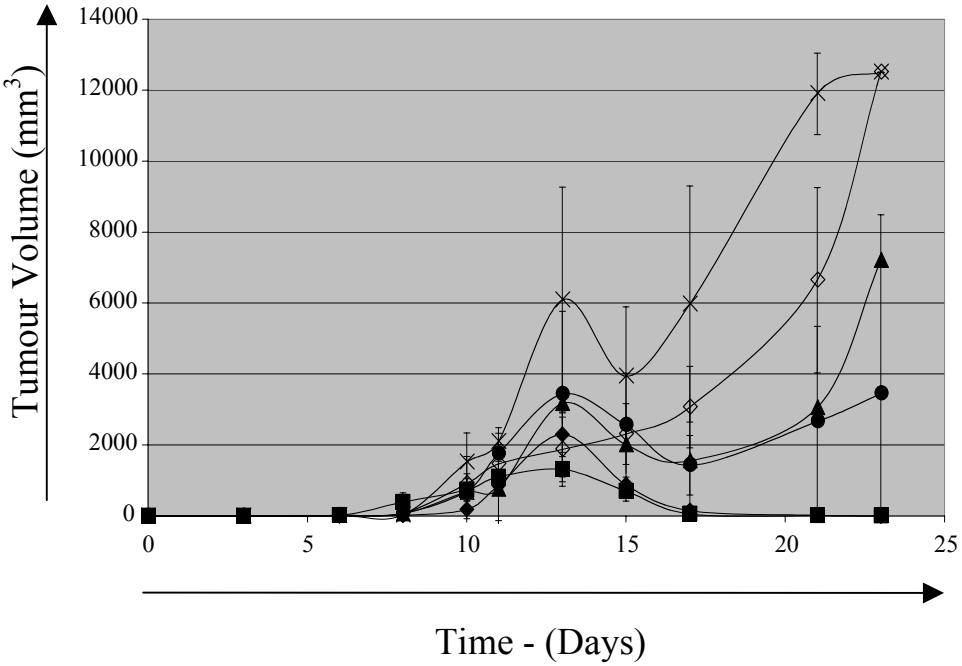

Figure 26: Growth kinetics of plasmid transfected J558L cell lines treated with Cy. Parental J558L◆ , Parental J558L and MC-2 peptide■ , J558LpMC-2 NoTag △ , J558L pMC-2-Tag ◇ ,J558L-Alanine^{8}-NoTag× , J558L pTag ● , Tumour volumes were determined using a calliper, each group (n=7). Representative of 3 experiments. Tumours in untreated mice grew out by day 20-25 and had to be euthanised (n=4).

4 DISCUSSION

4.1 THE ORIGIN OF INTERFERON GAMMA IN TUMOUR RESPONSES

Interferon gamma is the principle effector cytokine of cell-mediated immunity. It plays a critical role in promoting host resistance to microbial infection and is also involved in pathological circumstances such as trauma, autoimmunity and cancer (Billiau et al., 1998). Until recently, it was assumed that the main source of IFN-γ involved in anti-tumour responses was lymphocyte derived, however it was demonstrated that macrophages could secrete large amounts of IFN-γ and that this may operate by an autocrine positive feedback loop in which IL-12/IL-18 stimulation was critical. During tumour rejection mediated by the DNA-alkylating agent, cyclophosphamide, it was concluded that while production of IFN-γ by macrophages was necessary, it was not entirely sufficient for mediating tumour rejection (Ibe et al., 2001). In the experiments carried out by Ibe and colleagues, IFN-$\gamma R^{-/-}$ mice were unable to reject the tumour upon Cy treatment, however there was a delay in tumour growth, which could not be explained. The purpose of this thesis was to further analyse the role of IFN-γinvolved in Cy mediated rejection and determine whether matrix interactions with the cytokine had any function within this model.

It has been shown that IFN-γ is an important participant in Cy mediated tumour rejection. The model on which most of the animal experiments were based for the thesis demonstrated that IFN-$\gamma^{-/-}$ mice are incapable of rejecting J558L tumours after Cy treatment and therefore appear to be severely impaired when generating anti-tumour immune responses. There was a short delay in the tumour growth but eventually tumours grew out. This behaviour is similar to the response of the IFN-$\gamma R^{-/-}$ mice with MC51.9 tumours, however the kinetics in this model indicated a small decrease in size of the tumour before outgrowth. Additionally, the rapid destruction of the vasculature demonstrated by the CD31 stainings confirmed what was seen in the IFN-γR mice with MC51.9 tumours treated with Cy.

Confirmation of the results from the IFN-$\gamma^{-/-}$ mice was carried out by antibody neutralisation of IFN-γ in wild type BALB/c mice, as it has been recently suggested that effects seen in mice with targeted gene deletions may be misleading due to the possible indirect effects, such as the over compensatory expression of other genes, that can not be controlled (Wu et al., 2004).

Neutralisation of IFN-γ works as a temporary blockade of a specific signalling pathway. The neutralising antibody XMG6 was used to inactivate the effect of IFN-γ before tumour cell injection. The potency of a single injection or multiple injections at different time points throughout the growth period of the tumour had the same effect. Mice were incapable of rejecting a tumour after Cy treatment. Neutralising antibodies are known to be effective for two to four weeks, therefore it is reasonable to assume that XMG6 remained in the mice over the observation period, presumably blocking the anti-angiogenic effect of IFN-γ and allowing tumour outgrowth.

It was important to determine whether the source of IFN-γ required in tumour rejection arose locally or from the whole body. It is clear from several studies that T cell and NK cell derived IFN-γ is important in mediating tumour rejection. Nevertheless, it was never shown *in vivo* if there was an augmentation of systemic IFN-γ production in response to Cy. By using the Cincinnati Cytokine Capture (CCC) assay, over 96 hours in IFN-γ competent mice, there was a steady increase of detectable IFN-γ in the serum after Cy treatment. Levels rose from the baseline 250 pg/ml in tumour free mice to over 700 pg/ml, 96 hours after Cy treatment. This result can be explained by two hypotheses, (i) that matrix may release IFN-γ into the serum in response to Cy and/or (ii) there was homeostatic proliferation after lymphocyte depletion caused by Cy. It is known that IFN-γ is released by haematopoietic cells following homeostatic proliferation. This IFN-γ release into the serum correlates with the documented recovery of lymphocytes, particularly T cells after Cy treatment. It is known that Cy treated animals become lymphopenic within the first few hours after drug administration, and that it takes approximately three days for the T and B lymphocytes to begin to recover and 10 days for complete recovery of pretreatment total spleen numbers (Lutsiak et al., 2005)

In order to confirm the origin of IFN-γrequired for rejection, bone marrow chimeras were made to elucidate the role of haematopoietic and non-haematopoietic cells in the immunological response to cyclophosphamide. Four groups of bone marrow chimeras were generated from IFN-γgene deficient and competent mice (IFN-$\gamma^{-/-}$ to IFN-$\gamma^{-/-}$, IFN-$\gamma^{-/-}$ to IFN-$\gamma^{+/-}$, IFN-$\gamma^{+/-}$ to IFN-$\gamma^{-/-}$, IFN-$\gamma^{+/-}$ to IFN-$\gamma^{+/-}$). Those mice that had haematopoietic cells, which were capable of producing IFN-γ were capable of rejecting tumours with similar kinetics to the BALB/c wild type mice. It appeared in these two groups that the non-bone marrow derived cells did not play a major role in the rejection mediated by Cy. It was only essential that the donor bone marrow cells be capable of producing IFN-γ and these cells are most

likely responsible for the increase of IFN-γ after 48-72 hours in the serum detected by the CCC assay.

Whilst, there was no rejection of J558L tumours in mice that had received IFN-$\gamma^{-/-}$ haematopoietic cells, there was an interesting response in the IFN-$\gamma^{-/-}$ to IFN-$\gamma^{+/-}$ group. The tumours within this group decreased in size for approximately four days, after which there was expansion of the tumour mass. The total delay of outgrowth was approximately 6 days. The unexpected stay in tumour growth within the IFN-$\gamma^{-/-}$ to IFN-$\gamma^{+/-}$ group led to the hypothesis that matrix bound IFN-γ may influence immune responses.

The two variables in this experiment were the IFN-γ competent non-haematopoietic host cells and an IFN-γ pre-loaded extracellular matrix. It was shown by Lortat-Jacob and colleagues, that the half life ($t_{1/2}$) of circulating IFN-γcould be increased from 1.5 to 99 minutes when it was heparin bound, however the kinetics of matrix bound IFN-γ *in vivo* are presently unknown. This delay in tumour rejection could be due to the release of matrix bound IFN-γ by matrix metalloprotease 9 (MMP-9) produced by polymorphonuclear neutrophils in response to Cy treatment (Hirsh et al., 2004). MMP-9 is important in the proteolytic modelling of the matrix and is known to cleave and release cytokines and chemokines (Ma et al., 2005). However, it is clear that for complete tumour rejection, sustained production of haematopoietic cell derived IFN-γ was required.

While the IFN-γ derived from the haematopoietic system has a relatively short half-life *in vivo*, it is expected that the $t_{1/2}$ of matrix bound IFN-γ *in vivo* would be longer. A mechanism has been proposed whereby the integrity of the C-terminal of IFN-γ that is crucial to biological activity, remains intact from proteolytic cleavage by binding to heparan sulphate (Lortat-Jacob et al., 1996a). Therefore, biological functions of the cytokine might be prolonged *in vivo* through such an interaction (storage reservoir). It was shown that numerous growth factors, including FGFs, insulin growth factor (IGF), TGF-β and VEGFs, which bind to heparan sulphate, can be released from storage and/or be activated from latent forms (Taipale and Keski-Oja, 1997). Stabilisation of IFN-γ with heparan sulfate results in conformational changes of the secondary and tertiary structure enabling better recognition of the molecule by the receptor (Balasubramanian and Ramanathan, 2000). Therefore, it was appropriate to investigate whether IFN-γand heparan sulphate could interact within the tumour matrix.

4.2 THE BINDING AND INFLUENCE OF INTERFERON GAMMA ON THE TUMOUR EXTRACELLULAR MATRIX

In general, the ability of growth factors and various cytokines to bind to the extracellular matrix has been well documented, but it is less clear for IFN-γ. Therefore, to determine the significance of the interaction of IFN-γ with heparan sulphate the evolutionary consensus of the cytokine sequence was investigated. The homology of the basic amino acid cluster responsible for IFN-γ/heparan sulphate interactions between different species was compared (Figure 3, page 11) and was highly conserved. The most variability was seen amongst the two fish species, however the amino acids were still basic. This indicated that it was likely to be functionally important.

Until recently, all previous studies analysing the interactions between IFN-γ and heparan sulphate were determined *in vitro*. Visualisation of the interaction between these molecules in tumour sections was confirmed through confocal microscopy. In order to do this, a number of murine IFN-γantibodies were screened. Caution in interpreting the results of immunohistochemistry has been suggested (van der Loos et al., 2001). In total, van der Loos and colleagues screened 13 anti-human IFN-γ antibodies. Twelve of the thirteen antibodies recognised IFN-γ positive cells only upon stimulation and permeabilisation of the cell membrane with saponin, the group also found staining for smooth muscle cells, endothelial cells, extracellular matrix and CD138 plasma cells. At the time of this publication there was little known regarding the possibility of cytokine interaction with the matrix. As a result they considered the staining to be unspecific. Wrenshall and colleagues demonstrated that the cytokine IL-2 can bind to the heparan sulphate. The tertiary structure of a cytokine is required for ionic and electrostatic contact with the ECM. IL-2 and IFN-γ have similar tertiary structures supporting the possibility of an IFN-γ/ heparan sulphate relationship (Wrenshall and Platt, 1999).

Within the normal tumour microenvironment there is very little IFN-γ present. Therefore, tumour models (J558l-IFN-γ and MC51.9-IFN-γ) in which there was overexpression of this cytokine were used to create a basis for analysis of cytokine negative tumour cells. By doing this, the threshold of staining with XMG1.2 was contained to those areas where there were high IFN-γ deposits. Additionally, as matrix-cytokine interactions were of particular interest,

tumour sections were not treated with saponin. Specific staining of the IFN-γ transfected tumours was confirmed by isotype controls and the fact that cellular IFN-γ was limited to those cells that had been cross-sectioned by the microtome. Additionally, there was no staining in IFN-$\gamma^{-/-}$ mice. The secreted IFN-γ being detected in these tissues could be seen in scattered areas though out the central body and rim of the tumour section.

At least two forms of the basement membrane protein, HSPG, have been identified; a large core protein (> 400 kD) and a small core protein (30 kD). The large HSPG is probably the most abundant basement membrane proteoglycan. It is located predominantly in the lamina lucida, where it forms clustered aggregates and interacts with other basement membrane components to form the matrix. In addition, it also plays a critical role in attachment of cells to the basal membrane via integrin receptors.

Heparan sulphate was bound by the monoclonal antibody A7L6 which specifically recognizes domain IV of the core protein of the large heparan sulphate proteoglycan or perlecan. The reactivity is independent of the galactosaminoglycan moieties. As such the epitope is not sensitive to heparitinase treatment. However, HS chains can be degraded either enzymatically by heparanase or non-enzymatically by nitric oxide (Mani et al., 2004), which is capable of cleaving HS chains at glucosamines lacking N-substitution. Therefore, while the HS signal from the different tumours within the different mice was strong there was noticeable variation in their HS structures. This could be a result of the amount of heparan degrading enzymes produced by the tumour and the mouse.

In co-localisation studies of the two molecules HS and IFN-γ in the J558L-IFN-γ producer, approximately 10-15% of the tumour tissue was stained positive for IFN-γ (by visual assessment of the defined tumour area of over 40 sections), and 60% of that IFN-γ positive area was also heparan sulphate positive. In comparison, approximately 1-3% of the tumour section was positive for IFN-γ and similarly 60% of that IFN-γ co-localised to heparan sulphate in the cytokine negative parental J558L tumours. As expected, the staining for IFN-γ was weaker than the over-expresser, however there was an association between this cytokine and the basement membrane component heparan sulphate. By establishing the parameters of analysis using the J558L-IFN-γ producer as a basis for the confocal protocols, this approach allowed the specific interaction between heparan sulphate and IFN-γ to be seen in the normal microenvironment of J558L tumours.

During the co-localisation studies using the confocal microscope slight differences in the structure of HS were revealed, therefore more detailed analysis was carried out to determine if there were any more structural alterations in the tumour matrices of IFN-$\gamma^{-/-}$ and WT mice. IFN-γ is known to suppress matrix protein deposition (Niwa et al., 2004). Genes involved in matrix metabolism that are negatively regulated by IFN-γ include MMP 1, -9, -13 and stromelysin and type II collagen. However, the relevance of these differences for the tumour microenvironment remains unclear.

Whilst there are no macroscopic differences in the organogenesis or development of the cells of the immune system in IFN-γ gene deficient mice, there appears to be diminished capacity to respond to infection and immunological stimuli. The tumour stroma is known to be an important target in aiding tumour rejection. The extracellular microenvironment is constantly being modified by matrix metalloproteinases and therefore is an active component of the tumour. It is highly likely that there would be microscopic differences within the tumour stroma of gene deficient and competent mice. Histological analysis of two different tumour types (J558L and TS/A) revealed the presence of a panel of molecules of the ECM that are important in the structural integrity of tumours (Collagen 1-4, heparan sulphate). However, there were minor differences in the characteristics of the molecules between IFN-γ competent and deficient mice. It is known from gene transcript studies that large amounts of IFN-γ are required to modify protein expression of collagens (Diaz and Jimenez, 1997), and heparan sulphate (Sharma and Iozzo, 1998), therefore, as there are limited amounts of circulating IFN-γ within tumour bearing IFN-γ competent mice, only subtle differences can be seen. This would account for the thin sheets of heparan sulphate and collagens in the tumours implanted in immuno-competent mice compared with the thick, dense deposits in the tumours of gene deficient mice.

Additional confirmation of the HS/IFN-γ interaction was provided by matrigel plug accumulation of human IFN-γ, which could be detected *ex vivo* by ELISA up to 24 hours after injection. The advantage of this system was that the human IFN-γ could bind to murine heparan sulphate (Lortat-Jacob et al., 1991) but not the murine cell surface IFN-γ receptor (Farrar and Schreiber, 1993). This experiment provided additional evidence that IFN-γ could be stored *in vivo* as a non-receptor bound cytokine (Lortat-Jacob et al., 1991). The results suggested that there were significant differences between the gene deficient and competent

mice, which could affect IFN-γ accumulation *in vivo*. Consequently, *in vivo* analysis was carried out by iodinating human IFN-γ as it provided a more sensitive level of detection than immunohistochemistry. The iodination was achieved by chloramine T and not the Bolton Hunter method commonly used in cytokine labelling. Bolton Hunter usually labels the arginines and lysines, which in this case are essential for IFN-γ binding to heparan sulphate, therefore the tyrosines were labelled instead using chloramine T.

The amount of I^{125} labelled IFN-γ found in the blood was low (between 4-6%) indicating that there was rapid clearance or blood to tissue transfer, which confirmed previous findings (Lortat-Jacob et al., 1996b). Previously it had been described that the key time point in determining organ accumulation was 1 hour. As cytokine retention capability was of particular interest, analysis of I^{125}-IFN-γ in organs was also made at 24 hours. At the early time point of one hour after injection there was significantly more accumulation of IFN-γ in the tumours of knockout mice compared with their wild type litter-mates. This was indicative of competition between endogenous IFN-γ in the WT mice for the extracellular binding sites.

Day 5 tumours had higher accumulation of I^{125}-IFN-γ compared to their day 8 counterparts, 1 hour after cytokine transfer in both gene deficient (three fold) and competent (two fold) groups. Whilst the standard deviation remained high for the knockout mice there were still clear differences. Early tumours are highly vascularised and matrix deposition has just begun. Therefore, this could account for the high signal from day 5 gene deficient mice where there was no competition for heparan sulphate binding sites and there was a high percentage dose per gram ratio. The differences in the tumour matrix of the IFN-$\gamma^{-/-}$ mice compared to their WT counterparts might also contribute to the higher accumulation of human I^{125}-IFN-γ in the IFN-$\gamma^{-/-}$ mice as a result of the structural differences as discussed earlier.

Accumulation of radioactive cytokine in the tumour is significantly different to other organs due to large deposits of basement membrane matrix, which make up the major part of the tumour body. The presence of I^{125}-IFN-γ in organs (spleen, liver, kidney, heart, lung and tumour) 24 hours and 72 hours after injection were analysed, however no significant differences between the knockout and wild type mice was seen. The fact that by 24 hours there is significant reduction in the amount of IFN-γ present in the organs might indicate that there is rapid turnover of the cytokine.

For the first time binding and accumulation *in vivo* of IFN-γ to heparan sulphate of the tumour matrix was shown. However, the exact function of this interaction remains unclear. Heparan sulphate glycosaminoglycans, present at the cell surface and the extracellular matrix that surrounds cells are important mediators of biological processes. Furthermore, it has become apparent that cells dynamically regulate the structure of their heparan sulphate "coat" to differentially regulate extracellular signals (Liu et al., 2002), or regulate matrix homeostasis (Taipale and Keski-Oja, 1997). The histological confirmation of the electrostatic interaction between IFN-γ and heparin sulphate *in vivo*, indicated a possible functional relationship as a result of contact between the two molecules. Therefore, the purpose and relevance of this interaction was investigated by interfering with the non-receptor mediated binding of IFN-γ to the matrix.

4.3 THE BLOCKADE OF HEPARAN SULPHATE AND INTERFERON GAMMA INTERACTIONS WITHIN THE TUMOUR STROMA

IFN-γ is theoretically capable of interacting with heparan sulphate within the matrix and on the endothelial vasculature (Yard et al., 1998), however reports vary regarding the function of bound IFN-γ. Heparin bound IFN-γ has been shown to have an inhibitory outcome on MHC class II expression as well as antiviral and anti-parasitic actions (Daubener et al., 1995). Contra to this, immobilised plate bound IFN-γ molecules have been shown to induce HLA-DR expression on COLO-205 tumour cells (Fernandez-Botran et al., 1999), suggesting cell surface GAGs could present IFN-γ to its receptor and that there was an important regulatory role for heparan sulphate on the activity of IFN-γ *in vivo*.

In an effort to determine the functional consequences of inhibiting IFN-γ binding to heparan sulphate, a peptide was generated by Fernandez-Botran and co-workers, 1999, from the small basic amino acid sequence (murine IFN-$\gamma_{128-135}$) at the C-terminal end of IFN-γ. This sequence is responsible for the electrostatic interaction with heparan sulphate and this cluster was additionally identified as crucial in increasing the on rate of the IFN-γ/IFN-γ-R binding reaction (Sadir et al., 1998). Therefore, confirmation of the functional inhibition *in vitro* of the murine peptide (LRKRKRSR) was required in order to determine whether a response could

possibly be analysed *in vivo*. It was evident that the peptide was capable of preventing human I^{125}-IFN-γ binding to plate-bound heparan sulphate within the matrigel *in vitro*. This was the first time that inhibition was shown in relation to matrigel, as previously the assay was carried out with purified plate-bound heparan sulphate (Fernandez-Botran et al., 2002). In order to study the effects of the peptide *in vivo*, plasmids were constructed that were capable of secreting the peptide from transfected J558L tumour cells.

The murine IFN-$\gamma_{128-135}$ sequence was inserted into the pSecTag-2 plasmid under the control of the EF1-α promoter. Substitution of the original CMV promoter was necessary as it becomes methylated and consequently shuts down *in vivo* (French Anderson, 1994). Additionally, EF1-α is known to be a strong promoter of gene expression (Tokushige et al., 1997). Four plasmids were constructed due to evidence suggesting that histidine repeats can bind to heparin and heparan sulphate with high affinity (Jones et al., 2005). Hereby masking the cleavage sites of the heparan sulphate chains recognised by the β-D-endoglycosidase heparanase.

The supernatants from the cell lines expressing the MC-2 peptide were capable of inhibiting the binding of human I^{125}-IFN-γ to matrigel *in vitro*, when compared to the non-expressing MC-2 controls and the untransfected parental tumour line. These results confirmed the functional significance of the murine IFN-$\gamma_{128-135}$ peptide sequence in preventing the binding of I^{125}-IFN-γ *in vitro*. Hence, production of the peptide from the tumours was confirmed, and the influence of blocking the HS/IFN-γ interaction by the tumour lines was investigated *in vivo* in the Cy model.

Non-receptor binding may be related to several aspects of cytokine activity and may have physiological consequences. Thus, in concordance with the previous functional experiments using cyclophosphamide, the transfected tumours were subjected to the same protocol. The cell lines all appeared to grow with similar kinetics *in vitro* and *in vivo*, however the $Alanine^{8}$ secreting tumours always grew slightly faster. At the same time, mice bearing the parental J558L tumour were treated daily with 1mg of the murine IFN-$\gamma_{128-135}$ peptide. Tumours were slightly smaller compared with untreated parental tumours. This may have been a result of the inflammatory response to the daily MC-2 peptide injections or that the peptide may have prevented the non-receptor mediated binding of the IFN-γ molecule and therefore could contribute to its influence on growth and the subsequent clearance of the cytokine.

Tumours expressing the MC-2 fragment were not rejected when treated with Cy at day 11. There was a slight reduction in tumour mass but the tumour continued to grow out. Among the mice of the J558L-pTAG group only 35% of the challenged mice were capable of rejecting the tumour which may have been due to the influence of the 6-HIS-repeat sequence that might have prevented remodelling and cleavage of the heparan sulphate side chains (Jones et al., 2005) in response to Cy treatment. Mice challenged with the J558L-pAlanine-NoTAG tumour did not reject the tumour. The neutral alanine fragment is unlikely to have bound to the matrix through electrostatic or ionic interactions as the frame-shifted tail sequence is relatively uncharged. Some other component of the plasmid backbone may have influenced the way in which J558L tumour cells would normally be rejected by Cy. Recently, it was shown that data obtained from plasmids containing the Zeocin resistance marker could be misleading as Zeocin could not be completely detoxified by the *Sh ble* gene and was still capable of cleaving DNA (Trastoy et al., 2005). Ultimately, recombinant cells could have cumulative damages indicating that their genomic integrity and metabolism may have been altered. Whilst there appears to be an effect of the murine IFN-$\gamma_{128\text{-}135}$ peptide as seen by the I^{125} IFN-γ binding assay, the role of IFN-γand heparan sulphate interactions in this model remains to be further investigated. Ultimately, the development of a mouse in which the IFN-γ molecule could bind to heparan sulphate and not to the receptor (or vice-versa) would enable the role of this interaction to be fully understood in relation to Cy mediated tumour rejection.

By using a chemotherapy induced, immune response mediated tumour rejection model the critical importance of haematopoietic cell induced IFN-γ was elucidated. For the first time, it has been demonstrated that IFN-γ levels were elevated in the serum after Cy treatment and the presence of matrix bound IFN-γ *in vivo* was described. Additionally, the accumulation of radioactive human IFN-γ in the tumour stroma, *in vivo*, confirmed and proved the presence of non receptor mediated binding of the cytokine and that this accumulation could be inhibited in the presence of the peptide fragment MC-2 (LRKRKRSR). Whilst the effect of inhibiting IFN-γ/HS interactions in the plasmid transfected tumour model remains unclear at present, the importance of heparan sulphate within the Cy tumour model could be investigated using perlecan knock out mice. At present these mice are not on the BALB/c background and would need to be backcrossed.

The existence of this species conserved C-terminal sequence that facilitates IFN-γ binding to the matrix indicates that there may be an important function for this interaction. Evidence from the allotransplantation experiments carried out by Fernandez-Botran and coworkers, 2001, indicate that there may be an impaired immune response due to the presence of the MC-2 peptide (Fernandez-Botran et al., 2002), however its function within this Cy dependent tumour rejection model remains unclear. Lastly, it is clear that for tumour rejection IFN-γ is required, however haematopoietic cell induced and matrix bound IFN-γ may not be mutually exclusive and could possibly function together to generate an adequate anti-tumour immune response.

5 SUMMARY

Interferon gamma (IFN-γ) is a pro-inflammatory cytokine that is produced primarily by T and NK cells. Previously, it has been shown that IFN-γ is necessary for cyclophosphamide mediated tumour rejection, however, the source of this IFN-γ remained unclear. The aim of this work was to identify the source and characterise the role of IFN-γ in this scenario. Using the Cincinnati Cytokine Capture Assay it was shown for the first time that the IFN-γ serum levels steadily increased over a 96 hour time period after cyclophosphamide administration. Furthermore, with the help of bone marrow chimeras, I was able to show that IFN-γ required for tumour rejection was produced by haematopoietic cells. Interestingly, there was a delay in tumour outgrowth in bone marrow chimeras that had received IFN-γ deficient bone marrow cells when compared to IFN-γ deficient mice. I concluded that there must have been an additional source of IFN-γ and therefore extended the investigation.

The ability of IFN-γ to bind to matrix proteins such as heparan sulphate *in vitro* has been reported. The binding of IFN-γ to the extracellular matrix *in vivo* has so far not been shown. Therefore, I investigated whether matrix bound IFN-γ was responsible for the growth delay observed in IFN-$\gamma^{-/-}$ to IFN-$\gamma^{+/-}$ bone marrow chimeras. Using confocal microscopy I was able to show that IFN-γ could bind to heparan sulphate in various tumour models. In a xenotypic model I used human IFN-γ in mice. The advantage of this system was that the human IFN-γ could bind to murine heparan sulphate but not the murine cell surface receptor. I could confirm the binding of human IFN-γ to heparan sulphate, as it had accumulated in matrigel plugs. Additionally, using human I^{125} IFN-γ, binding and accumulation to heparan sulphate of the tumour matrix was shown for the first time. The electrostatic co-operation between IFN-γ and heparin sulphate *in vivo* supported the possibility there was functionality as a result of contact between the two molecules.

In an effort to determine the functional consequences of inhibiting IFN-γ binding to heparan sulphate, I made use of a previously identified peptide that was generated based on the highly conserved, small basic amino acid sequence (murine IFN-$\gamma_{128\text{-}135}$) at the C-terminal end of IFN-γ. This peptide has been shown to block *in vitro* binding of IFN-γ to heparan sulphate. In order to study the effects of the peptide *in vivo*, plasmid transfected J558L tumour cells were constructed that secreted the peptide. Tumours that expressed the peptide could not be

rejected after cyclophosphamide treatment. However, rejection of the empty vector control tumours was also not complete.

This work demonstrates that haematopoietic cells are responsible for the production of IFN-γ required for complete rejection of the tumour in our model, that there is a steady increase of IFN-γ during the first 4 days after cyclophosphamide treatment, that IFN-γ binding to the extracellular matrix occurs *in vivo* (this interaction can be partially inhibited by the MC-2 peptide), and that IFN-γ influences matrix deposition. Since the results of the functional experiments using this model are inconclusive, further investigational modifications will be required.

6 ZUSAMMENFASSUNG

Interferon gamma (IFN-γ) ist ein pro-inflammatorisches Zytokin, das primär durch T- und NK-Zellen gebildet wird. Es wurde kürzlich berichtet, dass IFN-γ für eine durch Cyclophosphamid-vermittelte Tumorabstoßung notwendig ist. Die Quelle dieses IFN-γ blieb jedoch unklar. Das Ziel dieser Arbeit war, diese Quelle zu identifizieren und die Rolle des IFN-γ in diesem Szenario zu charakterisieren. Mit dem Cincinnati Zytokin Capture Assay konnte ich zum ersten Mal zeigen, dass die IFN-γ Serumspiegel über einen Zeitraum von 96 Stunden nach der Verabreichung von Cyclophosphamid kontinuierlich anstiegen. Des Weiteren konnte ich mit Hilfe von Knochenmarks-Chimären zeigen, dass das IFN-γ, welches für die Tumorabstoßung erforderlich war, durch hämotopoetische Zellen gebildet wurde. Interessanterweise gab es im Vergleich zu IFN-γ-defizienten Mäusen eine Verzögerung im Tumorwachstum der Knochenmarks-Chimären, die IFN-γ-defiziente Knochenmarkzellen erhalten hatten. Ich schloss daraus, dass es eine zusätzliche Quelle von IFN-γ geben musste, und erweiterte daher die Untersuchung.

Über die Fähigkeit von IFN-γ, Matrix-Proteine wie Heparan-Sulfat *in vitro* zu binden, wurde berichtet. Die Bindung von IFN-γ an die extrazelluläre Matrix *in vivo* war bisher nicht gezeigt worden. Daher untersuchte ich, ob Matrix-gebundenes IFN-γ für das langsamere Wachstum, das ich in IFN-$\gamma^{-/-}$ gegenüber IFN-$\gamma^{+/-}$ Knochenmarks-Chimären beobachtet hatte, verantwortlich war. Durch konfokale Mikroskopie konnte ich zeigen, dass IFN-γ in verschiedenen Tumormodellen Heparan-Sulfat binden konnte. In einem xenotypischen Modell verwendete ich humanes IFN-γ in Mäusen. Der Vorteil dieses Systems war, dass das humane IFN-γ zwar Maus-Heparan-Sulfat, nicht jedoch die Zelloberflächenrezeptoren der Maus binden konnte. Ich konnte die Bindung von humanem IFN-γ an Heparan-Sulfat, wie es in Matrigel Plugs akkumuliert war, bestätigen. Zusätzlich konnte ich durch humanes I^{125} IFN-γ erstmalig die Bindung und Akkumulation an Heparan-Sulfat der Tumor-Matrix zeigen. Die elektrostatische Wechselwirkung zwischen IFN-γ und Heparan-Sulfat *in vivo* deutet darauf hin, dass Funktionalität als Ergebnis eines Kontaktes zwischen den zwei Molekülen vorhanden war.

In einem Versuch, die funktionellen Konsequenzen der Inhibition der Wechselwirkung zwischen IFN-γ Heparan-Sulfat aufzuklären, verwendete ich ein kürzlich identifiziertes Peptid, das von der hoch konservierten Aminosäurensequenze am C-Terminal-Ende von IFN-

γ (Maus-IFN-$\gamma_{128-135}$) abgeleitet worden war und das reich an kleinen basischen Aminosäuren ist. Es zeigte sich, dass dieses MC-2 Peptid die *in vitro* Bindung von IFN-γ an Heparan-Sulfat blockierte. Um die Effekte dieses Peptids *in vivo* untersuchen zu können, wurden transfizierte J558L Tumorzellen hergestellt, welche die Peptide absonderten. Tumore, die Peptide exprimierten, konnten nach Cyclophosphamid-Behandlung nicht abgestoßen werden. Jedoch war ebenso die Abstoßung der Kontrolltumore nicht vollständig.

Diese Arbeit demonstriert, dass hämatopoetische Zellen für die Produktion von IFN-γ, welches für die komplette Tumorabstoßung in unserem Modell benötigt wird, verantwortlich sind, dass es einen kontinuierlichen Anstieg von IFN-γ während der ersten vier Tage nach Cyclophosphamid-Behandlung gibt, dass die IFN-γ-Bindung an die extrazelluläre Matrix auch *in vivo* stattfindet (diese Interaktion kann durch das MC-2 Peptid partiell inhibiert werden), und dass INF-γ die Zusammensetzung der Matrix beeinflusst. Da die Ergebnisse der funktionalen Experimente, die dieses Model verwenden, nicht eindeutig sind, sind weitere, modifizierte Untersuchungen erforderlich.

7 ADDITIONAL ABBREVIATIONS

aa	Amino acid
BM	Basement membrane
BMC	Bone marrow chimera
bp	Base pair
C	Carboxyl
Cpm	Counts per minute
Cy	Cyclophosphamide
DAB	Diaminobenzidine
DMEM	Dulbeccos modified Eagles medium
DNA	Deoxyribonucleic acid
ECM	Extracellular matrix
EGF	Epidermal growth factor
EHS	Engelbreth Holm Swarm
FCS	Foetal calf serum
FGF	Fibroblast growth factor
GAG	Glycosaminoglycan
GAS	Gamma activated sequences
Gy	Gray
HPLC	High performance liquid chromotography
HS	Heparan sulphate
HSPG	Heparan sulphate proteoglycan
IFN-γ	Interferon gamma
IFN-γR	Interferon gamma receptor
IGF	Insulin growth factor
IL-2	Interleukin-2
IL-4	Interleukin-4
IL-8	Interleukin 8
JAK	Janus tyrosine kinases
kb	Kilobase
K_d	Dissociation constant
kg	Kilogram
LB	Luria Bertani
M	Marker
mAb	Monoclonal antibody
MCA	Methylcholanthrene
MCP	Macrophages chemotactic proteins
mg	Milligram
MHC	Major histocompatability complex
ml	Millilitre
MMP	Matrix metalloproteases
N	Amino
ng	Nanogram
NK	Natural killer
PBMC	Peripheral blood monocyte cells
PCR	Polymerase chain reaction
PDGF	Platelet derived growth factor
PG	Proteoglycan

pg	Picogram
SAV	Streptavidin-HRP conjugate
SLRP	Small leucine rich repeats
STAT-1α	Signal transducer and activator of transcription-1α
$t_{1/2}$	half-life
TAF	Tumour-associated fibroblast
Taq	Thermus aquaticus
TGF-β1	Transforming growth factor beta
VEGF	Vascular endothelial growth factor
µg	Microgram
WT	Wild type

8 REFERENCES

Awwad, M., and North, R. J. (1988). Cyclophosphamide (Cy)-facilitated adoptive immunotherapy of a Cy-resistant tumour. Evidence that Cy permits the expression of adoptive T-cell mediated immunity by removing suppressor T cells rather than by reducing tumour burden. Immunology *65*, 87-92.

Azouz, A., Razzaque, M., El-Hallak, M., and Taguchi, T. (2004). Immunoinflammatory response and fibrogenesis. Med Electron Microsc *37*, 141-148.

Balasubramanian, V., and Ramanathan, M. (2000). Glycosaminoglycans alter the conformation of interferon-gamma. Cytokine *12*, 466-471.

Becker, C., Pohla, H., Frankenburger, B., Schuler, T., Assenmacher, M., Schendel, D. J., and Blankenstein, T. (2001). Adoptive tumor therapy with T lymphocytes enriched through and IFN-γ capture assay. Nat Med *7*, 1159-1162.

Berd, D., Mastrangelo, M. J., Engstrom, P. F., Paul, A., and Maguire, H. (1982). Augmentation of the human immune response by cyclophosphamide. Cancer Res *42*, 4862-4866.

Billiau, A., Heremans, H., Vermeire, K., and Matthys, P. (1998). Immunomodulatory properties of interferon-gamma. An update. Ann N Y Acad Sci *856*, 22-32.

Blankenstein, T., and Qin, Z. (2003). The role of IFN-γ in tumor transplantation immunity and inhibition of chemical carcinogenesis. Curr Opin Immunol *15*, 148-154.

Capila, I., and Lindhardt, R. J. (2002). Heparin - Protein Interactions. Angew Chem Int Ed Engl *41*, 390-412.

Cavallo, F., Martin-Fontecha, A., Bellone, M., Heltai, E., Tornaghi, P., Freschi, M., Forni, G., Dellabona, P., and Casorati, G. (1995). Co-expression of B7-1 and ICAM-1 on tumors is required for rejection and the establishment of a memory response. Eur J Immunol *25*, 1154-1162.

Chiocca, E. A. (1995). Brain tumor therapy in mice with a novel "suicide" gene: The cyclophosphamide-activating CYP2B1 gene).

Dalton, D. K., Pitts-Meek, S., Keshav, S., Figari, I. S., Bradley, A., and Stewart, T. A. (1993). Multiple defects of immune cell function in mice with disrupted interferon-gamma genes. Science *259*, 1739-1742.

Daubener, W., Nockemann, S., Gutsche, M., and Hadding, U. (1995). Heparin inhibits the antiparasitic and immune modulatory effects of human recombinant interferon-gamma. Eur J Immunol *25*, 688-692.

De Wever, O., and Mareel, M. (2003). Role of tissue stroma in cancer cell invasion. J Pathol *200*, 429-447.

Diaz, A., and Jimenez, S. A. (1997). Interferon-gamma regulates collagen and fibronectin gene expression by transcriptional and post-transcriptional mechanisms. Int J Biochem Cell Biol *29*, 251-260.

Dighe, A. S., Richards, E., Old, L. J., and Schreiber, R. D. (1994). Enhanced in vivo growth and resistance to rejection of tumor cells expressing dominant negative IFN gamma receptors. Immunity *1*, 447-456.

Douglas, M. S., Rix, D. A., Dark, J. H., Talbot, D., and Kirby, J. A. (1997). Examination of the mechanism by which heparin antagonizes activation of a model endothelium by interferon-gamma (IFN-gamma). Clin Exp Immunol *107*, 578-584.

Dvorak, H. F. (1986). Tumors: wounds that do not heal. Similarities between tumor stroma generation and wound healing. N Engl J Med *315*, 1650-1659.

Elenbaas, B., and Weinberg, R. A. (2001). Heterotypic signaling between epithelial tumor cells and fibroblasts in carcinoma formation. Exp Cell Res *264*, 169-184.

Farrar, M. A., and Schreiber, R. D. (1993). The molecular cell biology of interferon-gamma and its receptor. Annu Rev Immunol *11*, 571-611.

Fernandez-Botran, R., Gorantla, V., Sun, X., Ren, X., Perez-Abadia, G., Crespo, F. A., Oliver, R., Orhun, H. I., Quan, E. E., Maldonado, C.*, et al.* (2002). Targeting of glycosaminoglycan-cytokine interactions as a novel therapeutic approach in allotransplantation. Transplantation *74*, 623-629.

Fernandez-Botran, R., Romanovskis, P., Sun, X., and Spatola, A. F. (2004). Linear basic peptides for targeting interferon-gamma-glycosaminoglycan interactions: synthesis and inhibitory properties. J Pept Res *63*, 56-62.

Fernandez-Botran, R., Yan, J., and Justus, D. E. (1999). Binding of interferon gamma by glycosaminoglycans: a strategy for localization and/or inhibition of its activity. Cytokine *11*, 313-325.

Finkelman, F. D., and Morris, S. C. (1999). Development of an assay to measure in vivo cytokine production in the mouse. Int Immunol *11*, 1811-1818.

French Anderson, W. (1994). Making clinical grade gene therapy vectors. Hum Gene Ther *5*, 925-926.

Gallagher, J. T., and Walker, A. (1985). Molecular distinctions between heparan sulphate and heparin. Analysis of sulphation patterns indicates that heparan sulphate and heparin are separate families of N-sulphated polysaccharides. Biochem J *230*, 665-674.

Hengst, J. C., Mokyr, M. B., and Dray, S. (1980). Importance of timing in cyclophosphamide therapy of MOPC-315 tumor-bearing mice. Cancer Res *40*, 2135-2141.

Hirsh, M., Carmel, J., Kaplan, V., Levine, E., and Krausz, M. M. (2004). Activity of lung neutrophils and matrix metalloproteinases in cyclophosphamide-treated mice with experimental sepsis. Int J Exp Path *85*, 147-157.

Hock, H., Dorsch, M., Kunzendorf, U., Qin, Z., Diamantstein, T., and Blankenstein, T. (1993). Mechanisms of rejection induced by tumor cell-targeted gene transfer of interleukin 2, interleukin 4, interleukin 7, tumor necrosis factor, or interferon gamma. Proc Natl Acad Sci U S A *90*, 2774-2778.

Ibe, S., Qin, Z., Schuler, T., Preiss, S., and Blankenstein, T. (2001). Tumor rejection by disturbing tumor stroma cell interactions. J Exp Med *194*, 1549-1559.

Iivanainen, E., Kahari, V. M., Heino, J., and Elenius, K. (2003). Endothelial cell-matrix interactions. Microsc Res Tech *60*, 13-22.

Iozzo, R. V. (1998). Matrix proteoglycans: from molecular design to cellular function. Annu Rev Biochem *67*, 609-652.

Iozzo, R. V., and San Antonio, J. D. (2001). Heparan sulfate proteoglycans: heavy hitters in the angiogenesis arena. J Clin Invest *108*, 349-355.

Jain, R. K., and Duda, D. G. (2003). Role of bone marrow-derived cells in tumor angiogenesis and treatment. Cancer Cell *3*, 515-516.

Jiang, X., and Couchman, J. R. (2003). Perlecan and tumor angiogenesis. J Histochem Cytochem *51*, 1393-1410.

Jones, A. L., Hulett, M. D., and Parish, C. R. (2005). Histidine-rich glycoprotein: A novel adaptor protein in plasma that modulates the immune, vascular and coagulation systems. Immunol Cell Biol *83*, 106-118.

Kalluri, R. (2003). Basement membranes: structure, assembly and role in tumour angiogenesis. Nat Rev Cancer *3*, 422-433.

Klein, G., and Klein, E. (2005). Surveillance against tumors - is it mainly immunological? Immunol Lett *100*, 29-33.

Klein, G., Vellenga, E., Fraaije, M. W., Kamps, W. A., and de Bont, E. S. (2004). The possible role of matrix metalloproteinase (MMP)-2 and MMP-9 in cancer, e.g. acute leukemia. Crit Rev Oncol Hematol *50*, 87-100.

Li, A. C., and Thompson, R. P. (2003). Basement membrane components. J Clin Pathol *56*, 885-887.

Liu, D., Shriver, Z., Venkataraman, G., El Shabrawi, Y., and Sasisekharan, R. (2002). Tumor cell surface heparan sulfate as cryptic promoters or inhibitors of tumor growth and metastasis. Proc Natl Acad Sci U S A *99*, 568-573.

Lortat-Jacob, H., Baltzer, F., and Grimaud, J. A. (1996a). Heparin decreases the blood clearance of interferon-gamma and increases its activity by limiting the processing of its carboxyl-terminal sequence. J Biol Chem *271*, 16139-16143.

Lortat-Jacob, H., Brisson, C., Guerret, S., and Morel, G. (1996b). Non-receptor-mediated tissue localization of human interferon-gamma: role of heparan sulfate/heparin-like molecules. Cytokine *8*, 557-566.

Lortat-Jacob, H., and Grimaud, J. A. (1991). Interferon-gamma C-terminal function: new working hypothesis. Heparan sulfate and heparin, new targets for IFN-gamma, protect, relax the cytokine and regulate its activity. Cell Mol Biol *37*, 253-260.

Lortat-Jacob, H., and Grimaud, J. A. (1992). Binding of interferon-gamma to heparan sulfate is restricted to the heparin-like domains and involves carboxylic--but not N-sulfated--groups. Biochim Biophys Acta *1117*, 126-130.

Lortat-Jacob, H., Grosdidier, A., and Imberty, A. (2002). Structural diversity of heparan sulfate binding domains in chemokines. Proc Natl Acad Sci U S A *99*, 1229-1234.

Lortat-Jacob, H., Kleinman, H. K., and Grimaud, J. A. (1991). High-affinity binding of interferon-gamma to a basement membrane complex (matrigel). J Clin Invest *87*, 878-883.

Lubineau, A., Lortat-Jacob, H., Gavard, O., Sarrazin, S., and Bonnaffe, D. (2004). Synthesis of tailor-made glycoconjugate mimetics of heparan sulfate that bind IFN-gamma in the nanomolar range. Chemistry *10*, 4265-4282.

Lutsiak, M. E., Semnani, R. T., De Pascalis, R., Kashmiri, S. V., Schlom, J., and Sabzevari, H. (2005). Inhibition of CD4(+)25+ T regulatory cell function implicated in enhanced immune response by low-dose cyclophosphamide. Blood *105*, 2862-2868.

Ma, Z., Chang, M. J., Shah, R. C., and Benveniste, E. N. (2005). Interferon-{gamma}-activated STAT-1{alpha} suppresses MMP-9 gene transcription by sequestration of the coactivators CBP/p300. J Leukoc Biol.

Mani, K., Cheng, F., Sandgren, S., Van der Born, J., Havsmark, B., Ding, K., and L.A, F. (2004). The heparan sulfate-specific epitope 10E4 is NO-sensitive and partly inaccessible in glypican-1. Glycobiology *14*, 599-607.

Matar, P., Rozados, V. R., Gervasoni, S. I., and Scharovsky, G. O. (2002). Th2/Th1 switch induced by a single low dose of cyclophosphamide in a rat metastatic lymphoma model. Cancer Immunol Immunother *50*, 588-596.

Mocellin, S., Wang, E., and Marincola, F. M. (2001). Cytokines and immune response in the tumor microenvironment. J Immunother *24*, 392-407.

Nanni, P., de Giovanni, C., Lollini, P. L., Nicoletti, G., and Prodi, G. (1983). TS/A: a new metastasizing cell line from a BALB/c spontaneous mammary adenocarcinoma. Clin Exp Metastasis *1*, 373-380.

Niwa, T., Wada, H., Ohashi, H., Iwamoto, N., Ohta, H., Kirii, H., Fujii, H., Saito, K., and Seishima, M. (2004). Interferon-gamma produced by bone marrow-derived cells attenuates atherosclerotic lesion formation in LDLR-deficient mice. J Atheroscler Thromb *11*, 79-87.

Noonan, D. M., Fulle, A., Valente, P., Cai, S., Horigan, E., Sasaki, M., Yamada, Y., and Hassell, J. R. (1991). The complete sequence of perlecan, a basement membrane heparan sulfate proteoglycan, reveals extensive similarity with laminin A chain, low density lipoprotein-receptor, and the neural cell adhesion molecule. J Biol Chem *266*, 22939-22947.

Nurcombe, V., Ford, M. D., Wildschut, J. A., and Bartlett, P. F. (1993). Developmental regulation of neural response to FGF-1 and FGF-2 by heparan sulfate proteoglycan. Science *260*, 103-106.

O'Reilly, M. S., Holmgren, L., Shing, Y., Chen, C., Rosenthal, R. A., Moses, M., Lane, W. S., Cao, Y., Sage, E. H., and Folkman, J. (1994). Angiostatin: a novel angiogenesis inhibitor that mediates the suppression of metastases by a Lewis lung carcinoma. Cell *79*, 315-328.

Pass, G. J., Carrie, D., Boylan, M., Lorimore, S., Wright, E., Houston, B., C.J., H., and Wolf, C. R. (2005). Role of hepattic cytochrome P450s in the pharmacokinetics and toxicity of cyclophosphamide: Studies with the hepatic cytochrome P450 reductase null mouse. Cancer Res *65*, 4211-4217.

Philip, M., Rowley, D. A., and Schreiber, H. (2004). Inflammation as a tumor promoter in cancer induction. Semin Cancer Biol *14*, 433-439.

Pupa, S. M., Menard, S., Forti, S., and Tagliabue, E. (2002). New insights into the role of extracellular matrix during tumor onset and progression. J Cell Physiol *192*, 259-267.

Qiao, D., Meyer, K., Mundhenke, C., Drew, S. A., and Friedl, A. (2003). Heparan sulfate proteoglycans as regulators of fibroblast growth factor-2 signaling in brain endothelial cells. Specific role for glypican-1 in glioma angiogenesis. J Biol Chem *278*, 16045-16053.

Qin, Z., and Blankenstein, T. (2000). CD4+ T cell--mediated tumor rejection involves inhibition of angiogenesis that is dependent on IFN gamma receptor expression by nonhematopoietic cells. Immunity *12*, 677-686.

Qin, Z., Schwartzkopff, J., Pradera, F., Kammertoens, T., Seliger, B., Pircher, H., and Blankenstein, T. (2003). A critical requirement of interferon gamma-mediated angiostasis for tumor rejection by CD8+ T cells. Cancer Res *63*, 4095-4100.

Sadir, R., Forest, E., and Lortat-Jacob, H. (1998). The heparan sulfate binding sequence of interferon-gamma increased the on rate of the interferon-gamma-interferon-gamma receptor complex formation. J Biol Chem *273*, 10919-10925.

Sadir, R., Lortat-Jacob, H., and Morel, G. (2000). Internalization and nuclear translocation of IFN-gamma and IFN-gammaR: an ultrastructural approach. Cytokine *12*, 711-714.

Sasisekharan, R., Shriver, Z., Venkataraman, G., and Narayanasami, U. (2002). Roles of heparan-sulphate glycosaminoglycans in cancer. Nat Rev Cancer *2*, 521-528.

Seljelid, R., Jozefowski, S., and Sveinbjornsson, B. (1999). Tumor stroma. Anticancer Res *19*, 4809-4822.

Sharma, B., and Iozzo, R. V. (1998). Transcriptional silencing of perlecan gene expression by interferon-gamma. J Biol Chem *273*, 4642-4646.

Silzle, T., Randolph, G. J., Kreutz, M., and Kunz-Schughart, L. A. (2004). The fibroblast: sentinel cell and local immune modulator in tumor tissue. Int J Cancer *108*, 173-180.

Somasundaram, R., Ruehl, M., Tiling, N., Ackermann, R., Schmid, M., Riecken, E. O., and Schuppan, D. (2000). Collagens serve as an extracellular store of bioactive interleukin 2. J Biol Chem *275*, 38170-38175.

Stamenkovic, I. (2003). Extracellular matrix remodelling: the role of matrix metalloproteinases. J Pathol *200*, 448-464.

Subramaniam, P. S., Larkin, J., 3rd, Mujtaba, M. G., Walter, M. R., and Johnson, H. M. (2000). The COOH-terminal nuclear localization sequence of interferon gamma regulates STAT1 alpha nuclear translocation at an intracellular site. J Cell Sci *113 (Pt 15)*, 2771-2781.

Subramaniam, P. S., Mujtaba, M. G., Paddy, M. R., and Johnson, H. M. (1999). The carboxyl terminus of interferon-gamma contains a functional polybasic nuclear localization sequence. J Biol Chem *274*, 403-407.

Taipale, J., and Keski-Oja, J. (1997). Growth factors in the extracellular matrix. Faseb J *11*, 51-59.

Tokushige, K., Moradpour, D., Wakita, T., Geissler, M., Hayashi, N., and Wands, J. R. (1997). Comparison between cytomegalovirus promoter and elongation factor-1 alpha

promoter-driven constructs in the establishment of cell lines expressing hepatitis C virus core protein. J Virol Methods *64*, 73-80.

Trastoy, M. O., Defais, M., and Larminat, F. (2005). Resistance to the antibiotic Zeocin by stable expression of the Sh ble gene does not fully suppress Zeocin-induced DNA cleavage in human cells. Mutagenesis *20*, 111-114.

Tsung, K., Meko, J. B., Tsung, Y. L., Peplinski, G. R., and Norton, J. A. (1998). Immune response against large tumors eradicated by treatment with cyclophosphamide and IL-12. J Immunol *160*, 1369-1377.

van der Loos, C. M., Houtkamp, M. A., de Boer, O. J., Teeling, P., van der Wal, A. C., and Becker, A. E. (2001). Immunohistochemical detection of interferon-gamma: fake or fact? J Histochem Cytochem *49*, 699-710.

Wegrowski, Y., and Maquart, F. X. (2004). Involvement of stromal proteoglycans in tumour progression. Crit Rev Oncol Hematol *49*, 259-268.

Wetzel, R., Perry, L. J., Veilleux, C., and Chang, G. (1990). Mutational analysis of the C-terminus of human gamma-interferon. Protein Eng *4*, 105.

Willimsky, G., and Blankenstein, T. (2005). Sporadic immunogenic tumors avoid destruction by inducing T-cell tolerance. Nature *437*, 141-146.

Wrenshall, L. E., and Platt, J. L. (1999). Regulation of T cell homeostasis by heparan sulfate-bound IL-2. J Immunol *163*, 3793-3800.

Wu, T. H., Pabin, C. N., Qin, Z., Blankenstein, T., Philip, M., Dignam, J., Schreiber, K., and Schreiber, H. (2004). Long-term suppression of tumor growth by TNF requires a Stat1- and IFN regulatory factor 1-dependent IFN-gamma pathway but not IL-12 or IL-18. J Immunol *172*, 3243-3251.

Yard, B. A., Lorentz, C. P., Herr, D., and van der Woude, F. J. (1998). Sulfation-dependent down-regulation of interferon-gamma-induced major histocompatibility complex class I and II and intercellular adhesion molecule-1 expression on tubular and endothelial cells by glycosaminoglycans. Transplantation *66*, 1244-1250.

Zigrino, P., Löffek, S., and Mauch, C. (2005). Tumor-stroma interactions: their role in the control of tumor cell invasion. Biochemie *87*, 321-328.

Zou, J., Carrington, A., Collet, B., Dijkstra, J. M., Yoshiura, Y., Bols, N., and Secombes, C. (2005). Identification and bioactivities of IFN-γ in Rainbow Trout *Oncorhynchus mykiss*: The first Th-1-type cytokine characterised functionally in fish. J Immunol *175*, 2484-2494.

9 CURRICULUM VITAE

DATE OF BIRTH:	31.05.1977
PLACE OF BIRTH:	Swan District, Perth, Western Australia
NATIONALITY:	Australian, Spanish
MARITAL STATUS:	Single

EDUCATION:

PRIMARY SCHOOL**:**

1983	Normanhurst Primary, Normanhurst, New South Wales
1984-1985	Nightcliff Primary, Nightcliff, Northern Territory
1986-1988	Saint Patrick's Primary, Katanning, Western Australia
1988	Star of the Sea Primary, Rockingham, Western Australia

SECONDARY SCHOOL:

1989-1994	Iona Presentation College, Mosman Park, Western Australia

UNIVERSITY:

1996-1998	Bachelor of Science in Biotechnology at Murdoch University, Perth, Western Australia
1999	Honours in Pathology at the University of Melbourne, Melbourne, Victoria

PROMOTION:	since 2001
Group:	Molekulare Immunologie und Gentherapie Prof. Dr. Thomas Blankenstein
Institute:	Max-Delbrück-Centrum für Molekulare Medizin und Institut für Immunologie, Charite-UKBF

10 PUBLICATIONS

Qin Z, Schwartzkopff J, **Pradera F**, Kammertoens T, Seliger B, Pircher H, Blankenstein T. A critical requirement of interferon gamma-mediated angiostasis for tumor rejection by CD8+ T cells. Cancer Res. 2003 Jul 15;63(14):4095-100

11 ACKNOWLEDGEMENTS

I would like to acknowledge the help of many people during my PhD.

First, I wish to thank Thomas Blankenstein for the opportunity to work within the laboratory, and for offering direction.

Thomas Kammertoens my arm of support and trust when things were going well or were falling apart. Your dedication to science is infectious, your inspirational ideas either verged on insanity or genius. Thankyou, I wouldn't be here without you.

To my colleagues: Zhihai Qin for teaching me the basics of science and the yin and yan of life, Boris Engels for his patience, whenever I needed to give someone an earbashing, Hye-Jung Kim for her wisdom, friendship, strength and intelligence, Martin Textor for the laughs and coffee in the stairwell, Jehad Charo the Molecular Biology Master for teaching me the ways of the force, and the technical assistance I received from Tanja Specowius, Nahid Hakiy and Christel Westen

Most importantly I wish to thank my family. My parents Juan and Christine who showed me the infinite possibilities the world had to offer. My brothers Michael and Robert, who were here in Europe and supported me during this time. I hope one day I can return all the kindness and love you have given me.

.

12 APPENDIX

A

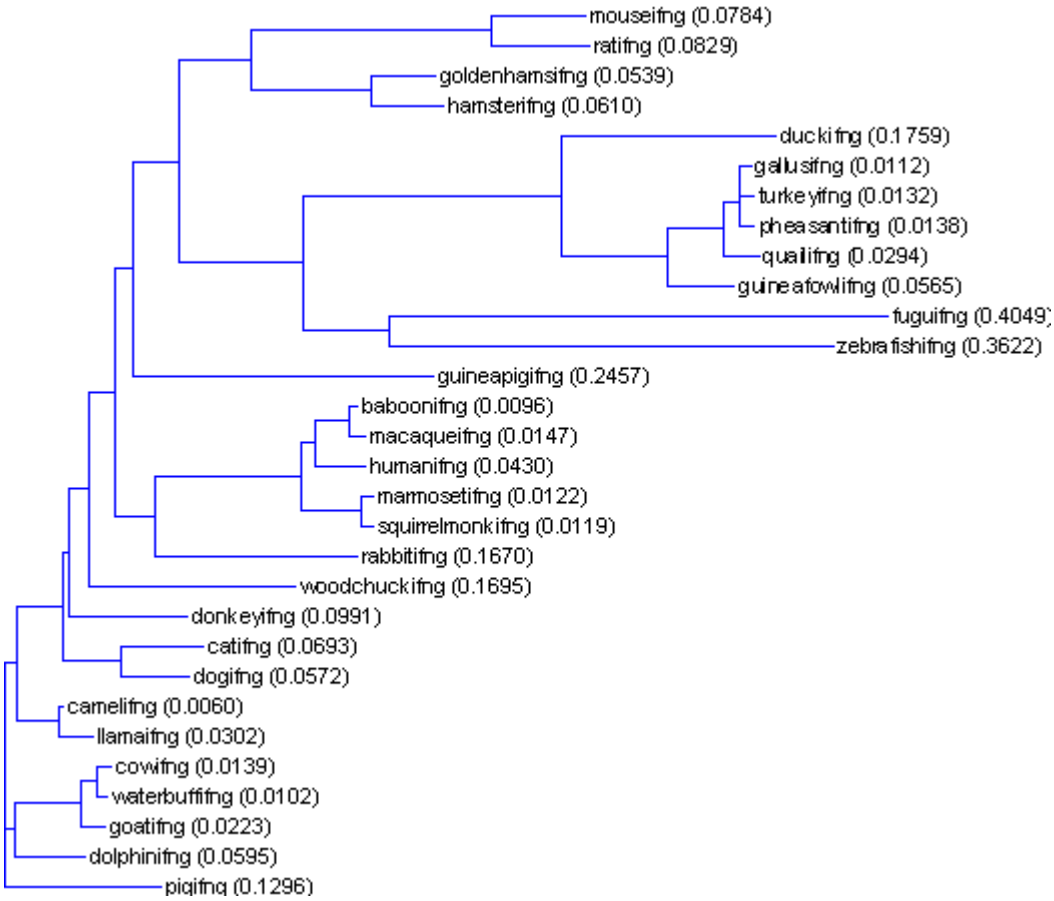

B

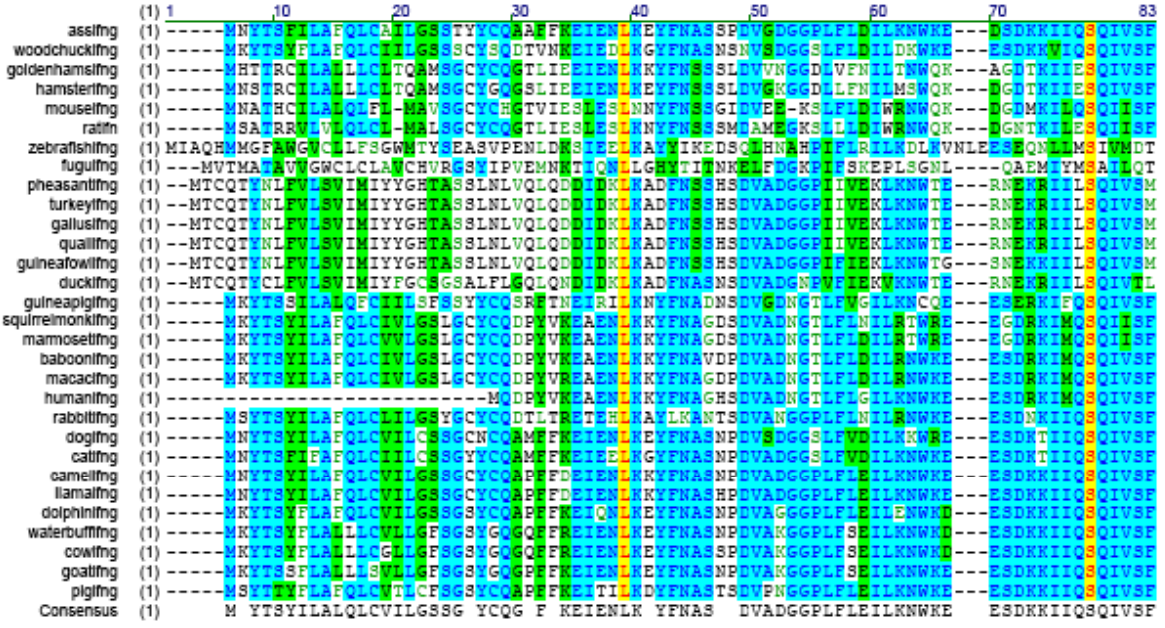

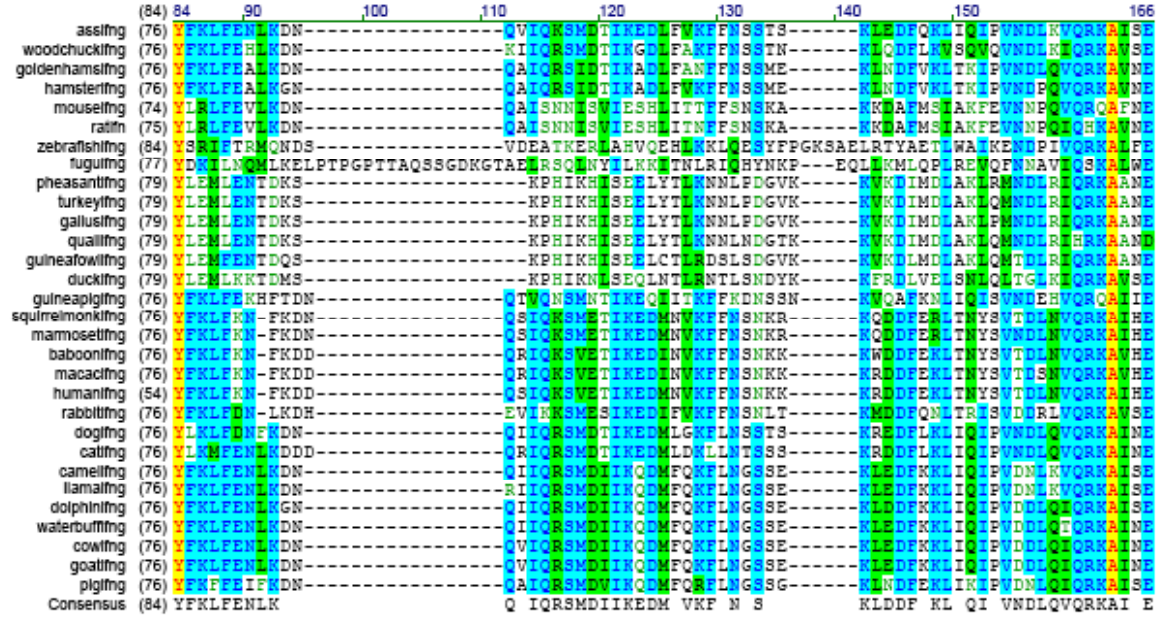

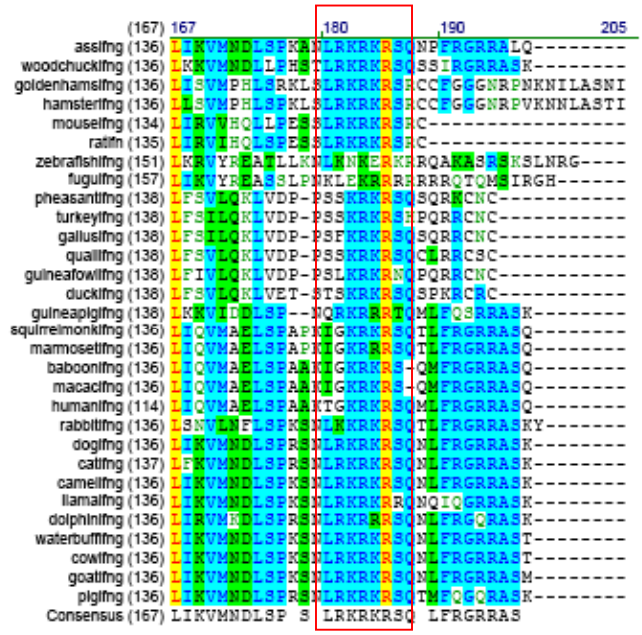

Figure 27: Phylogenetic tree (A) and IFN-γ sequences (B) showing the homology of known IFN-γ molecules from different species as determined by Vector Alignment™. In **(A)** the phylogenetic tree is built using the Neighbour Joining (NJ) method of Saitou and Nei. The NJ method works on a matrix of distances between all pairs of sequences to be analysed and these distances are related to the degree of divergence between the sequences. The values in parenthesis are the calculated distance values. The colours in **(B)** indicate identical (yellow), similar (blue) and weakly similar (green) amino acids. The red box highlights the C-terminal LRKRKRSR sequence capable of binding to heparan sulphate.

A

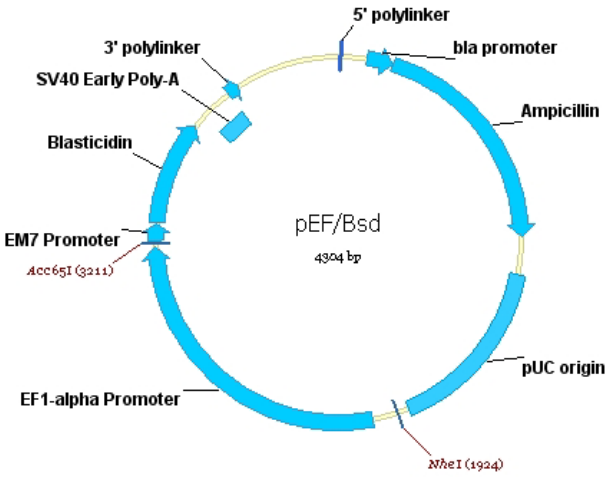

B

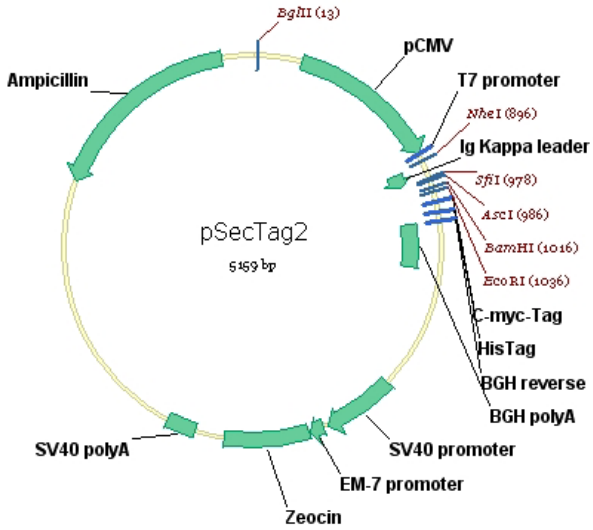

C

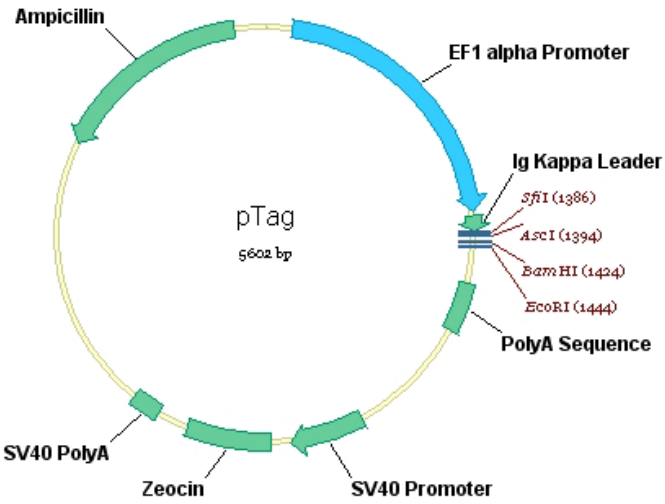

Figure 28: **Plasmid Map of the constructs used to transfect J558L tumour cells**. The Human EF-1 alpha promoter from the pEF/Bsd vector **(A)** replaced the pCMV promoter from the pSecTag2 vector **(B)** to create the backbone plasmid pTag **(C)**.

A

gacggatcgggagatcctcgaggagacctgcaaagatggataaagttttaaacagagaggaatctttgcagctaatggaccttctaggt
cttgaaaggagtgggaattggctccggtgcccgtcagtgggcagagcgcacatcgcccacagtccccgagaagttgtggggagggg
tcggcaattgaaccggtgcctagagaaggtggcgcggggtaaactgggaaagtgatgtcgtgtactggctccgccttttcccgaggg
tgggggagaaccgtatataagtgcagtagtcgccgtgaacgttcttttcgcaacgggtttgccgccagaacacaggtaagtgccgtgt
gtggttcccgcgggcctggcctctttacgggttatggcccttgcgtgccttgaattacttccacctggctgcagtacgtgattcttgatccc
gagcttcgggttggaagtgggtgggagagttcgaggccttgcgcttaaggagccccttcgcctcgtgcttgagttgaggcctggcctg
ggcgctggggccgccgcgtgcgaatctggtggcaccttcgcgcctgtctcgctgctttcgataagtctctagccatttaaaatttttgatg
acctgctgcgacgctttttttctggcaagatagtcttgtaaatgcgggccaagatctgcacactggtatttcggttttggggccgcgggcg
gcgacggggcccgtgcgtcccagcgcacatgttcggcgaggcggggcctgcgagcgcggccaccgagaatcggacgggggtag
tctcaagctggccggcctgctctggtgcctggcctcgcgccgccgtgtatcgccccgccctgggcggcaaggctggcccggtcggc
accagttgcgtgagcggaaagatggccgcttcccggccctgctgcagggagctcaaaatggaggacgcggcgctcgggagagcg
ggcgggtgagtcacccacacaaaggaaaagggcctttccgtcctcagccgtcgcttcatgtgactccacggagtaccgggcgccgtc
caggcacctcgattagttctcgagcttttggagtacgtcgtctttaggttgggggggagggtttttatgcgatggagtttccccacactgagt
gggtggagactgaagttaggccagcttggcacttgatgtaattctccttggaatttgccctttttgagtttggatcttggttcattctcaagcct
cagacagtggttcaaagttttttttcttccatttcaggtgtcgtgaggaattagcttggtacctagccaccatggagacagacacactcctgc
tatgggtactgctgctctgggttccaggttccactggtgacgcggcccagccggccaggcgcgccgtacgaagcttggtaccgagctc
ggatccactccagtgtggtggaattctgcagatatccagcacagtggcggccgctcgaggagggcccgaacaaaaactcatctcaga
agaggatctgaatagcgccgtcgaccatcatcatcatcatcattgaatagcgccgtcgaccatcatcatcatcatcattgagtttaaaccc
gctgatcagcctcgactgtgccttctagttgccagccatctgttgtttgcccctcccccgtgccttccttgaccctggaaggtgccactccc
actgtcctttcctaataaaatgaggaaattgcatcgcattgtctgagtaggtgtcattctattctgggggggtggggtggggcaggacagca
agggggaggattgggaagacaatagcaggcatgctggggatgcggtgggctctatggcttctgaggcggaaagaaccagctgggg
ctctagggggtatccccacgcgccctgtagcggcgcattaagcgcggcgggtgtggtggttacgcgcagcgtgaccgctacacttgc
cagcgccctagcgcccgctcctttcgctttcttcccttcctttctcgccacgttcgccggctttccccgtcaagctctaaatcggggcatcc
ctttagggttccgatttagtgctttacggcacctcgaccccaaaaaacttgattagggtgatggttcacgtagtgggccatcgccctgata
gacggtttttcgccctttgacgttggagtccacgttctttaatagtggactcttgttccaaactggaacaacactcaaccctatctcggtctat
tcttttgatttataagggattttggggatttcggcctattggttaaaaaatgagctgatttaacaaaaatttaacgcgaattaattctgtggaat
gtgtgtcagttagggtgtggaaagtccccaggctccccagcaggcagaagtatgcaaagcatgcatctcaattagtcagcaaccaggt
gtggaaagtccccaggctccccagcaggcagaagtatgcaaagcatgcatctcaattagtcagcaaccatagtcccgcccctaactcc
gcccatcccgcccctaactccgcccagttccgcccattctccgccccatggctgactaatttttttttatttatgcagaggccgaggccgcc
tctgcctctgagctattccagaagtagtgaggaggctttttggaggcctaggcttttgcaaaaagctcccgggagcttgtatatccattttc
ggatctgatcagcacgtgttgacaattaatcatcggcatagtatatcggcatagtataatacgacaaggtgaggaactaaaccatggcca
agttgaccagtgccgttccggtgctcaccgcgcgcgacgtcgccggagcggtcgagttctggaccgaccggctcgggttctcccggg
acttcgtggaggacgacttcgccggtgtggtccgggacgacgtgaccctgttcatcagcgcggtccaggaccaggtggtgccggaca
acaccctggcctgggtgtgggtgcgcggcctggacgagctgtacgccgagtggtcggaggtcgtgtccacgaacttccgggacgcc
tccgggccggccatgaccgagatcggcgagcagccgtgggggcgggagttcgccctgcgcgacccggccggcaactgcgtgcac
ttcgtggccgaggagcaggactgacacgtgctacgagatttcgattccaccgccgccttctatgaaaggttgggcttcggaatcgttttc
cgggacgccggctggatgatcctccagcgcggggatctcatgctggagttcttcgcccaccccaacttgtttattgcagcttataatggtt
acaaataaagcaatagcatcacaaatttcacaaataaagcatttttttcactgcattctagttgtggtttgtccaaactcatcaatgtatcttatc
atgtctgtataccgtcgacctctagctagagcttggcgtaatcatggtcatagctgtttcctgtgtgaaattgttatccgctcacaattccaca
caacatacgagccggaagcataaagtgtaaagcctggggtgcctaatgagtgagctaactcacattaattgcgttgcgctcactgcccg
ctttccagtcgggaaacctgtcgtgccagctgcattaatgaatcggccaacgcgcggggagaggcggtttgcgtattgggcgctcttcc
gcttcctcgctcactgactcgctgcgctcggtcgttcggctgcggcgagcggtatcagctcactcaaaggcggtaatacggttatccac
agaatcaggggataacgcaggaaagaacatgtgagcaaaaggccagcaaaaggccaggaaccgtaaaaaggccgcgttgctggc
gtttttccataggctccgccccctgacgagcatcacaaaaatcgacgctcaagtcagaggtggcgaaacccgacaggactataaaga
taccaggcgtttcccccctggaagctccctcgtgcgctctcctgttccgaccctgccgcttaccggatacctgtccgcctttctcccttcgg
gaagcgtggcgctttctcaatgctcacgctgtaggtatctcagttcggtgtaggtcgttcgctccaagctgggctgtgtgcacgaacccc
ccgttcagcccgaccgctgcgccttatccggtaactatcgtcttgagtccaacccggtaagacacgacttatcgccactggcagcagcc
actggtaacaggattagcagagcgaggtatgtaggcggtgctacagagttcttgaagtggtggcctaactacggctacactagaagga
cagtatttggtatctgcgctctgctgaagccagttaccttcggaaaaagagttggtagctcttgatccggcaaacaaaccaccgctggta
gcggtggtttttttgtttgcaagcagcagattacgcgcagaaaaaaaggatctcaagaagatcctttgatcttttctacggggtctgacgct
cagtggaacgaaaactcacgttaagggattttggtcatgagattatcaaaaaggatcttcacctagatccttttaaattaaaaatgaagtttt

aaatcaatctaaagtatatatgagtaaacttggtctgacagttaccaatgcttaatcagtgaggcacctatctcagcgatctgtctatttcgtt
catccatagttgcctgactccccgtcgtgtagataactacgatacgggagggcttaccatctggccccagtgctgcaatgataccgcga
gacccacgctcaccggctccagatttatcagcaataaaccagccagccggaagggccgagcgcagaagtggtcctgcaactttatcc
gcctccatccagtctattaattgttgccgggaagctagagtaagtagttcgccagttaatagtttgcgcaacgttgttgccattgctacagg
catcgtggtgtcacgctcgtcgtttggtatggcttcattcagctccggttcccaacgatcaaggcgagttacatgatcccccatgttgtgca
aaaaagcggttagctccttcggtcctccgatcgttgtcagaagtaagttggccgcagtgttatcactcatggttatggcagcactgcataa
ttctcttactgtcatgccatccgtaagatgcttttctgtgactggtgagtactcaaccaagtcattctgagaatagtgtatgcggcgaccgag
ttgctcttgcccggcgtcaatacgggataataccgcgccacatagcagaactttaaaagtgctcatcattggaaaacgttcttcggggcg
aaaactctcaaggatcttaccgctgttgagatccagttcgatgtaacccactcgtgcacccaactgatcttcagcatcttttactttcaccag
cgtttctgggtgagcaaaaacaggaaggcaaaatgccgcaaaaaagggaataagggcgacacggaaatgttgaatactcatactcttc
ctttttcaatattattgaagcatttatcagggttattgtctcatgagcggatacatatttgaatgtatttagaaaaataaacaaatagggttcc
gcgcacatttccccgaaaagtgccacctgacgtc

B

```
                1                                                  50
pAlaNoTag     (1) ATGGAGACAGACACACTCCTGCTATGGGTACTGCTGCTCTGGGTTCCAGG
pMC2NoTag     (1) ATGGAGACAGACACACTCCTGCTATGGGTACTGCTGCTCTGGGTTCCAGG
  pMC2Tag     (1) ATGGAGACAGACACACTCCTGCTATGGGTACTGCTGCTCTGGGTTCCAGG
     pTag     (1) ATGGAGACAGACACACTCCTGCTATGGGTACTGCTGCTCTGGGTTCCAGG

               51                                                 100
pAlaNoTag    (51) TTCCACTGGTGACGCGGCCCAGCCGGCCAGGCGCGCCGTACGAAGCTTGG
pMC2NoTag    (51) TTCCACTGGTGACGCGGCCCAGCCGGCCAGGCGCGCCGTACGAAGCTTGG
  pMC2Tag    (51) TTCCACTGGTGACGCGGCCCAGCCGGCCAGGCGCGCCGTACGAAGCTTGG
     pTag    (51) TTCCACTGGTGACGCGGCCCAGCCGGCCAGGCGCGCCGTACGAAGCTTGG

               101                                                150
pAlaNoTag   (101) TACCGAGCTCGGATCCTGCC--GCAGCGGCTGC-----AGCCGCCGCTGC
pMC2NoTag   (101) TACCGAGCTCGGATCCTCTCAGGAAGCGGAAA------AGGAGTCGCTGC
  pMC2Tag   (101) TACCGAGCTCGGATCCTCTC---AGGAAGCGGAAAAGGAGTCGCTGCGAA
     pTag   (101) TACCGAGCTCGGATCCACTC---CAG-----------------TGTGGT

               151                                                200
pAlaNoTag   (144) CGAATTCTGCAGATATCCAGCACAGTGGCGGCCGCTCGAGGAGGGCCCGA
pMC2NoTag   (145) -GAATTCTGCAGATATCCAGCACAGTGGCGGCCGCTCGAGGAGGGCCCGA
  pMC2Tag   (148) TTAATTCTGCAGATATCCAGCACAGTGGCGGCCGCTCGAGGAGGGCCCGA
     pTag   (130) GGAATTCTGCAGATATCCAGCACAGTGGCGGCCGCTCGAGGAGGGCCCGA

               201                                                250
pAlaNoTag   (194) ACAAAAACTCATCTCAGAAGAGGATC------------------------
pMC2NoTag   (194) ACAAAAACTCATCTCAGAAGAGGATC------------------------
  pMC2Tag   (198) ACAAAAACTCATCTCAGAAGAGGATCTGAATAGCGCCGTCGACCATCATC
     pTag   (180) ACAAAAACTCATCTCAGAAGAGGATCTGAATAGCGCCGTCGACCATCATC

               251     261
pAlaNoTag   (220) -----------
pMC2NoTag   (220) -----------
  pMC2Tag   (248) ATCATCATCAT
     pTag   (230) ATCATCATCAT
```

C

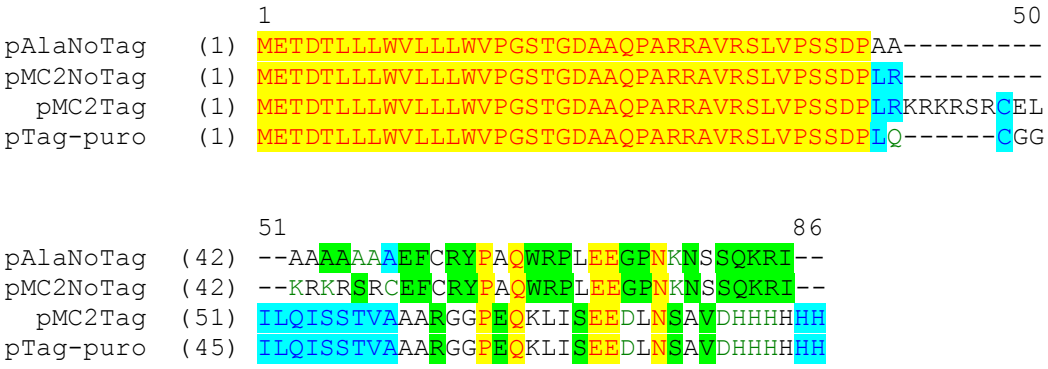

Figure 29: Nucleotide and Amino acid sequences of the plasmids used to transfect J558L tumour cells. The sequence of the plasmid backbone pTag **(A)** was used to create plasmids pAla^{8}NoTag, pMC2NoTag and pMC2Tag. Oligonucleotides were cloned between BamH1 and Eco R1. The nucleotide sequence **(B)** and amino acid sequences **(C)** of the secreted fragments are included.

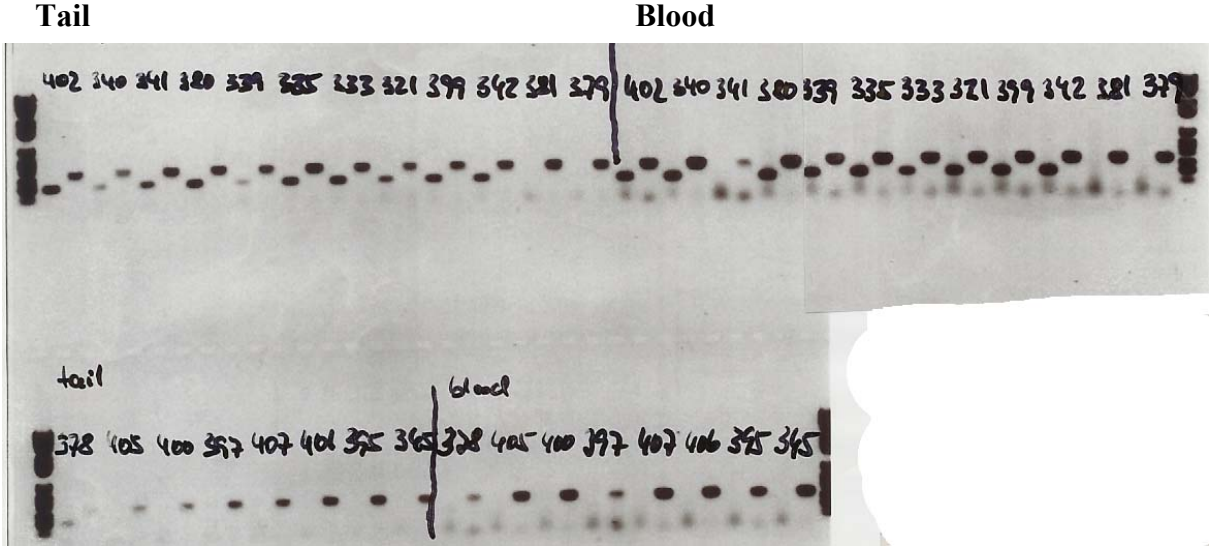

Figure 30: IFN-γ gene PCR of the blood and tail from selected mice from the bone marrow chimera experiment.
Each number represents an individual mouse within the experimental group. 12 weeks after irradiation with 10 Gy and reconstitution with bone marrow mouse tail and blood were lysed and DNA was isolated for PCR using primers specific for IFN-γ (See materials and methods).

Berlin 2006

Ich erkläre an Eides Statt, dass die vorliegende Dissertation in allen Teilen von mir selbständig angefertigt wurde und die benutzten Hilfsmittel vollständig angegeben worden sind.

Veröffentlichungen von irgendwelchen Teilen der vorliegenden Dissertation sind von mir nicht / wie folgt vorgenommen worden.

Weiter erkläre ich, dass ich nicht schon anderweitig einmal die Promotionsabsicht angemeldet oder ein Promotionseröffnungsverfahren beantragt habe.

Felicia Pradera, Berlin, 2006